



National Library
of Canada

Acquisitions and
Bibliographic Services Branch

395 Wellington Street
Ottawa, Ontario
K1A 0N4

Bibliothèque nationale
du Canada

Direction des acquisitions et
des services bibliographiques

395, rue Wellington
Ottawa (Ontario)
K1A 0N4

Your file - Votre référence

Our file - Notre référence

NOTICE

The quality of this microform is heavily dependent upon the quality of the original thesis submitted for microfilming. Every effort has been made to ensure the highest quality of reproduction possible.

If pages are missing, contact the university which granted the degree.

Some pages may have indistinct print especially if the original pages were typed with a poor typewriter ribbon or if the university sent us an inferior photocopy.

Reproduction in full or in part of this microform is governed by the Canadian Copyright Act, R.S.C. 1970, c. C-30, and subsequent amendments.

AVIS

La qualité de cette microforme dépend grandement de la qualité de la thèse soumise au microfilmage. Nous avons tout fait pour assurer une qualité supérieure de reproduction.

S'il manque des pages, veuillez communiquer avec l'université qui a conféré le grade.

La qualité d'impression de certaines pages peut laisser à désirer, surtout si les pages originales ont été dactylographiées à l'aide d'un ruban usé ou si l'université nous a fait parvenir une photocopie de qualité inférieure.

La reproduction, même partielle, de cette microforme est soumise à la Loi canadienne sur le droit d'auteur, SRC 1970, c. C-30, et ses amendements subséquents.

UNIVERSITY OF ALBERTA

COLLAPSE BEHAVIOR OF VERY LOOSE DRY SAND

BY

PETER SKOPEK ©

A THESIS

SUBMITTED TO THE FACULTY OF GRADUATE STUDIES AND
RESEARCH IN PARTIAL FULFILLMENT OF THE REQUIREMENTS

FOR

THE DEGREE OF DOCTOR OF PHILOSOPHY

IN

GEOTECHNICAL ENGINEERING

DEPARTMENT OF CIVIL ENGINEERING

EDMONTON, ALBERTA

FALL, 1994



National Library
of Canada

Bibliothèque nationale
du Canada

Acquisitions and
Bibliographic Services Branch

Direction des acquisitions et
des services bibliographiques

395 Wellington Street
Ottawa, Ontario
K1A 0N4

395, rue Wellington
Ottawa (Ontario)
K1A 0N4

Your file *Votre référence*

Our file *Notre référence*

The author has granted an irrevocable non-exclusive licence allowing the National Library of Canada to reproduce, loan, distribute or sell copies of his/her thesis by any means and in any form or format, making this thesis available to interested persons.

L'auteur a accordé une licence irrévocable et non exclusive permettant à la Bibliothèque nationale du Canada de reproduire, prêter, distribuer ou vendre des copies de sa thèse de quelque manière et sous quelque forme que ce soit pour mettre des exemplaires de cette thèse à la disposition des personnes intéressées.

The author retains ownership of the copyright in his/her thesis. Neither the thesis nor substantial extracts from it may be printed or otherwise reproduced without his/her permission.

L'auteur conserve la propriété du droit d'auteur qui protège sa thèse. Ni la thèse ni des extraits substantiels de celle-ci ne doivent être imprimés ou autrement reproduits sans son autorisation.

ISBN 0-315-95266-0

Canada

Name PETER SKOPEK

Dissertation Abstracts International is arranged by broad, general subject categories. Please select the one subject which most nearly describes the content of your dissertation. Enter the corresponding four-digit code in the spaces provided.

CIVIL ENGINEERING

SUBJECT TERM

0543

SUBJECT CODE

U·M·I

Subject Categories

THE HUMANITIES AND SOCIAL SCIENCES

COMMUNICATIONS AND THE ARTS

Architecture 0729
Art History 0377
Cinema 0900
Dance 0378
Fine Arts 0357
Information Science 0723
Journalism 0391
Library Science 0399
Mass Communications 0708
Music 0413
Speech Communication 0459
Theater 0465

EDUCATION

General 0515
Administration 0514
Adult and Continuing 0516
Agricultural 0517
Art 0273
Bilingual and Multicultural 0282
Business 0688
Community College 0275
Curriculum and Instruction 0727
Early Childhood 0518
Elementary 0524
Finance 0277
Guidance and Counseling 0519
Health 0680
Higher 0745
History of 0520
Home Economics 0278
Industrial 0521
Language and Literature 0279
Mathematics 0280
Music 0522
Philosophy of 0998
Physical 0523

Psychology 0525
Reading 0535
Religious 0527
Sciences 0714
Secondary 0533
Social Sciences 0534
Sociology of 0340
Special 0529
Teacher Training 0530
Technology 0710
Tests and Measurements 0288
Vocational 0747

LANGUAGE, LITERATURE AND LINGUISTICS

Language 0679
General 0289
Ancient 0290
Linguistics 0291
Modern 0401
Literature 0294
General 0295
Classical 0297
Comparative 0298
Medieval 0316
Modern 0591
African 0305
American 0352
Asian 0355
Canadian (English) 0593
Canadian (French) 0311
English 0312
Germanic 0315
Latin American 0313
Middle Eastern 0314
Romance 0370
Slavic and East European 0372

PHILOSOPHY, RELIGION AND THEOLOGY

Philosophy 0422
Religion 0318
General 0321
Biblical Studies 0319
Clergy 0320
History of 0322
Philosophy of 0469
Theology 0323

SOCIAL SCIENCES

American Studies 0323
Anthropology 0324
Archaeology 0326
Cultural 0327
Physical 0310
Business Administration 0272
General 0770
Accounting 0454
Banking 0338
Management 0385
Marketing 0501
Canadian Studies 0503
Economics 0505
General 0508
Agricultural 0509
Commerce-Business 0510
Finance 0511
History 0358
Labor 0366
Theory 0351
Folklore 0578
Geography 0578
Gerontology 0578
History 0578
General 0578

Ancient 0579
Medieval 0581
Modern 0328
Black 0331
African 0332
Asia, Australia and Oceania 0334
Canadian 0335
European 0336
Latin American 0333
Middle Eastern 0377
United States 0585
History of Science 0398
Law 0615
Political Science 0616
General 0617
International Law and Relations 0814
Public Administration 0452
Recreation 0626
Social Work 0627
Sociology 0938
General 0631
Criminology and Penology 0628
Demography 0629
Ethnic and Racial Studies 0630
Individual and Family Studies 0700
Industrial and Labor Relations 0344
Public and Social Welfare 0709
Social Structure and Development 0999
Theory and Methods 0453
Transportation 0453
Urban and Regional Planning 0453
Women's Studies 0453

THE SCIENCES AND ENGINEERING

BIOLOGICAL SCIENCES

Agriculture 0473
General 0285
Agronomy 0475
Animal Culture and Nutrition 0476
Animal Pathology 0359
Food Science and Technology 0478
Forestry and Wildlife 0479
Plant Culture 0480
Plant Pathology 0817
Plant Physiology 0777
Range Management 0306
Wood Technology 0287
Biology 0308
General 0309
Anatomy 0379
Biostatistics 0329
Botany 0353
Cell 0369
Ecology 0793
Entomology 0410
Genetics 0307
Limnology 0317
Microbiology 0416
Molecular 0433
Neuroscience 0821
Oceanography 0778
Physiology 0472
Radiation 0786
Veterinary Science 0760
Zoology 0425
Biophysics 0996
General 0425
Medical 0996

EARTH SCIENCES

Biochemistry 0425
Geochemistry 0996

Geodesy 0370
Geology 0372
Geophysics 0373
Hydrology 0388
Mineralogy 0411
Paleobotany 0345
Paleoecology 0426
Paleontology 0418
Paleozoology 0985
Palynology 0427
Physical Geography 0368
Physical Oceanography 0415

HEALTH AND ENVIRONMENTAL SCIENCES

Environmental Sciences 0768
Health Sciences 0566
General 0300
Audiology 0992
Chemotherapy 0567
Dentistry 0350
Education 0769
Hospital Management 0758
Human Development 0982
Immunology 0564
Medicine and Surgery 0347
Mental Health 0569
Nursing 0570
Nutrition 0380
Obstetrics and Gynecology 0354
Occupational Health and Therapy 0381
Ophthalmology 0571
Pathology 0419
Pharmacology 0572
Pharmacy 0382
Physical Therapy 0573
Public Health 0574
Radiology 0575
Recreation 0575

Speech Pathology 0460
Toxicology 0383
Home Economics 0386

PHYSICAL SCIENCES

Pure Sciences 0485
Chemistry 0749
General 0486
Agricultural 0487
Analytical 0488
Biochemistry 0738
Inorganic 0490
Nuclear 0491
Organic 0494
Pharmaceutical 0495
Physical 0754
Polymer 0405
Mathematics 0605
Physics 0986
General 0606
Acoustics 0608
Astronomy and Astrophysics 0748
Atmospheric Science 0607
Atomic 0798
Electronics and Electricity 0759
Elementary Particles and High Energy 0609
Fluid and Plasma 0610
Molecular 0752
Nuclear 0756
Optics 0611
Radiation 0463
Solid State 0346
Statistics 0984
Applied Sciences 0346
Applied Mechanics 0984
Computer Science 0984

Engineering 0537
General 0538
Aerospace 0539
Agricultural 0540
Automotive 0541
Biomedical 0542
Chemical 0543
Civil 0544
Electronics and Electrical 0348
Heat and Thermodynamics 0545
Hydraulic 0546
Industrial 0547
Marine 0794
Materials Science 0548
Mechanical 0743
Metallurgy 0551
Mining 0552
Nuclear 0549
Packaging 0765
Petroleum 0554
Sanitary and Municipal 0790
System Science 0428
Geotechnology 0796
Operations Research 0795
Plastics Technology 0994
Textile Technology 0994

PSYCHOLOGY

General 0621
Behavioral 0384
Clinical 0622
Developmental 0620
Experimental 0623
Industrial 0624
Personality 0625
Physiological 0989
Psychobiology 0349
Psychometrics 0632
Social 0451



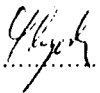
UNIVERSITY OF ALBERTA

RELEASE FORM

NAME OF AUTHOR Peter Skopek
TITLE OF THESIS Collapse behavior of very loose dry sand
DEGREE Doctor of Philosophy
YEAR THIS DEGREE GRANTED 1994

Permission is hereby granted to the University of Alberta Library to reproduce single copies of this thesis and to lend or sell such copies for private scholarly or scientific purposes only.

The author reserves all other publication and other rights in association with the copyright in the thesis, and except as hereinbefore provided neither the thesis nor any substantial portion thereof may be printed or otherwise reproduced without in any material form whatever without the author's prior written permission.

(Signed) 

Peter Skopek

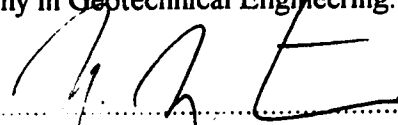
3139 - 109 Street

Edmonton, Alberta, T6J 4N6


DATE October 7, 1994

UNIVERSITY OF ALBERTA
FACULTY OF GRADUATE STUDIES AND RESEARCH

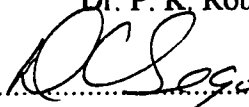
The undersigned certify that they have read, and recommend to the Faculty of Graduate Studies and Research for acceptance, a thesis entitled Collapse Behavior of Very Loose Dry Sand submitted by Peter Skopek in partial fulfillment of the requirements for the degree of Doctor of Philosophy in Geotechnical Engineering.



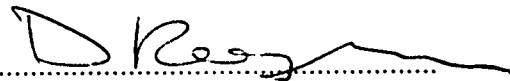
Dr. N. R. Morgenstern



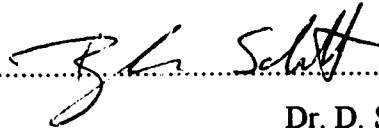
Dr. P. K. Robertson



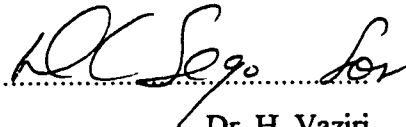
Dr. D. C. Sego



Dr. D. M. Rogowsky



Dr. D. Schmitt



Dr. H. Vaziri

Date: October 7, 1999

To my wife Andrea

Abstract

The objective of this thesis is to advance the understanding of the processes governing the collapse of very loose sands leading to flow liquefaction. Current methods of flow liquefaction analysis assume that once liquefaction is triggered the subsequent deformation is undrained. This is a gross over-simplification of the process since it does not take into account differing rates of drainage. For example with gravel the rate of dissipation of pore pressures could be commensurate with the rate of pore pressure generation. This would result only in volume changes without any loss of strength required for full scale failure, i.e., flow liquefaction.

An effective stress based theory is introduced to calculate the pore pressures developing during flow liquefaction is proposed in this thesis. The theory emanates from the state boundary surface concept that provides a constitutive relation between volume change and stress change during the collapse of very loose sand. It is shown that material instabilities exist on the state boundary surface that manifest themselves as increments of volumetric creep. In this study both the structural contraction along the state boundary surface and the structural collapse phenomena have been incorporated into a simple theory of pore pressure generation.

Material properties and parameters for the state boundary surface have been obtained by testing very loose dry sand under a variety of triaxial stress paths. Necessary monitoring of volume changes was accomplished by direct measurement of axial and lateral deformations. For measurement of lateral deformations a new resistance wire transducer was developed and is described in this study.

Acknowledgments

I would like to express my gratitude to Dr. N. R Morgenstern for his guidance and advice. The opportunity to work with him and witness his unparalleled insight covering the entire field of geotechnical engineering was an invaluable and amazing experience.

The support, direction and energetic devotion offered by Dr. P. K. Robertson was critical to this research and greatly appreciated.

I greatly appreciate the encouragement and support by Dr. D. C. Sego especially during the difficult early stages of research.

The never-ending help of the technicians Steve Gamble and Gerry Cyre is gratefully acknowledged.

I would also like to thank my fellow graduate students Annajirao Chillarige and Richard Dawson for the challenging discussions and fresh ideas.

At last, but most certainly not least, I want to thank Dr. Z. Eisenstein for his friendship and never failing support during the research and beyond.

Table of Contents

Chapter 1	INTRODUCTION	1
Chapter 2	COLLAPSE OF DRY SAND	7
	Introduction	7
	Collapse surface and state boundary	11
	Objective of the study	12
	Testing program	13
	Test results	14
	Explanation of observed phenomenon	16
	Conclusions	17
Chapter 3	STATE BOUNDARY SURFACE FOR VERY LOOSE SAND	30
	Introduction	30
	State boundary surface	33
	Mechanism of collapse	34
	Collapse criterion	35
	Testing program	35
	Interpretation of test results	36
	Practical implications of observed phenomenon	40
	Conclusions	43
Chapter 4	EFFECTIVE STRESS APPROACH TO EVALUATE FLOW LIQUEFACTION	57
	Introduction	57
	State boundary surface	59
	Structural contraction/collapse	61
	Mode of liquefaction failure	61
	Mathematical modeling	62
	Detailed calculation algorithm of the effect of structural contraction on the effective stress path during a q = constant loading	66

	Detailed calculation algorithm of the effect of structural collapse on pore pressure generation	67
	Results	68
	Conclusions	71
Chapter 5	A RESISTANCE WIRE TRANSDUCER FOR CIRCUMFERENTIAL STRAIN MEASUREMENT IN TRIAXIAL TESTS	82
	Introduction	82
	Proposed method	83
	Application	86
	Summary.....	87
Chapter 6	SUMMARY AND CONCLUSIONS.....	95
	RECOMMENDATIONS FOR FUTURE WORK	98
APPENDIX I	Summary of test characteristics	102
APPENDIX II	Course of the tests	105

List of Tables

Table 2.1	Summary of test initial parameters, parameters at the onset of structural contraction and characteristics of structural collapses
Table 3.1	Initial characteristics of presented tests

List of Figures

Figure 2.1	Definition of the elements of state boundary surface
Figure 2.2	Typical strain development during the $q = \text{constant}$ test (test #12)
Figure 2.3	Stress paths and contraction during the $q = \text{constant}$ tests
Figure 2.4	Typical strain development during structural collapse (test #8, 1 st jump)
Figure 2.5	Mobilized friction angle at points of observed structural collapse for $q = \text{constant}$ tests on very loose dry Ottawa sand (test #8, #9, #12)
Figure 2.6	Mobilized friction angle during $q = \text{constant}$ tests on very loose dry Ottawa sand
Figure 3.1	Definition of the elements of state boundary surface
Figure 3.2	Stress path deflection due to the state boundary surface for two $q = \text{constant}$ tests (test #9, #14)
Figure 3.3	Stress path deflection due to the state boundary surface for the conventional strain controlled compression test (test #compr2)
Figure 3.4	Stress path deflection due to the state boundary surface for the $p = \text{constant}$ test (test #p1)
Figure 3.5	Stress path deflection due to the state boundary surface for the special path test (test #spec)
Figure 3.6	The effect of the state boundary surface on a $q = \text{constant}$ loading path
Figure 3.7	Normalized plot of the state condition of the loose and dense samples (test #9, #14, #spec, #dns1, #dns2)
Figure 4.1	Definition of the elements of state boundary surface
Figure 4.2	Distribution of structural collapses during a typical $q = \text{constant}$ test (test #9)
Figure 4.3	Elements of mathematical model for the effective stress path during structural contraction
Figure 4.4	Calculated transition between drained and undrained behavior during structural contraction

- Figure 4.5** **Calculated effective stress paths and volume contraction structural contraction**
- Figure 4.6** **Calculated maximum pore pressure generation during one structural collapse**
- Figure 5.1** **Top view of the resistance wire transducer assembly**
- Figure 5.2** **Front view of the resistance wire transducer assembly**
- Figure 5.3** **Wheatstone Bridge schematic for the resistance wire transducer**
- Figure 5.4** **Calibration setup for the resistance wire transducer**
- Figure 5.5** **Calibration for resistance wire transducer**
- Figure 5.6** **Typical axial and circumferential deformation record during a test and associated calculated void ratio**

List of Symbols

c_v	coefficient of consolidation (m^2/s)
e	void ratio
E_{def}	deformation modulus (kPa)
E_r	rebound modulus (kPa)
K_w	bulk modulus of water (m^2/kN)
M	slope of steady state line in $p' - q$ plane
p'	effective mean principal stress (kPa); $= 1/3 \cdot (\sigma'_1 + 2 \cdot \sigma'_3)$
p'_{ss}	effective mean principal stress at the ultimate steady state for given void ratio
q	deviatoric stress (kPa); $= (\sigma'_1 - \sigma'_3)$
β	slope of the state boundary line
γ_w	specific gravity of water (kN/m^3)
Γ	void ratio at $\ln(p') = 1$
ϕ'_m	effective mobilized friction angle ($^\circ$)
λ	slope of the steady state line in $\ln p' - e$ plane
σ'	effective normal stress (kPa)
σ'_1	major principal stress (kPa)
σ'_3	minor principal stress, cell pressure in triaxial cell (kPa)
τ	shear stress (kPa)

Chapter 1

INTRODUCTION

Liquefaction phenomena have attracted serious research attention over the last decade as the geotechnical community became increasingly concerned with the lack of understanding of processes governing liquefaction. The endeavor to bridge this gap resulted in the development of a number of design procedures, primarily for design against earthquake triggered liquefaction failures. These procedures are most commonly based on the work of Seed and Idriss (1971). The empirical relationships between the SPT $(N_1)_{60}$ blowcount and the liquefaction resistance developed by Seed are able to discriminate, for a given earthquake, between liquefiable and stable sand. Experience has shown that these empirical relationships provide a reasonable and conservative approach. However, recently with increasing pressure for economical and safe designs these methods have been under intensive scrutiny for their possible excessive built-in conservatism. Foundation soils of Duncan Dam, Canada, evaluated using the above methodology were found susceptible to liquefaction. Extremely high quality sampling and testing provided a convincing basis for re-evaluating the site and as a result very expensive anti-liquefaction ground improvement measures were eliminated (Byrne et al. 1993). This experience contributed to the desire to replace methods based on empiricism with fundamental concepts. It is an often repeated story in geotechnical engineering that designs are initially based on general or regional experience and only later with the advance of our understanding of the governing processes can they be explained and thoroughly quantified. In addition, the original Seed empirical relationship has been reevaluated on a case by case basis to check its consistency (Fear and McRoberts 1994).

Another frequent problem relates to the terminology used to define liquefaction. The term liquefaction often has been used to describe fundamentally different

phenomena. So Castro (1969) defined liquefaction as the strain softening of a loose sand to an ultimate steady state of constant effective stress and deformation. Seed et al. (1983) defined liquefaction as the condition of zero effective stress due to cyclic loading. Ishihara (1993) proposed that liquefaction can be defined in terms of the magnitude of cyclic stress ratio required to produce a given level of strain, typically 5% double amplitude axial strain. Recently a more consistent terminology which recognizes gravitational flow liquefaction and seismic cyclic liquefaction has been introduced (Robertson 1994). In the literature dating back as far as 1956 (Terzaghi) flow liquefaction was also referred to as spontaneous liquefaction or static liquefaction. This thesis deals in general with this type of failure but it appears that the fundamental concepts discovered during the course of the research apply to the cyclic events as well.

The objective of this thesis is to study the fundamental mechanics of the flow liquefaction phenomenon rather than provide design guidelines. This task is accomplished by testing dry sand wherein the behavior is controlled solely by the material itself (pore pressures controlling the effective stresses during liquefaction flow are excluded by definition). The study also attempts to quantify the amount of material weakening during collapse and flow liquefaction. The state boundary surface approach (Sasitharan et al. 1994) based on the collapse surface concept (Sladen et al. 1986) is explored for a very loose dry sand, proven applicable for very loose dry sand, and used as a basis for addressing the objective of this research.

Outline of Thesis

This thesis is presented in paper format. Each chapter is a modified version of a paper submitted for publication in a major geotechnical journal. The chapters describe the testing program, observations on the fundamentals of the behavior of very loose dry sand and present an effective stress based theory for evaluation of liquefaction.

The contents are as follows. The second chapter introduces the results of the experimental study on collapse behavior of very loose dry sand. It is based on testing of very loose dry Ottawa sand under loading conditions that are known to initiate collapse followed by flow liquefaction in an identical very loose saturated sand. It is demonstrated that the very loose dry sand exhibits discontinuous behavior at stress states when the flow liquefaction is triggered in an identical, i.e., same density, saturated Ottawa sand. It is shown that this discontinuous behavior is associated with increased compressibility presented as structural contraction and occasionally with vigorous stress independent contractive events named structural collapse. A framework is proposed to relate the behavior of saturated sand to dry very loose sand. It is concluded that flow liquefaction is a result of a specific contractive response of a very loose sand structure and that this response is independent of drainage conditions, and it can be triggered by a loading path with no excess pore pressures, i.e., drained.

Based on the discontinuous phenomenon described in the second chapter, a testing program is outlined in the third chapter to characterize the conditions at which the discontinuity is initiated. The testing program is composed of a variety of different triaxial stress paths. It is concluded that these conditions obey the state boundary surface concept (Roscoe et al. 1958). This state boundary surface is shown to be geometrically similar to that found for very loose saturated sand (Sasitharan et al. 1994). In addition, two tests on dense dry sand are shown to investigate the behavior of dilatant sand within the framework of state boundary surface concept. It is shown that the sand exhibits a temporary contractive stage before it starts to dilate towards the steady state. This observation appears to be consistent with a phenomenon associated with the instability (Lade 1993) or critical stress ratio line (Vaid and Chern 1985) for saturated sand.

The fourth chapter applies the observations reported in the previous two chapters and introduces an effective stress based theory for evaluation of the potential for liquefaction. Two models are presented to calculate the magnitude of pore

pressures generated when an element of soil travels along the state boundary surface and when structural collapse is initiated. These two models make use of linking a perfectly drained response of dry sand to the response of saturated sand controlled by specific boundary conditions and material properties. It is shown that the significant pore pressures needed for material weakening and progressive propagation are generated during a structural collapse. It is also shown that the travel of the stress state of a soil element along the state boundary surface alone can generate excess pore pressures due to the enhanced compressibility especially if substantial loading rates related to rapid construction are imposed.

A novel solution to the problem of measurement of local strains inside a triaxial cell used for calculating volume changes of dry triaxial specimens is described in the fifth chapter. This measuring system utilizes a resistance wire transducer mounted on the wall of a sample. The system appears to be suitable for a wide variety of direct displacement measurements, especially in situation, when space restrictions apply.

Conclusions and recommendations for further studies are presented in the sixth chapter. The last section of the thesis includes processed test data from the sixteen tests carried out in the course of this study.

REFERENCES

- Byrne, P. M. , Imrie, A. S., and Morgenstern, N. R. (1993). "Results and implications of seismic performance studies - Duncan Dam." *Proc. 46th Canadian Geotechnical Conference*, 271-281.
- Castro, G. (1969). "Liquefaction of sands." *Harvard Soil Mechanics Series*, No. 81, Harvard University, Cambridge, MA.
- Seed, H. B., Idriss, I. M., and Arango, I. (1983). "Evaluation of liquefaction potential using field performance data." *ASCE Journal of the Soil Mechanics and Foundations Division*, 109, GT3, 458-482.
- Fear, C., and McRoberts, E. (1994). "A re-consideration of the initiation of liquefaction in sandy soils." *ASCE Journal of the Soil Mechanics and Foundations Division*, in press.
- Ishihara, K. (1993). "Liquefaction and flow failure during earthquakes." *33rd Rankine lecture*, March 1993.
- Lade, P. V. (1993). "Initiation of static instability in the submarine Nerlerk berm." *Canadian Geotechnical Journal*, 30(6), 895-904.
- Robertson, P. K. (1994). "Terminology for soil liquefaction." *Proc. 47th Canadian Geotechnical Conference, Halifax*, in press.
- Roscoe, K. H., Schofield, A. N., and Wroth, C. P. (1958). "On the yielding of soils." *Géotechnique*, 8(1), 22-53
- Seed, H. B., and Idriss, I. M. (1971). "Simplified procedure for evaluating soil liquefaction." *ASCE Journal of the Soil Mechanics and Foundations Division*, 97(No.SM9), 1249-1273.

- Sasitharan, S., Robertson, P. K., Sego, D. C. and Morgenstern, N. R. (1994). "A state boundary surface for very loose sand and its practical implications." *Canadian Geotechnical Journal*, in press.
- Seed, H. B., Idriss, I. M., and Arango, I. (1983). "Evaluation of liquefaction potential using field performance data." *ASCE Journal of the Soil Mechanics and Foundations Division*, 109, GT3, 458-482.
- Sladen, J. A., D'Hollander, R. D., and Krahn, J. (1985b). "The liquefaction of sands, a collapse surface approach." *Canadian Geotechnical Journal*, 22, 564-578.
- Terzaghi, K. 1956. "Varieties of submarine slope failure." *Proc. 8th Texas Conference on Soil Mechanics and Foundation Engineering*, U. Texas, Austin, 1-41.
- Vaid, Y. P., and Chern, J. C. (1985). "Cyclic and monotonic undrained response of saturated sands." *Advances in the Art of Testing Soils Under Cyclic Conditions*, Edited by V. Khosla, ASCE, New York, N. Y., 120-147.

Chapter 2

COLLAPSE OF DRY SAND¹

INTRODUCTION

Liquefaction is an important phenomenon. Dramatic effects of earthquake triggered liquefaction failures in 1964 in Japan and Alaska marked the onset of a concentrated research effort to understand the triggering mechanisms of such events. The result of this endeavor is a fairly solid understanding of the behavior of sands under cyclic loading conditions.

Nevertheless, failures have also been observed for which no source of cyclic loading has been identified. Terzaghi (1956) describes several cases of submarine slope failures where only minor triggering mechanisms could be detected. He refers to this phenomenon of sudden liquefaction as **spontaneous liquefaction**. Such failures of natural or man made slopes, commonly called **flowslides**, are believed to be initiated by minor changes in stresses such as ground water table fluctuations or toe erosion, hence essentially by static loading. Therefore, today the term spontaneous liquefaction is often used interchangeably with the term **static liquefaction**.

Casagrande (1936) described an experiment in which a weight had been placed on the surface of a very loose saturated sand and a stick was driven into the sand adjacent to the weight. The slight disturbance produced by the penetration of the stick initiated a collapse of the essentially metastable sand structure which quickly

¹ A version of this paper has been accepted for publication. Skopek, P., Morgenstern, N. R., Robertson, P. K., and Sego, D. C. (1994). *Canadian Geotechnical Journal*.

propagated throughout the entire mass with the simultaneous generation of pore pressures. The pore pressures decreased the frictional resistance so that the weight could no longer be supported and it sank below the surface. The stick penetration essentially simulates a minor change in stresses in a metastable sand structure resulting in statically triggered liquefaction.

Further studies on liquefaction behavior of sands under static loading (e.g. Castro 1969, Castro and Poulos 1977, Poulos et al. 1985, Kramer and Seed 1988, and Alarcon-Guzman et al. 1988) concluded that for liquefaction to occur the material must be loose, i.e., contractive during shearing at large strains, and the loading path must not allow for excessive volume changes prior to the collapse. Also the material must be saturated and have a sufficiently low permeability to sustain the generated pore pressures. The ultimate steady state shear strength must be less than the in situ driving shear stress, i.e., there must be a potential for weakening and associated stress redistribution possibly leading to full scale liquefaction. The underlying assumption of these criteria is that the deformation during liquefaction is undrained. Based on this a number of evaluation methods and parameters have been developed for design against static liquefaction (Poulos et al. 1985, Casagrande 1976, Bishop 1967, and Kramer and Seed 1988).

Recently the concept of the collapse surface, which will be discussed later in this paper, has been introduced to explain the 1983 submarine flowslides at Nerlerk in the Beaufort Sea (Sladen et al. 1985a). A total of six liquefaction slides occurred during the construction of a subsea berm. These slides were apparently triggered by static loading arising from the hydraulic placement of sand. The void ratio of the sand within the berm was approximately 0.8 with a permeability in the order of 10^{-5} m/s. The initial slopes and height of the berm were in the range between 10° to 12° and 25 to 30 meters, respectively. The flowslides came to rest at very flat postfailure slopes of 1° to 2° after a runout of up to 100 meters.

Similar events were observed in coking coal stockpiles at northern Australian coal export terminals. The stockpiles were about 15 meters high and failed within 10 to 20 seconds reaching runouts of about 60 meters. A laboratory testing program at James Cook University (Eckersley 1990) investigated these events by conducting a series of 19 model tests to induce flowslides in an instrumented test tank. The stockpiles were modeled by placement of the moist coal in a tank 1 meter high, sloping at 36° , and at various average void ratios depending on the placement method used. Flowslides were then induced by slowly raising the water table in the model from behind the slope. The failure of the loose coal berms occurred in a period from 2 to 10 seconds at movement velocities of about 1 m/s and reached flat postfailure slopes of approximately 5° . Furthermore, the instrumentation supplied information on pore pressure generation in the collapse zone. Hence, it could be established that the excess pore pressures were generated after the first movements and were consequent to the collapse.

The occurrence of collapse liquefaction (collapse followed by liquefaction) phenomena in coal mine waste dumps is more enigmatic. A study of Rocky Mountain coal mine waste dumps (Golder Associates - private communication) shows that there have been a number of slope failures with long runouts up to 2.5 kilometers, typical of flowslides. The common belief prevails that there is insufficient saturation inside the waste dumps because of the natural particle segregation during dumping resulting in a free draining toe. A study by Dawson et al. (1992) shows that when somewhat finer material is deposited from the dump crest a blanket of a considerable thickness can be created and is subsequently covered by successive dumping. This finer layer inside the dump can be very loose, can retain water and its permeability can be sufficiently low to sustain pore pressures necessary for the development of liquefaction flowslides.

In all cases presented above, calculations based on limit equilibrium along a distinct failure plane yielded Factors of Safety well above unity. In the case of the

Nerlerk failures the calculated Factors of Safety were as high as 3 (Lade 1993). In the case of Rocky Mountain coal mine waste dumps the Factor of Safety was usually calculated around 1.2 (Dawson et al. 1994). Hence, the concepts embraced in the classical equilibrium approach were insufficient to properly assess the behavior of these loose materials. A Rocky Mountain waste dump failure and Eckersley's flowslide model test were analyzed by Dawson et al. (1992) using the finite element liquefaction model developed by Gu (1992) and Gu et al. (1993). The calculations demonstrated the progressive propagation of pore pressures due to weakening of the material in undrained loading during collapse and confirmed Casagrande's opinion that there is no need for the liquefaction of the entire failing body, since "*the overlying mass can slide out as if suddenly placed on roller bearings*" (Casagrande 1936).

The common factor of the above events are dramatic failures without warning and without any obvious trigger followed by long runouts at high speeds and very flat postfailure slopes suggesting significant loss of internal friction resistance. Classical equilibrium methods of geotechnical engineering consistently overestimate the Factor of Safety of these structures, because they are based on ultimate steady state friction values and pre-failure pore pressures. The catastrophic nature of these events, i.e., the collapse of the metastable material followed by very mobile flow liquefaction, makes this problem very real and its understanding is crucial to certain geotechnical designs.

Throughout this thesis some generic terms will often be used to describe certain events or conditions of sand behavior. Therefore, in this paper the term **collapse** refers to the specific response of the very loose structure which can be exhibited either as rapid contractive strains under fully drained conditions with no pore pressure generation or as vigorous pore pressure generation under undrained conditions. The term **liquefaction** or **flow liquefaction** (Robertson 1994) refers to the behavior of a saturated material immediately after the collapse when the generated pore pressures significantly decrease the effective stresses and the mass strains in a manner resembling

the flow of a thick viscous liquid. The combination of the above two terms yields the term **collapse liquefaction** to describe the behavior when the material collapse results in flow liquefaction. The term **very loose** is used in this paper to describe the metastable sand structure which can collapse at certain stress states.

COLLAPSE SURFACE AND STATE BOUNDARY

The collapse surface concept adopted to explain the Nerlerk subsea berm flowslide was first published by Sladen et al. (1985b). They observed that the peaks of the undrained effective stress path for Nerlerk sand samples at the same void ratio but at various initial stress states fell on a straight line in the $p' - q$ (mean principal stress - deviatoric stress) plane and that these stress paths eventually reached the same state, i.e., the ultimate steady state. The line joining the peaks of the stress paths to the ultimate steady state was called the **collapse line**. The same material tested at different void ratios yielded collapse lines of the same slope but ending at different ultimate steady state points. The global picture could then be obtained in $p' - q - e$ (mean principal stress - deviatoric stress - void ratio) space where the collapse lines compose the collapse surface and the ultimate steady state points compose the **ultimate steady state or critical state line**. The collapse surface can be imagined as the locus of state conditions (combination of void ratio and stress state) at which the collapse of a very loose soil structure is initiated during undrained loading. Hence, the collapse surface constitutes a triggering criterion for collapse in undrained loading.

This concept was further examined by Alarcon-Guzman et al. (1988) and Ishihara et al. (1991). They demonstrated that a **state boundary surface** can be defined in $p' - q - e$ space above which a state condition for a particular material is not admissible. The state boundary surface is positioned above the collapse surface and is an envelope composed of the post peak portions of the undrained stress paths (Fig. 2.1). Sasitharan et al. (1993) demonstrated that an attempt to cross this

boundary for a very loose saturated sand by a $q = \text{constant}$ stress path resulted in collapse and flow liquefaction. Such a stress path essentially simulates the natural condition of a rising water table investigated in Eckersley's flowslide modeling. Furthermore, Sasitharan et al. (1994) showed that when a sample was brought to a stress state on the state boundary surface during undrained strain controlled loading and the loading was changed to triaxial compression or to $p' = \text{constant}$ stress path, the state condition remained on and traveled along the same state boundary surface. These tests demonstrate that the state boundary surface controls the state condition of an soil element by forcing it to adjust and follow along the state boundary surface.

OBJECTIVE OF THE STUDY

The objective of this study is to investigate the phenomenon of collapse of very loose sand by exploring the behavior of very loose dry sand. From the work by Eckersley (1990) and Sasitharan et al. (1993) it appears that the mechanism of flow liquefaction is not controlled by drainage conditions. Both studies reported triggering of flow liquefaction during fully drained, i.e., without any excess pore pressures, $q = \text{constant}$ loading. This suggests that the liquefaction phenomenon is driven by the material response rather than by specific drainage conditions and that the generated pore pressures are the consequence and not the cause of the collapse. The absence of the pore water in a dry sand predicates fully drained conditions by definition and ensures that the response is controlled exclusively by the material properties. If the collapse is found to be a material property and shown to be related to pore pressure generation during flow liquefaction of saturated sand, a theory of liquefaction in terms of effective stresses can be later advanced.

TESTING PROGRAM

In this study samples of essentially dry Ottawa sand were subjected to triaxial $q \cong \text{constant}$ stress paths. Tests were conducted using a Wykeham Farrance loading frame modified to accommodate the application of dead load to the top of the sample. During the test, readings of axial load, cell pressure, axial deformation and sample circumference changes were recorded on a computer through a DAS16 interface board. A high speed data acquisition system (10 readings/second) was utilized, since monitoring of time development of volume changes was essential.

The novel technical challenge was the need for accurate volume change measurements. This is particularly difficult, since there is no pore fluid in the dry sample. For this purpose a special transducer for circumference change measurement was developed (Skopek and Cyre 1994). A high resistance wire, 0.063 mm diameter, 390 Ω/m was wrapped once around the sample, tensioned by a 20 g load and excited by 6V. The voltage potential difference was then measured in the wire between the two fixed points on the sample circumference. As the sample deforms the length of the wire between the two fixed points changes and this is reflected in the voltage differential signal output. The signal is amplified 50 times and recorded by the data acquisition system. This wire transducer has a resolution of 0.01 mm/division and excellent output stability. It should be noted that, due to the conductive character of the wire transducer, compressed air instead of water or oil was used as a cell pressure medium which required a little more care in cell pressure control, since the high compressibility of air hampers the control of pressure change. Sample volume was calculated after the deformed cross-section was established using the circumference change readings recorded at $\frac{1}{4}$, $\frac{1}{2}$ and $\frac{3}{4}$ of the height of the sample along with the axial deformation reading. The volume was calculated by integration of the deformed cross-section. Once the volume was calculated, the void ratio calculation was straightforward.

Ottawa sand (C109) from Ottawa, Illinois was used for this study. This sand is a uniform, medium sand composed primarily from round to subrounded quartz grains with a specific gravity of 2.67, mean grain size $D_{50} = 0.34$ mm, $e_{min} = 0.5$, $e_{max} = 0.82$ according to ASTM D2049. Samples were prepared in the laboratory using the moist tamping method with about 2.5% moisture. The samples were 64 mm in diameter and about 118 mm high. Prepared void ratios ranged between 0.75 - 0.85.

Only samples prepared by the moist tamping preparation technique were sufficiently loose for the purposes of the study. Dry pluviation produced samples too dense to exhibit collapse. It is believed that the low moisture content of about 2.5% did not affect the test results and the estimated suction in the samples of less than 5 kPa was much smaller than the applied stress levels during the test.

The tests were conducted in three stages. The samples in the triaxial cell were first subjected to an all round pressure and then the deviatoric load was applied in steps up to the desired magnitude. The third stage of the test was conducted at approximately $q = \text{constant}$ conditions. The cell pressure was slowly decreased manually at an overall average rate of 1 kPa/min. The resulting stress path is only approximately $q = \text{constant}$, since the magnitude of vertically transmitted load is affected by the decreasing cell pressure due to the fixed connection between the top cap and the loading ram. Thus, q is slowly increased as the cell pressure decreases.

TEST RESULTS

Only three tests from the total of sixteen tests are presented in detail in this chapter and their characteristics are summarized in Table 2.1.

Typical sand behavior during tests

The typical course of a test is shown in Figures 2.2 and 2.3.

1. In the first stage (Fig. 2.3, from a to b) the isotropic loading of the sample produced only minor axial deformation (less than 0.3%) and negligible lateral deformation. The associated void ratio change was a contraction of about -0.01. This stage usually lasted for about 10 to 20 minutes before all changes had stabilized.
2. During the second stage (Fig. 2.3, stretch from b to c) the application of the deviatoric stress, i.e., dead load, produced only a small effect on the lateral deformation of the sample. Axial deformations of about 0.5% were recorded. The void ratio changes resulted in a contraction of less than -0.02. The dead load was applied in steps for approximately 5-10 minutes each to completion of the volume changes.
3. In the following third stage (Fig. 2.3, from c to d) a gradual cell pressure decrease produced almost negligible volume changes and the sand behaved as an essentially elastic material. This behavior continued up to a certain distinct stress level when the material started to contract and both the axial and lateral strains increased slightly. This is shown in $p' - e$ plane as a deflection in the direction of the stress path (Fig. 2.3, point d). Shortly after, a new compressibility $\Delta e / \Delta p'$ was established. At this stage more pronounced time dependent deformation could be observed after each incremental cell pressure change but all movements stabilized within several minutes.
4. Further decreases in the confining pressure resulted in discrete contractive response during which the axial strain 'jumped' by about 2% with an associated void ratio contraction of -0.05. These discrete jumps accelerated in terms of seconds (20s) and decelerated over a minute (Fig. 2.4). Usually 2 or 3 contractive "jumps" could be recorded during each test.

EXPLANATION OF OBSERVED PHENOMENON

All tests have shown that very loose essentially dry Ottawa sand when subjected to triaxial $q \cong \text{constant}$ stress path first behaves essentially elastically, then at a certain point the deformation response abruptly changes. The material contracts and exhibits a significant increase in compressibility. Thus the initial direction of a stress path in the $p' - e$ plane is notably deflected. After this short transition period a new and significantly higher compressibility is observed (Fig. 2.3). As the sample is further loaded two different straining patterns can be detected. The first pattern is associated with moderate slips at grain contacts which have both a stress dependent and time dependent component (Fig. 2.2). This response will be referred to as **structural contraction**. The second straining pattern is characterized by rapid contractive strains of primarily time dependent (constant stress) nature (Fig. 2.2 and Fig. 2.4). These strains accelerate rapidly within 10 to 20 seconds and then slowly decelerate over a minute. It is believed that this second straining pattern is peculiar to the collapse of very loose saturated sand and it will be further referred to as the **structural collapse**.

The structural collapse of very loose dry sand is a result of progressive destabilization of the grain structure. This process of structural destabilization commences as small strains/slips at grain contacts. The grains try to reorient to accommodate the developing instability. This accounts for the first straining pattern. Later the ability of the material to compensate is insufficient and the entire structure collapses and contracts. The contractive strains densify (harden) the dry sand which results in self-stabilization of the collapse and all movements eventually cease. The new state condition of the material is still far from the ultimate steady state condition and so the process can repeat itself under further loading. The densification (hardening) of saturated sand during a structural collapse is inhibited by the pore water and so pore pressures are generated. The generation of pore pressures leads to

material weakening and progressive propagation of collapse, which may result in full scale flow liquefaction.

The mobilized friction angles at the points of observed structural collapse range from 20.4° to 30.1° which is below the ultimate steady state mobilized friction angle (Figure 2.5, Table. 2.1). This observation is consistent with the observations made for collapse of a very loose saturated sand and supports the fact that geotechnical design cannot always rely on the ultimate steady state mobilized friction angle as a guarantee of safety. The undrained collapse leading to flow liquefaction of a saturated sand, which appears to be equivalent to the structural collapse of a very loose dry sand, can occur at mobilized friction angles much below the ultimate steady state mobilized friction angle.

The relationship between the mobilized friction angle ϕ'_m and the vertical displacement dH during presented $q \cong \text{constant}$ tests is shown in Fig. 2.6. This diagram shows that the behavior of the sand is consistent with the behavior of the same sand tested by Sasitharan et al. (1994) and also that the tests are mutually consistent. The mobilized friction angle approaches the ultimate steady state value of about 30° which is expected for Ottawa sand.

CONCLUSIONS

The deflection of the original direction of the stress paths in $p' - q - e$ space is shown as an increased compressibility. This breakpoint in material response and onset of structural contraction resulting in establishment of a new path direction in the $p' - e$ plane is believed to be conceptually similar to the behavior of a very loose saturated sand attaining the state boundary surface. Figure 2.3 and Table 2.1 show that the mobilized friction angles at the observed breakpoints are significantly smaller than the ultimate steady state friction angle for Ottawa sand.

The contractive character of very loose dry Ottawa sand collapse is conceptually consistent with the behavior of very loose saturated sand. In very loose saturated sand the structural collapse of the sand matrix is exhibited by pore pressure generation and, if the pore pressures cannot dissipate sufficiently rapidly, a consequent decrease in effective stress and significant loss of shear strength can occur. This can result in flow liquefaction. In the dry sand there is no incompressible pore medium, therefore the collapse reflects itself in contractive volume change. The collapse is confined by self stabilization due to hardening as a result of densification.

The pore pressure generation in very loose saturated sand has already been shown to be a consequence and not a cause of collapse (Eckersley 1990, Sasitharan et al. 1993). This observation is supported in this study by means of structural collapse of dry sand, which did not have any triggering pore pressure levels available but collapse still occurred.

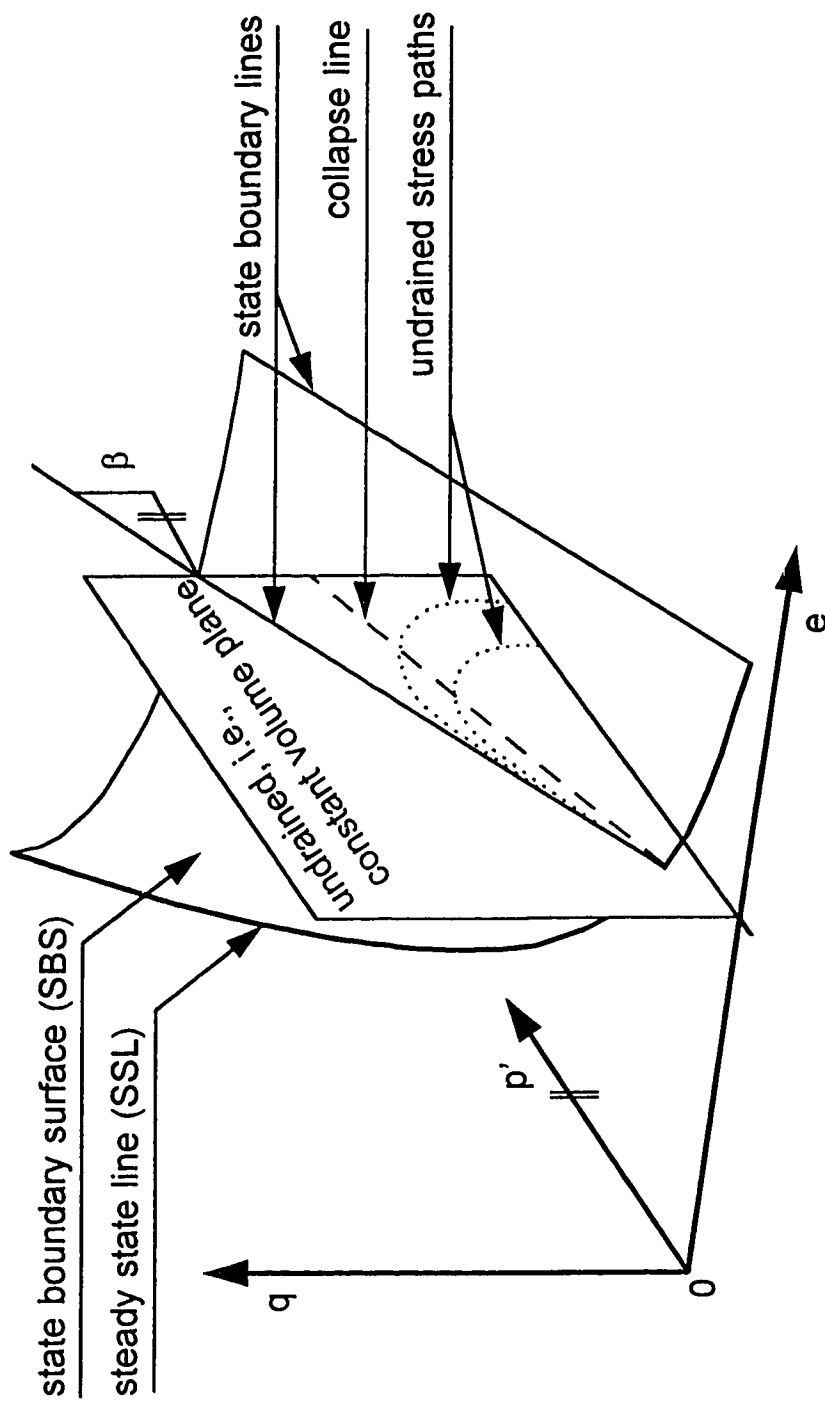
Conclusions of the presented study can be summarized as follows:

1. Very loose essentially dry Ottawa sand during $q \cong \text{constant}$ loading attains a discrete state condition where the loading path in $p' - q - e$ space is deflected and a new significantly higher compressibility associated with structural contraction is established. This change occurs at a mobilized friction angle considerably smaller than the ultimate steady state mobilized friction angle (Fig. 2.3) and agrees with the state boundary surface concept established for saturated sand.
2. Further loading of the element renders the structure increasingly unstable, which eventually results in discrete contractive time dependent “jumps”, which have been referred to as structural collapses. It is our opinion that these structural collapses are responsible for the pore pressure generation during the collapse of very loose saturated sand which results in flow liquefaction. The

structural collapses occur at mobilized frictional angles significantly smaller than the ultimate steady state mobilized friction angle.

Test identification	#8	#9	#12
<u>Initial parameters</u>			
void ratio e	0.825	0.833	0.813
moisture content (%)	2.73	2.54	2.51
p' / q (kPa)	300 / 98	240 / 77	246 / 130
<u>Onset of structural contraction</u>			
p' / q (kPa)	182 / 108	123 / 81	191 / 131
ϕ'_m (°)	15.7	17.3	17.9
Characteristics of structural collapse	$\sigma_3 / e / \phi'_m$	$\sigma_3 / e / \phi'_m$	$\sigma_3 / e / \phi'_m$
1 st	70 / 0.780 / 24.6	77 / 0.810 / 20.4	75 / 0.762 / 27.0
2 nd	64 / 0.768 / 26.5	54 / 0.786 / 26.2	68 / 0.754 / 27.9
3 rd	(units are kPa and degrees)	49 / 0.783 / 27.2	58 / 0.744 / 30.1

Table 2.1 Summary of test initial parameters, parameters at the onset of structural contraction and characteristics of structural collapses



Note: collapse line is BELOW the state boundary line in the shown undrained plane; collapse surface pertaining to this collapse line is NOT shown on this figure

Fig. 2.1 Definition of the elements of state boundary surface

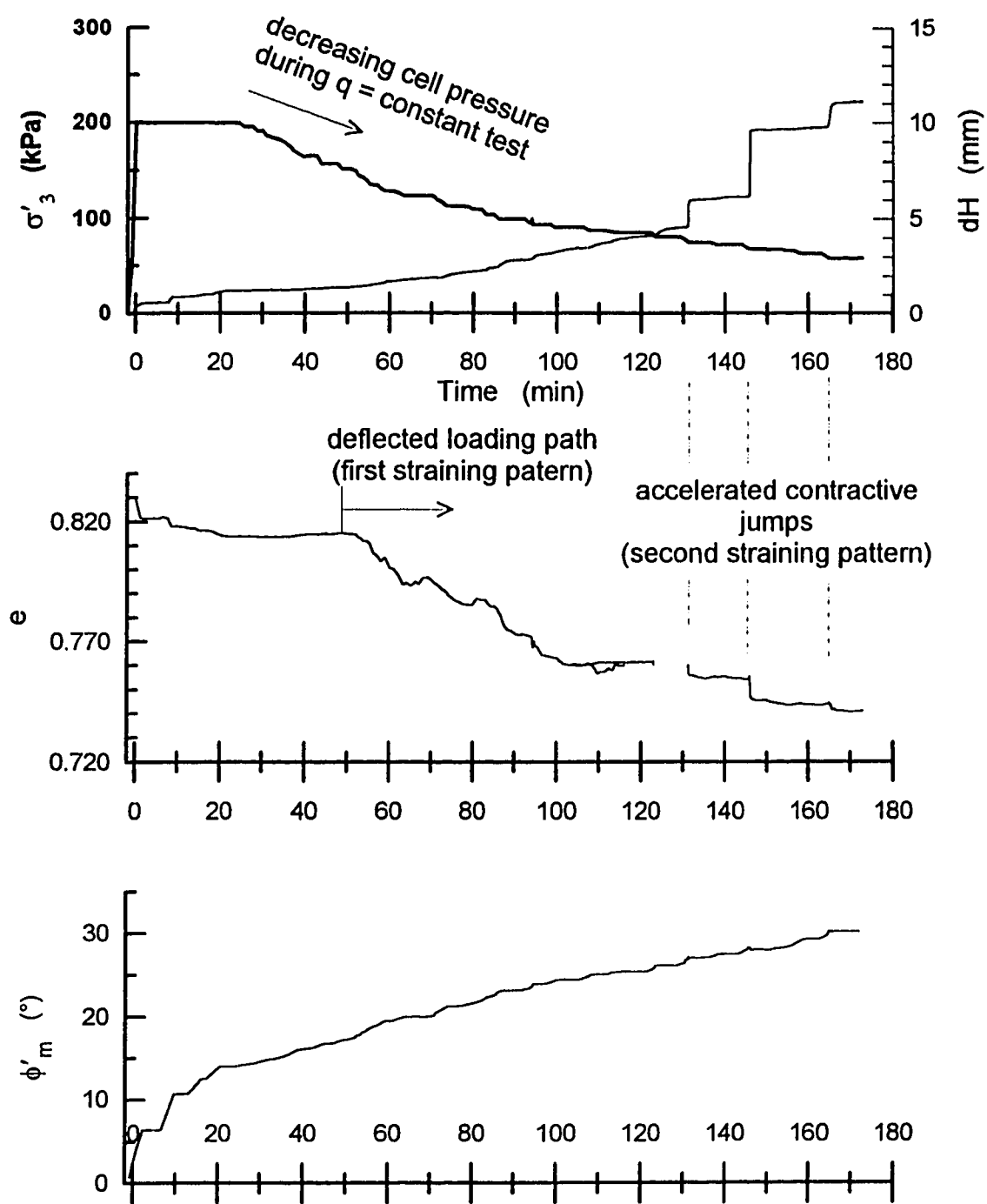


Fig. 2.2 Typical strain development during the $q = \text{constant}$ test (test #12)

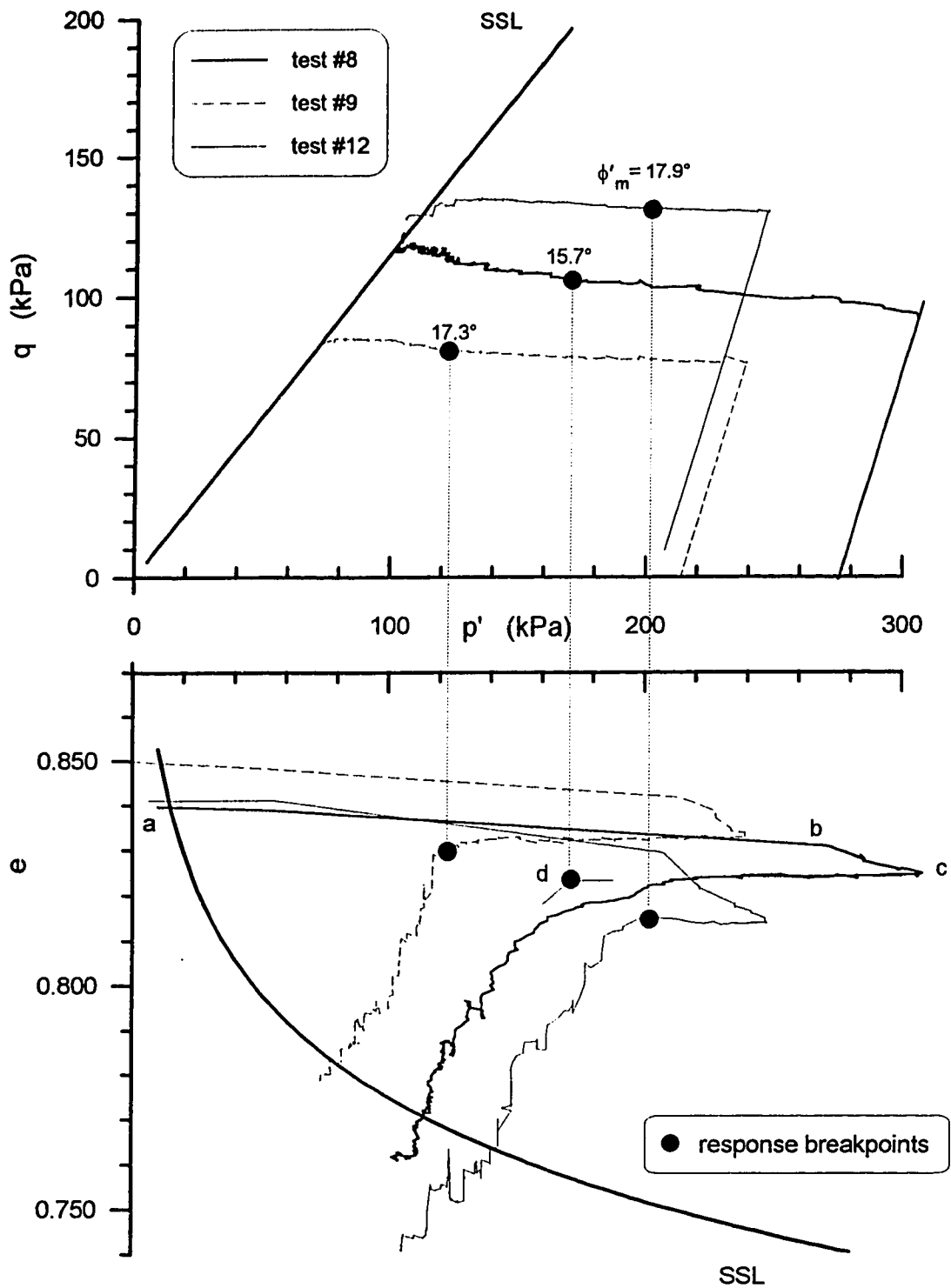


Fig. 2.3 Stress paths and contraction during the $q = \text{constant}$ tests

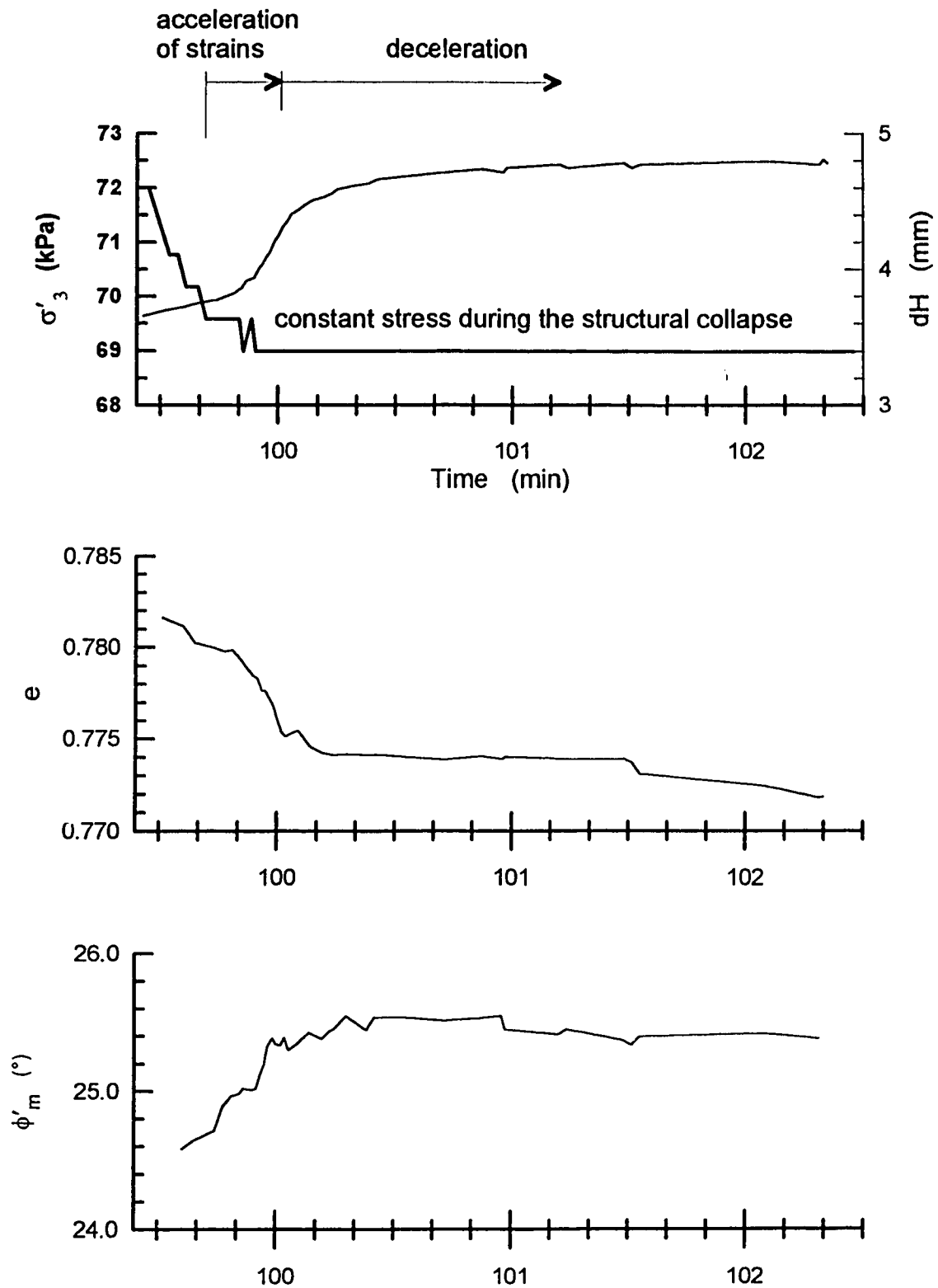


Fig. 2.4 Typical strain development during structural collapse (test #8, 1st jump)

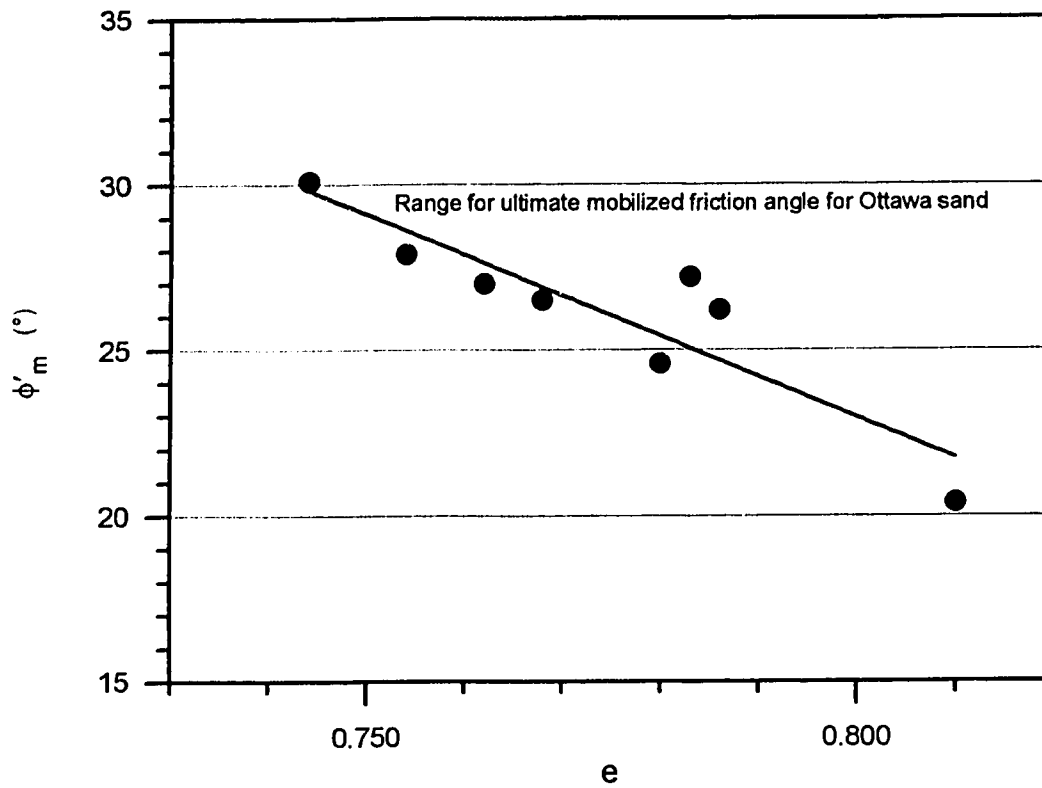


Fig. 2.5 Mobilized friction angle at points of observed structural collapse for all $q = \text{constant}$ tests on very loose dry Ottawa sand (tests #8, #9, #12)

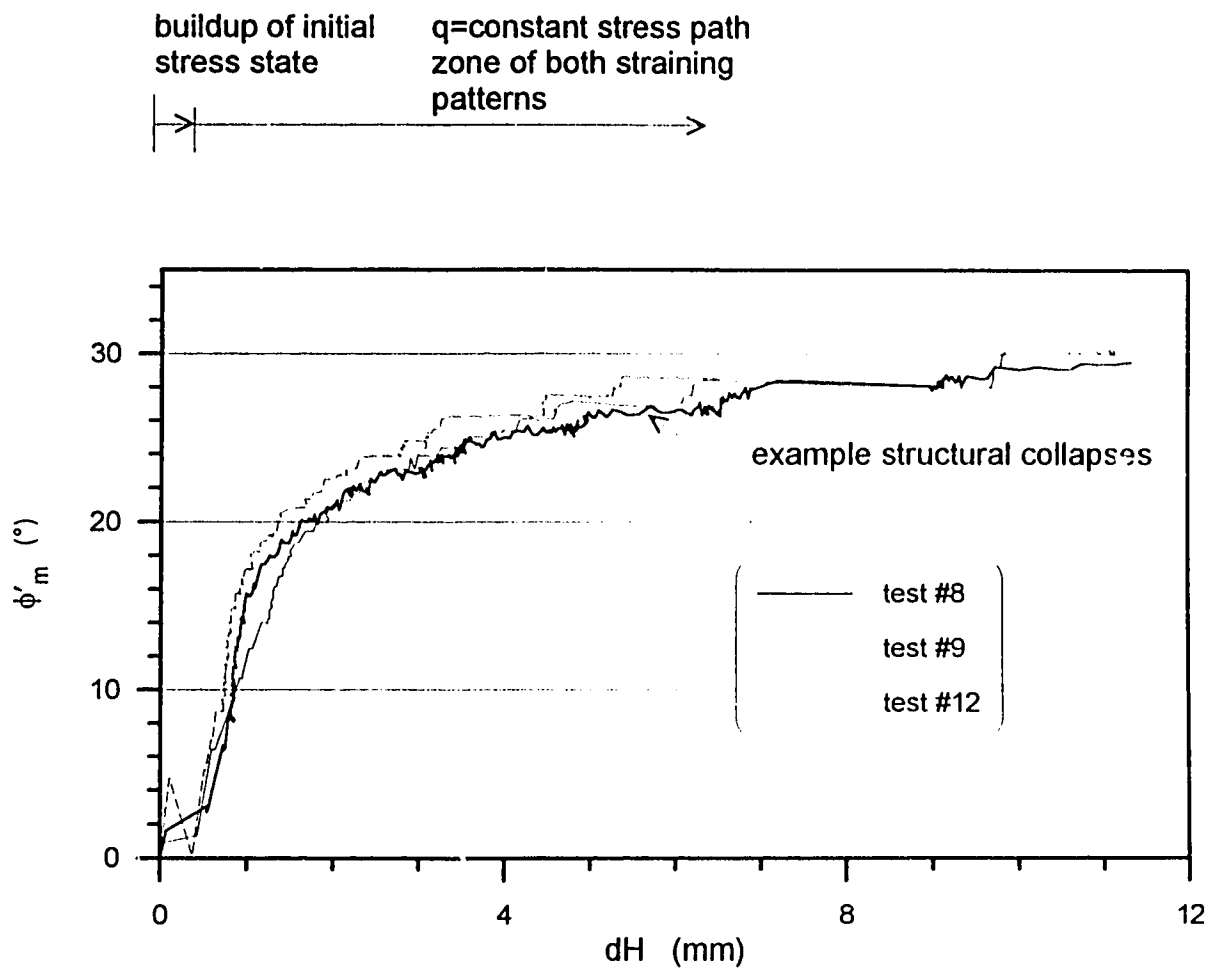


Fig. 2.6 Mobilized friction angle during $q = \text{constant}$ tests on very loose dry Ottawa sand

REFERENCES

- Alarcon-Guzman, A., Leonards, G. A., and Chameau, J. L. (1988). "Undrained monotonic and cyclic strength of sands." *ASCE Journal of the Geotechnical Engineering Division*, 114(No.10), pp. 1089-1109.
- Bishop, A. W. (1967). "Progressive failure - with special reference to the mechanism causing it. Panel discussion." *Proceedings of the Geotechnical Conference*, Oslo, Norway. Vol.2. pp. 142-150.
- Casagrande, A. (1936). "Characteristics of cohesionless soils affecting the stability of earth fills." *Journal of the Boston Society of Civil Engineers*, Vol. 23, No. 1, January, pp. 257-276.
- Casagrande, A. (1976). "Liquefaction and cyclic deformation of sands, a critical review." *Harvard Soil Mechanics Series*, No. 88, Harvard University, Cambridge, MA
- Castro, G. (1969). "Liquefaction of sands." *Harvard Soil Mechanics Series*, No. 81, Harvard University, Cambridge, MA.
- Castro, G., and Poulos, S. J. (1977). "Factors affecting liquefaction and cyclic mobility." *ASCE Journal of the Geotechnical Engineering Division*, 103(GT6), pp. 501-516.
- Dawson, R. F., Morgenstern, N. R., and Gu, W. H. (1992). "Instability mechanisms initiating flow failures in mountainous mine waste dumps - Phase I." *Study for Energy, Mines and Resources Canada*, DSS contract #23440-0-9198/01-X8G.
- Dawson, R. F., Morgenstern, N. R., and Gu, W. H. (1994). "Liquefaction flowslides in Western Canadian coal mine waste dumps - Phase II: case histories." *Study for*

Energy, Mines and Resources Canada, SSC file # XSG42-00138 (608), SSC contract 23440-2-9151/01-XSG.

Eckersley, J. (1990). "Instrumented laboratory flowslides." *Géotechnique*, 40(3), pp. 489-502.

Evans, M. D., Seed, H. B., and Seed, R. B. (1992). "Membrane compliance and liquefaction of sluiced gravel specimens." *ASCE Journal of the Geotechnical Engineering Division*, 118(No.6), pp. 856-867.

Gu, W. H., Morgenstern, N. R., and Robertson, P.K. (1993). "Progressive failure of The Lower San Fernando Dam." *ASCE Journal of the Geotechnical Engineering Division*, 119(No.2), pp. 333-348.

Gu, W. H. (1992). "Liquefaction and post earthquake deformation analysis." PhD thesis, University of Alberta, Alberta, Canada.

Ishihara, K., Verdugo, R. and Acacio, A. A. (1991). "Characterization of cyclic behavior of sand and post-seismic stability analysis." *9th Asian Regional Conference on Soil Mechanics and Foundation engineering*, Bangkok, Thailand. Vol.2. pp. 17-40.

Kramer, S. L., and Seed, H. B. (1988). "Initiation of soil liquefaction under static loading conditions." *ASCE Journal of the Geotechnical Engineering Division*, 114(No.4), pp. 412-430.

Lade, P. V. (1993). "Initiation of static instability in the submarine Nerlerk berm." *Canadian Geotechnical Journal*, 30(6), pp. 895-904.

Poulos, S. J., Castro, G., and France, J. W. (1985). "Liquefaction evaluation procedure." *ASCE Journal of the Geotechnical Engineering Division*, 111(No.6), pp. 772-792.

- Robertson, P. K. (1994). "Terminology for soil liquefaction." *Proc. 47th Canadian Geotechnical Conference*, Halifax, in press.
- Sasitharan, S., Robertson, P. K., Sego, D. C. and Morgenstern, N. R. (1993). "Collapse behavior of sand." *Canadian Geotechnical Journal*, 30(4), pp. 569-577.
- Sasitharan, S., Robertson, P. K., Sego, D. C. and Morgenstern, N. R. (1994). "A state boundary surface for very loose sand and its practical implications." *Canadian Geotechnical Journal*, in press.
- Skopek, P., and Cyre, G. (1994). "A resistance wire transducer for circumferential strain measurement in triaxial test." *Geotechnical Testing Journal*, in press.
- Sladen, J. A., D'Hollander, R. D., and Krahn, J. (1985a). "Back analysis of the Nerlerk berm liquefaction slides." *Canadian Geotechnical Journal*, 22, pp. 579-588.
- Sladen, J. A., D'Hollander, R. D., and Krahn, J. (1985b). "The liquefaction of sands, a collapse surface approach." *Canadian Geotechnical Journal*, 22, pp. 564-578.
- Terzaghi, K. (1956). "Varieties of submarine slope failure." *Proc. 8th Texas Conference on Soil Mechanics and Foundation Engineering*, U. Texas, Austin, 1-41.

STATE BOUNDARY SURFACE FOR VERY LOOSE SAND¹

INTRODUCTION

Loose cohesionless materials have been responsible for a number of serious or catastrophic liquefaction failures. Dramatic effects of earthquake triggered **flowslides** in Japan and Alaska in 1964 initiated a concentrated research effort to understand the mechanism of these events. The result of this endeavor is an improved understanding of the behavior of sands during cyclic loading. Nevertheless failures have also been observed for which no considerable source of cyclic loading has been detected. Terzaghi (1956) describes several cases of submarine flowslides where no external trigger could be identified. He refers to this phenomenon of sudden liquefaction without a presence of cyclic shear stresses as **spontaneous liquefaction**. Such failures of natural or man-made slopes are believed to be instigated by minor stress changes such as ground water table fluctuations or toe erosion, hence essentially by static loading.

Casagrande (1936) reported an elegant experiment to demonstrate this spontaneous (also called static) liquefaction. A tank was filled with sand in a loose, saturated state and a weight was placed on the surface. Then a stick was thrust into the sand adjacent to the weight. The slight disturbance produced by the penetration of

¹ A version of this paper has been submitted for publication. Skopek, P., Morgenstern, N. P., and Robertson, P. K. (1994). *Journal of the Geotechnical Engineering Division ASCE*.

the stick created local pore pressures which triggered collapse of the essentially metastable loose sand structure. Pore pressures quickly propagated throughout the entire soil mass resulting in significant loss of bearing capacity and the weight sank below the sand surface. The stick penetration simulated minor stress change which was by no means cyclic.

Cases have been recorded where structures have failed and reached long runouts over a short period of time even though the slopes were built at or even less than the angle of repose (Sladen et al. 1985a; Dawson et al. 1992). Hence conventional limit equilibrium methods of analysis have been incapable of accounting for these failures. This led to a need for a better understanding of the triggering mechanism of statically induced liquefaction events. Studies by Castro (1969), Castro and Poulos (1977), Poulos et al. (1985), Kramer and Seed (1988), Alarcon-Guzman et al. (1988), and many others concluded that for liquefaction to occur the material must be loose, i.e., contractive at the onset of liquefaction, saturated, and have sufficiently low permeability to sustain generated pore pressures. The ultimate steady state shear strength must be less than the in situ driving shear stress, i.e., there must be a potential for material weakening and associated stress redistribution leading to progressive propagation of liquefaction. Robertson (1993) has suggested the term **flow liquefaction** to describe the above phenomenon.

Sladen et al. (1985b) introduced the **collapse surface** concept which explained submarine flowslides at Nerlerk in the Beaufort Sea. In this instance conventional limit equilibrium analysis yielded Factors of Safety as high as 3 (Lade 1993). The collapse surface concept, based on critical state soil mechanics, defines a locus of state conditions in $p' - q - e$ (mean principle stress - deviatoric stress - void ratio) space at which weakening is initiated during undrained loading. The locus was shown to be composed of collapse lines. The **collapse line** was defined as a line in the $p' - q$ plane joining the peaks of the undrained stress paths at the same void ratio, therefore ending

at the same ultimate state. The same material tested at different void ratios yielded collapse lines of the same slope but ending at different ultimate state points along the ultimate steady state line. The complete picture could then be obtained in $p' - q - e$ space where the collapse lines compose the warped **collapse surface** and the ultimate steady state points compose the **ultimate steady state** or **critical void ratio line** (Fig. 3.1). Thus the collapse surface was defined as a concept peculiar to undrained loading of very loose saturated sands.

Sasitharan et al. (1993) showed that undrained loading is not a prerequisite for collapse to occur. They demonstrated experimentally that a very loose saturated sand can collapse and liquefy under fully drained conditions with no excess pore pressure during a $q = \text{constant}$ stress path at the moment when the loading path tries to cross a surface which is an envelope to the post peak portions of the undrained stress paths. Work by Alarcon-Guzman et al. (1988) and Ishihara et al. (1991) showed that for some materials the post peak portion of undrained stress paths may be curved, rising significantly above the collapse surface. Sasitharan et al. (1994) also showed that for any stress path the state condition would never exist above the enveloping surface and that it would stay on the surface even when the loading direction is changed. Hence such a surface complies with criteria set forth for a state boundary surface as defined in Roscoe et al. (1958).

It is believed that the state boundary surface for very loose dry sand can provide a fundamental insight in the mechanism of **collapse liquefaction**, i.e. collapse generating sufficient pore pressures to develop flow liquefaction. The objective of this study is to investigate the state boundary surface for very loose dry sand and to formulate the parameters for its mathematical form.

STATE BOUNDARY SURFACE

Roscoe et al. (1958) showed that there is a surface defined in $\sigma' - \tau - e$ space for remolded clays above which a state condition of a soil element is not admissible:

“Experimental evidence suggests that in each type of test the loading paths have a surface as their envelope in $\sigma' - \tau - e$ space, and as yield continues, the loading paths continue to lie on that surface.”

All stress paths terminate on the critical void ratio line characterizing the critical state. Stress path for normally consolidated clays originate on the virgin consolidation line, follow the above surface and end on the critical void ratio line. This implies that such a **yield surface**, also called the Roscoe surface, originates from the virgin consolidation line. Loading paths for overconsolidated clays first exist in the essentially elastic domain below the yield surface but eventually reach this surface and under further loading follow it to critical state (Schofield and Wroth 1968). Hence this yield surface was shown also to be a **state boundary surface**, i.e. a boundary above which a state condition for a given material is not admissible. The concept provided a means of predicting soil behavior based on its initial void ratio and stress state.

Initially the practical application of critical state soil mechanics and the state boundary surface to granular materials (Wroth and Basset 1965 and others) was somewhat limited due to the fact that there seemed to be no unique virgin consolidation line for most engineering stress ranges, which was required to define one side of the surface. Moreover, apart from liquefaction, sands were not considered to be a geotechnically difficult material and the rather complex critical state mechanics could be substituted with simple conventional methodologies.

MECHANISM OF COLLAPSE

For investigating the mechanism of collapse the $q = \text{constant}$ loading path was selected. The $q = \text{constant}$ test simulates a stress path which was believed to be responsible for the occurrence of flowslides in coking coal stockpiles at northern Australian coal export terminals (Eckersley 1990). The triggering mechanism was shown to be a very slow rise of the water table. This stress path is also considered as a possible triggering mechanism of coal mine waste dump flowslides in the Rocky Mountains (Dawson 1994).

The $q = \text{constant}$ loading path has another fundamental significance. Since the collapse is triggered under essentially drained loading with no excess pore pressures, consequent liquefaction cannot be explained as a result of undrained drainage conditions. Therefore, it must be some material property which generates the pore pressures and triggers flow liquefaction. Skopek et al. (1994) investigated this fundamental mechanics by examining the response of very loose dry sand. When testing a dry sand any pore pressure generation is excluded by definition and the response of a sand is controlled purely by the properties of the sand and sand structure. The $q = \text{constant}$ test on very loose saturated sand results in dramatic generation of pore pressures and is followed by significant loss of shear resistance and flow liquefaction. The $q = \text{constant}$ test on very loose dry sand results in significantly increased compressibility as well as in a distinct accelerated contractive volume changes. Hence, the pronounced volume change of very loose dry sand is believed to be an equivalent response of the same mechanism which generates pore pressures in very loose saturated sand.

COLLAPSE CRITERION

The state boundary surface provides a powerful concept which enables prediction of the constitutive behavior of an element of soil during any kind of loading.

The existence of the state boundary surface was successfully proven for very loose saturated sand (Sasitharan et al. 1994). It allowed formulation of a **triggering criterion** for weakening during certain loading paths. Evidence of increased compressibility and structural collapse given by Skopek et al. (1994) provides some insight into the fundamental mechanism of pore pressure generation during the initiation of collapse liquefaction. The formulation of a **collapse criterion** which would quantify the extent and the intensity of collapse can be attempted by investigating the rate of volume change of very loose dry sand and linking it to pore pressure generation in an identical saturated sand. In order to formulate such a criterion a concept which would enable prediction of the loading path after collapse is initiated is needed. The existence of a state boundary surface for very loose dry sand could fulfill this role.

TESTING PROGRAM

In this study samples of essentially dry Ottawa sand were subjected to several different triaxial stress paths while the three governing parameters p' , q , and e were closely monitored. The detailed testing procedure is described by Skopek et al. (1994).

The solution to the problem of monitoring abrupt and extensive volume changes in a dry material by special girth transducers is described by Skopek and Cyre (1994).

Samples were subjected to four different stress paths. One was a series of $q \cong \text{constant}$ stress paths which were previously shown to be “collapsible” for very loose saturated Ottawa sand (Sasitharan et al. 1993). This pilot series was complemented with a conventional triaxial strain controlled compression test, strain

and load controlled $p = \text{constant}$ stress path, and a special stress path, which was essentially $q \cong \text{constant}$ stress path with limited straining, when the deviatoric stress was released slightly upon developing strains. In addition two $q \cong \text{constant}$ tests were conducted on samples with the initial state on the dilatant (i.e. dense) side to investigate the behavior of dense sand within the framework of state boundary surface concept.

Ottawa sand (C109) from Ottawa, Illinois was used for this study. This sand is a uniform, medium sand composed primarily from round to subrounded quartz grains with a specific gravity of 2.67, mean grain size 0.34 mm, $e_{\min} = 0.5$, $e_{\max} = 0.82$ according to ASTM D2049. Samples were prepared in the laboratory using the moist tamping method with 2.5% moisture. The samples were 64 mm in diameter and about 118 mm high. Prepared void ratios ranged between 0.75 to 0.85. It is believed that the very low moisture content of about 2.5% did not affect the test results. The estimated suction in the samples was less than 10 kPa which was much smaller than the stress levels applied during the test.

INTERPRETATION OF TEST RESULTS

Only five tests from the total of sixteen tests on loose sand are presented in detail in this paper. These are two $q \cong \text{constant}$ tests at two extreme void ratios (Fig. 3.2), i.e. very loose and loose, a conventional strain controlled compression test (Fig. 3.3), a load controlled $p = \text{constant}$ test (Fig. 3.4), and a special stress path test (Fig. 3.5). The characteristics of each test are compiled in Table 3.1. For the mathematical formulation of the state boundary surface loading paths from all sixteen tests were used. All tests were plotted in $p' - q - e$ space and a surface containing the final portions of these stress paths was defined. The variety of different stress paths ensured that the formulation of the state boundary surface would not be biased by response peculiar to a specific family of loading paths.

Mathematical formulation of the state boundary surface in $p' - q - e$ space was based on the equation of a warped surface derived by Sasitharan et al. (1994):

$$q = \beta * p' + (M - \beta) * \exp\left(\frac{e - \Gamma}{-\lambda}\right), \text{ or after rearrangement}$$

$$e = \Gamma - \lambda * \ln\left(\frac{q - \beta * p'}{M - \beta}\right),$$

where: p' , q , and e are mean principle stress, deviatoric stress and void ratio respectively on the state boundary surface, M is the slope of the ultimate steady state line in the $p' - q$ plane, Γ and λ are the parameters defining the ultimate steady state line in $\ln(p')$ - e plane, and β is the approximate slope of the envelope to all undrained stress paths at the same void ratio, i.e., slope of the state boundary line in the $p' - q$ plane, i.e., constant volume plane (Fig. 3.1).

For this equation p' , q , and e were given by the measured loading path during a test, M , Γ and λ are constants based on the shape and location of the ultimate steady state line for a given material. The only missing parameter is the slope of the collapse line β . The triaxial testing of dry sand in this study did not have the benefit of containing the loading path within a constant volume, i.e. undrained, plane, and β is difficult to obtain. Therefore, β was used as a surface fitting parameter and varied in an attempt to obtain good agreement between the measured and expected loading paths. The comparison between the measured and expected loading path was accomplished by calculating the expected value for one of the three controlling parameters (p' , q or e) based on the other two measured parameters. For example, for a $q \cong \text{constant}$ tests, shown in Fig. 3.2 the expected void ratio (e) on the state boundary surface in the $p' - e$ plane (solid line) associated with the measured values of p' and q was compared with the actual measured void ratio (dots). There were three requirements for the surface fit to be considered successful:

1. Deflection of the loading path from its initial direction occurs in close vicinity of the state boundary surface (Fig. 3.2, point a).
2. The loading path after the deflection point follows closely the calculated state boundary surface (Fig. 3.2, zone b).
3. Both of the above requirements need to be satisfied with the same β for all tested stress paths.

The parameters for the state boundary surface were found to be as follows:

$$M = 1.154 \quad \Gamma = 0.9303 \quad \lambda = 0.0337 \quad \beta = 0.6$$

This state boundary surface for very loose dry sand compares reasonably well with the state boundary surface found for very loose saturated sand (Sasitharan et al. 1994). It is considered plausible that the exact parameters controlling the position and shape can vary for a saturated and dry sand. Further study on the relationship between the dry and saturated state boundary surface has to be undertaken.

The agreement between the measured and expected loading paths (Fig. 3.2 to Fig. 3.5 and Appendix B) is remarkably consistent over the whole range of tested stress paths. This consistency is compelling evidence of the existence of the state boundary surface for very loose dry sand. The fact that neither of the tested loading paths is allowed to cross this surface and rise significantly above it confirms that this surface is a state boundary.

It is evidenced in the figures that the state boundary surface dramatically affects the behavior of a sand and acts as an impenetrable wall for the loading paths. Since in any test there can be full control only over two of the three governing parameters p' , q , and e , the remaining parameter is forced to vary to keep the state condition on the state boundary surface. In undrained loading the void ratio remains constant, but in all other loading paths the void ratio is free to change. For all triaxial loading paths in this study the sample initially behaved essentially elastically with modest volume

change. This changed dramatically as the loading path approached the state boundary surface. The gross compressibility of the sample was greatly increased to adjust the direction of the loading path to follow along the state boundary surface. This phenomenon is shown schematically for a $q \cong \text{constant}$ stress path in Fig. 3.6.

This increased compressibility is a result of changed structural response on the state boundary surface and has been given the term **structural contraction** (Skopek et al. 1994). Structural contraction is initiated by a stress ratio increase, hence it is stress dependent. However, there is also a stress independent (creep) character which brings the state condition from an intrinsically unstable state on the state boundary surface into the stable essentially elastic domain below. Besides the slow structural contraction the sample can also undergo accelerated contractive strains which almost instantaneously bring the state condition below the state boundary surface. The dramatic “collapse” nature of these strains justifies the name **structural collapse**. The associated drop from the state boundary surface into the elastic domain temporarily stabilizes the structure due to densification. Consequently the response of the sample to further loading is again initially elastic and then at the approach to the state boundary the process of contraction repeats.

To aid in the presentation of results from this study, data for the tests #9, #14, and #spec have been shown in a normalized stress space of q/p'_{ss} versus p'/p'_{ss} (Fig. 3.7). This normalization was carried out with respect to the effective mean principal stress at the ultimate steady state (p'_{ss}) for the current void ratio. This normalized stress space allows results at different void ratio to be shown in one plane. Figure 3.7 shows a summary of the test results from this study in terms of the initial states of each test and the state at which a sudden change in void ratio (i.e. onset of contraction) was observed. Figure 3.7 clearly shows that for all the tests the onset of contraction occurs on a normalized state boundary surface passing through the

ultimate steady state point. The results of the remaining thirteen tests also plot on the normalized state boundary surface.

The additional two $q \equiv \text{constant}$ tests on dense dry sand were expected to behave essentially elastically until the state condition attained an equivalent of the Hvorslev's surface and then were expected to dilate to reach their ultimate steady state. However, both sand samples exhibited a small but distinct contraction during the test before they started to dilate. The amount of contraction was significantly smaller than that for the loose samples. It was found convenient for comparison of tests to plot this data in the normalized stress space along with the results of tests on very loose samples (Fig. 3.7). If the onset of the small contraction of the dense sand is plotted in this plot, it appears that they compose a line passing through the origin. Such a line seems to assume the same property as the instability line (Lade 1993) or the critical stress ratio line (Vaid and Chern 1985). This line is associated with temporary weakening of a saturated material under undrained conditions resulting in the so called quasi steady state (Ishihara 1993). The existence of this line for a dry sand would enable a fundamental insight into the mechanism of quasi steady state behavior. However, it is important to note that the amount of volumetric strain for dense sand samples was significantly smaller than that observed for the loose samples. If drainage were not restricted this small amount of contraction may not result in undrained behavior for the dense sand in situ.

PRACTICAL IMPLICATIONS OF OBSERVED PHENOMENA

For very loose saturated sand collapse liquefaction can be encountered on the state boundary surface during $q = \text{constant}$ loading. For very loose dry sand the collapse during the same loading path results in a structural contraction and structural collapses on the state boundary surface. Hence, it appears that these phenomena are only different responses to the same mechanism. Therefore, the intensity of structural

contraction/collapse of very loose dry sand can be indicative of the intensity of the pore pressure generation in very loose saturated sand. Of course, the consequences of such pore pressure generation in very loose saturated sand vary with the ability of the sand to sustain or dissipate the pore pressures. This ability is controlled by the permeability and compressibility of the sand, and the length of the drainage path in the particular soil formation.

For a body of very loose saturated sand to completely (or sufficiently) liquefy a sufficient pore pressure generation is required. The pore pressure generation is controlled by the propagation of structural contraction/collapse through the very loose granular structure. If no pore pressures are dissipated, the state condition follows the constant volume stress path along the state boundary, hence the element loses shear resistance, i.e., weakens and moves directly towards its ultimate steady state. The weakening of the element causes the adjacent elements to carry the excessive load, which can generate additional pore pressures due to structural contraction/collapse. Hence, the progressive propagation of collapse leading to full scale flow liquefaction failure can be established. This progressive propagation can be modeled numerically as shown by Gu et al. (1993).

In the case of drainage permitting the pore pressures to partially or fully dissipate, the associated volume change strengthens (densifies) the element and the loss of shear resistance may or may not be sufficient for the adjacent mass to collapse and liquefy due to the initial stress redistribution. If all the pore pressures dissipate during the structural contraction/collapse, fully drained behavior associated with no loss of shear strength inhibits progressive propagation of liquefaction and failure is impossible. This hypothesis is consistent with the observations published by Eckersley (1990) and Lade (1993). They showed that statically triggered flowslides were observed for saturated cohesionless materials with permeabilities less than 10^{-4} m/s. Evans et al. (1992) cite several case histories where liquefaction of gravels and

gravelly soil occurred. In all cases the sand content was at least 40% which must have contributed to the temporary impeded drainage conditions and reduced permeability. Yegian et al. (1994) cited several case histories where gravels liquefied during earthquake loading in cases where dissipation of pore pressures was impeded by a low permeability surface layer.

The ability to predict the amount and intensity of generated pore pressures based on the volume change during structural contraction/collapse provides the essential tools to formulate the **collapse criterion**. The collapse criterion should embrace factors similar to those listed in Casagrande (1936), i.e., rate of pore pressure generation during the structural contraction/collapse and its dissipation, the dissipation being a function of the amount of volume change, the size of the body, and permeability and compressibility of the soil.

The state boundary surface gives, for a given loading path, a prediction of the volume change which will take place before the ultimate state is achieved. This available volume change is dependent on the direction of a loading path and the location of the initial state condition relative to the state boundary surface. Slow structural contractions allow more time for the material to dissipate pore pressures as they are generated. The accelerated structural collapses may generate significant pore pressures almost instantaneously. They in turn can decrease effective stresses for sufficient time to trigger weakening resulting in stress redistribution and progressive propagation of collapse leading to flow liquefaction. It appears that the intensity of structural collapses decreases as the state condition approaches the ultimate state (Fig. 4.2).

Subsea flowslide failures encountered at Nerlerk were explained by the generation of temporary excess pore pressures in elements with in situ state conditions close to the collapse surface due to hydraulic fill dumping or wave action. Such a temporary undrained condition was believed to initiate the loss of shear strength

(weakening) of the nucleus soil elements causing stress redistribution and progressive propagation until the shear strength loss within a sufficient volume of the soil body was overcome by the acting shear stresses and the mass of sand started to move. The state boundary surface concept agrees with this except that it would suggest that the initial stress changes triggered structural contraction/collapse which elevated excess pore pressures and lead to progressive propagation of collapse and flow development due to the initial weakening.

Explanation of the flowslides in the coal stockpiles due to the slow raising water table is possible only within the framework of the state boundary surface. A slow raising water table represented a $q = \text{constant}$ stress path. The conditions were essentially drained, i.e., no excess pore pressures. Hence, there could not be a temporary excess of pore pressures to trigger the collapse, but flow liquefaction was initiated anyway. Hence, it must have been the structural contraction/collapse on the state boundary surface which generated elevated pore pressures resulting in shear strength loss and progressive propagation throughout the soil body.

The properties of the state boundary surface are very similar to the properties of a yield surface. The behavior of an element is essentially elastic and dramatically changes as the loading path attains the state boundary surface. Nevertheless, more tests are needed in order to be able to apply plasticity concepts to make a more definitive statement, if possible, about the direction of plastic strain increments on the state boundary surface.

CONCLUSIONS

The state boundary surface has been found for very loose dry Ottawa sand. This supports the concept of a fundamentally identical behavior of dry and saturated very loose sand. It reveals a discontinuous behavior of very loose materials on this boundary which renders the material intrinsically unstable. The collapse mechanism of

dry and saturated sand is the same and is independent of the drainage conditions; it is the resulting behavior which is different. The concept of the state boundary surface provides a way of explaining the dramatic phenomenon of flow liquefaction of very loose saturated sand as a structural property.

Two tests on dense dry sand exhibited a temporary minor contraction before dilating towards the ultimate steady state. It appears that this phenomenon agrees well with the observations during undrained tests on saturated sand at the same void ratio where the sand temporarily loses a portion of its shear strength and develops a so called quasi steady state. The existence of this effect for dense dry sand can provide a deeper insight into the fundamental mechanism of the quasi steady state. However more testing on dry samples is needed to justify this claim.

Any loading path for any degree of saturation which eventually reaches the state boundary surface will be forced into following along the surface by structural contraction. During certain loading paths a sand can also experience rapid stress independent structural collapses apart from the stress controlled structural contraction. These structural volume changes can initiate dramatic pore pressure generation in a saturated sand if the dissipation is impeded by boundary conditions or consolidation properties of the sand.

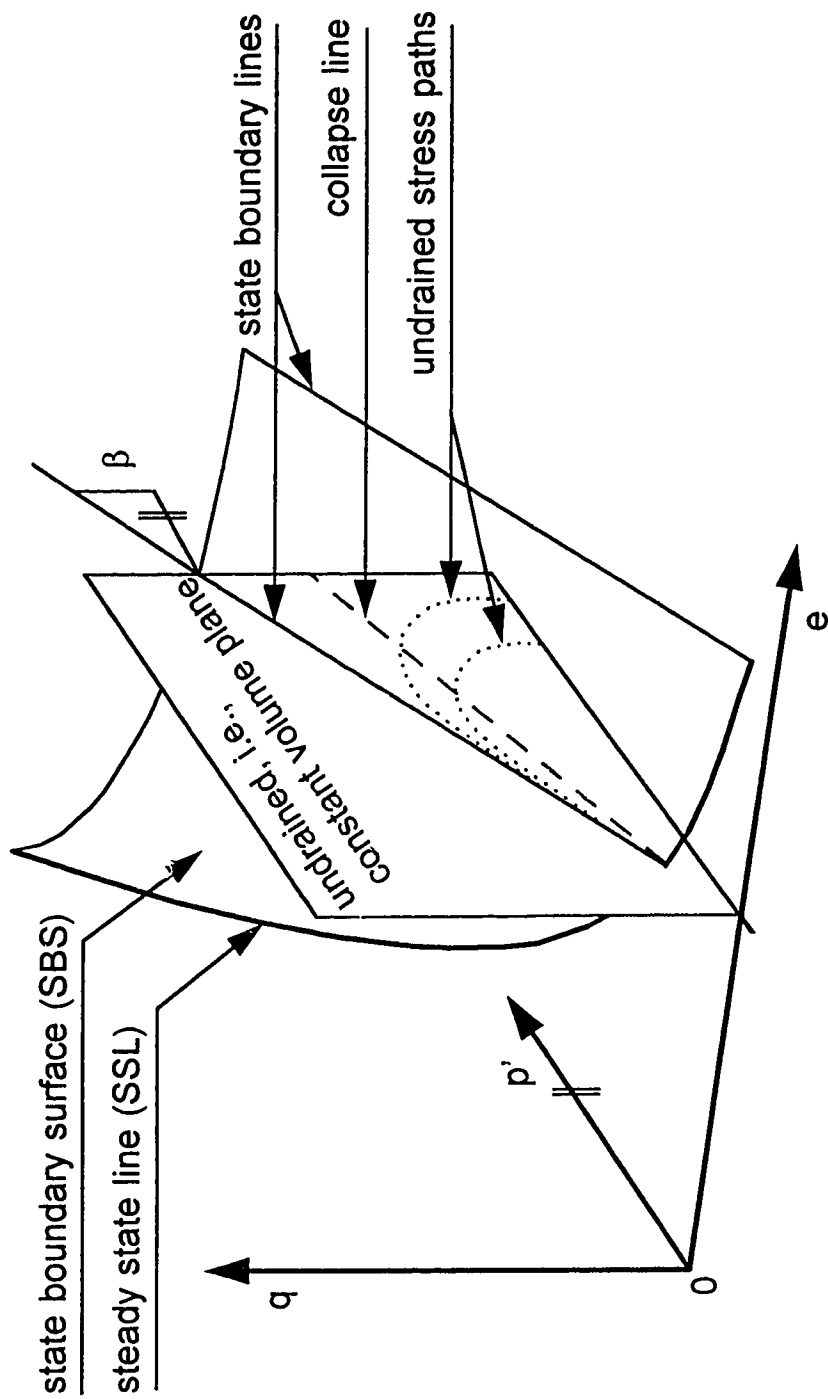
The intensity of the collapse liquefaction of very loose saturated sand is difficult, if not impossible, to quantify in the laboratory due to its sudden uncontrollable nature. The quantification of the intensity (rate) of a structural collapse of very loose dry sand is obtainable, since the collapse is not sustained by generated pore pressures, therefore the rate of volume change can be measured. Hence, the collapse criterion can be based on the quantification of the rate of structural collapse, which can be consequently directly linked to the pore pressure generation during collapse liquefaction. In addition the structural contraction itself has a potential to generate

additional pore pressures which can enhance material weakening necessary for progressive propagation.

The intrinsic instability of the sand on the state boundary surface has a direct implication on the kind of measures applicable to limit triggering of collapse liquefaction. Slow loading which would ensure complete dissipation of pore pressures may not be the solution, since it would not necessarily preclude the collapse. It is shown that the structural collapses take place independently of the presence of excess pore pressures and that they are the response of a material to certain stress paths on the state boundary surface. Therefore, collapse liquefaction appears to be a material property rather than a consequence of certain type of loading. Hence, in order to avoid collapse liquefaction the material must be changed so that it will not produce structural collapses, i.e., changed from a very loose state. Another solution would be to control the loading path so it would never reach the state boundary surface or force the loading path to follow the state boundary surface in a safe direction, which is not often a practical consideration.

		preparation parameters (before consolidation)		initial parameters (after consolidation, before shear)		
Test identification	Type of test	e	m. c. (%)	e	p' (kPa)	q (kPa)
very loose #9	load controlled, q = constant stress path	0.85	2.54	0.83	240	77
loose #14	ditto above	0.80	2.49	0.79	240	135
compression #compr2	strain controlled triaxial compression	0.85	2.72	0.85	55	0
p = constant p1	load controlled, p = constant stress path	0.84	2.70	0.82	105	0
special stress path #spec	load controlled test with load release	0.82	2.42	0.80	240	120

Table 3.1 Initial characteristics of presented tests



Note: collapse line is BELOW the state boundary line in the shown undrained plane; collapse surface pertaining to this collapse line is NOT shown on this figure

Fig. 3.1 Definition of the elements of state boundary surface

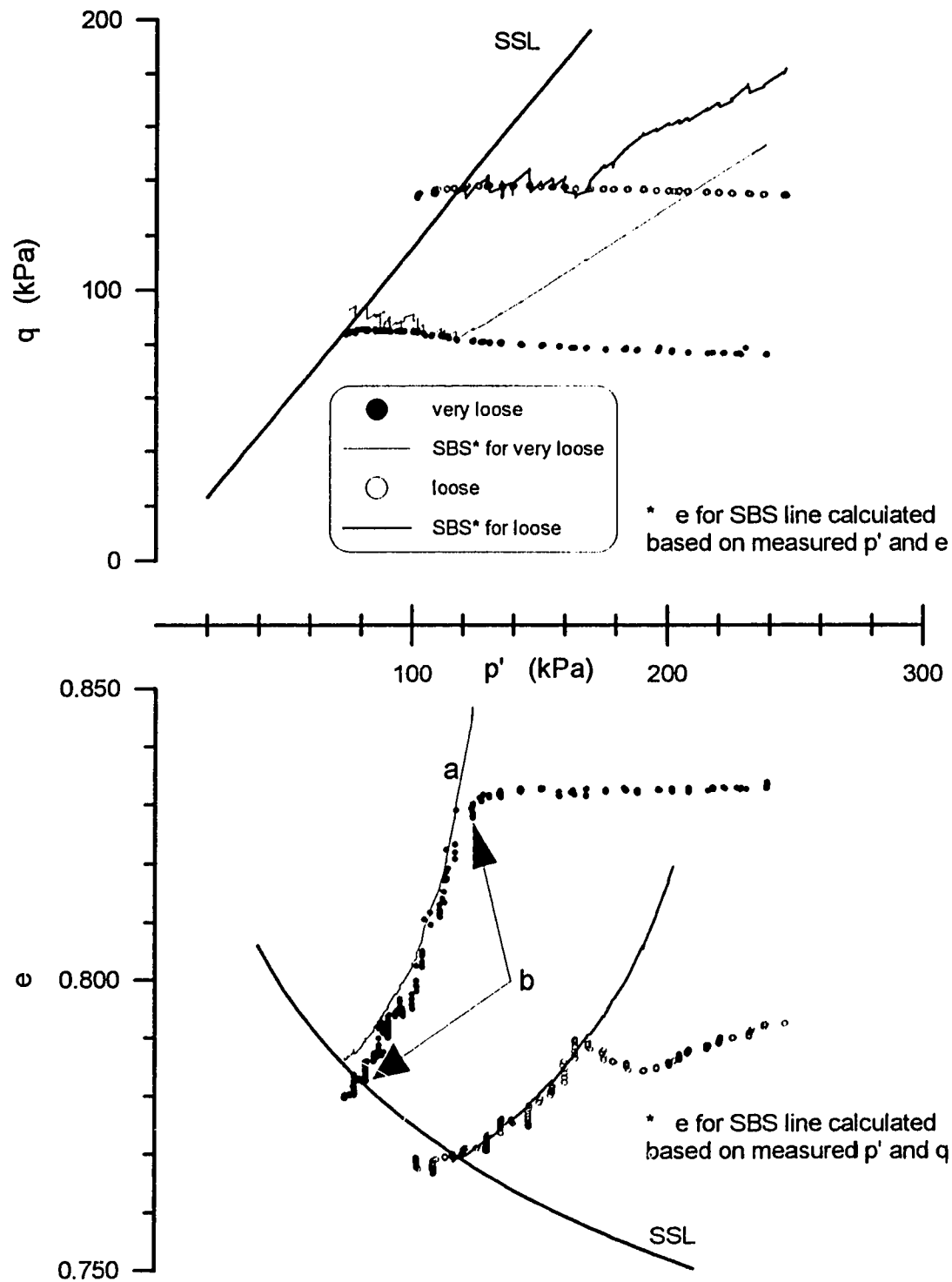


Fig. 3.2 Stress path deflection due to the state boundary surface for two $q = \text{constant}$ tests (test #9, #14)

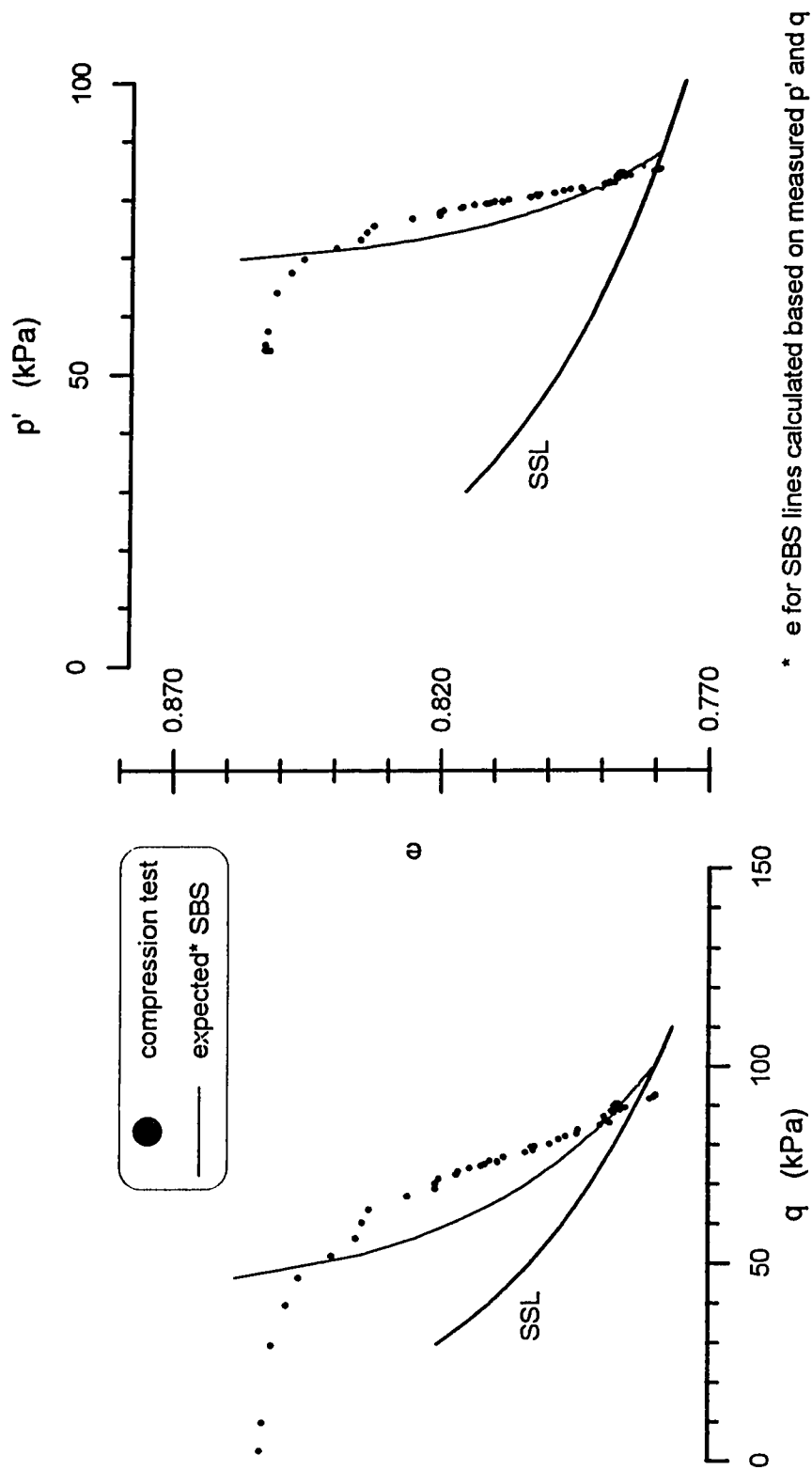


Fig. 3.3 Stress path deflection due to the state boundary surface for the conventional strain controlled compression test (test #comp2)

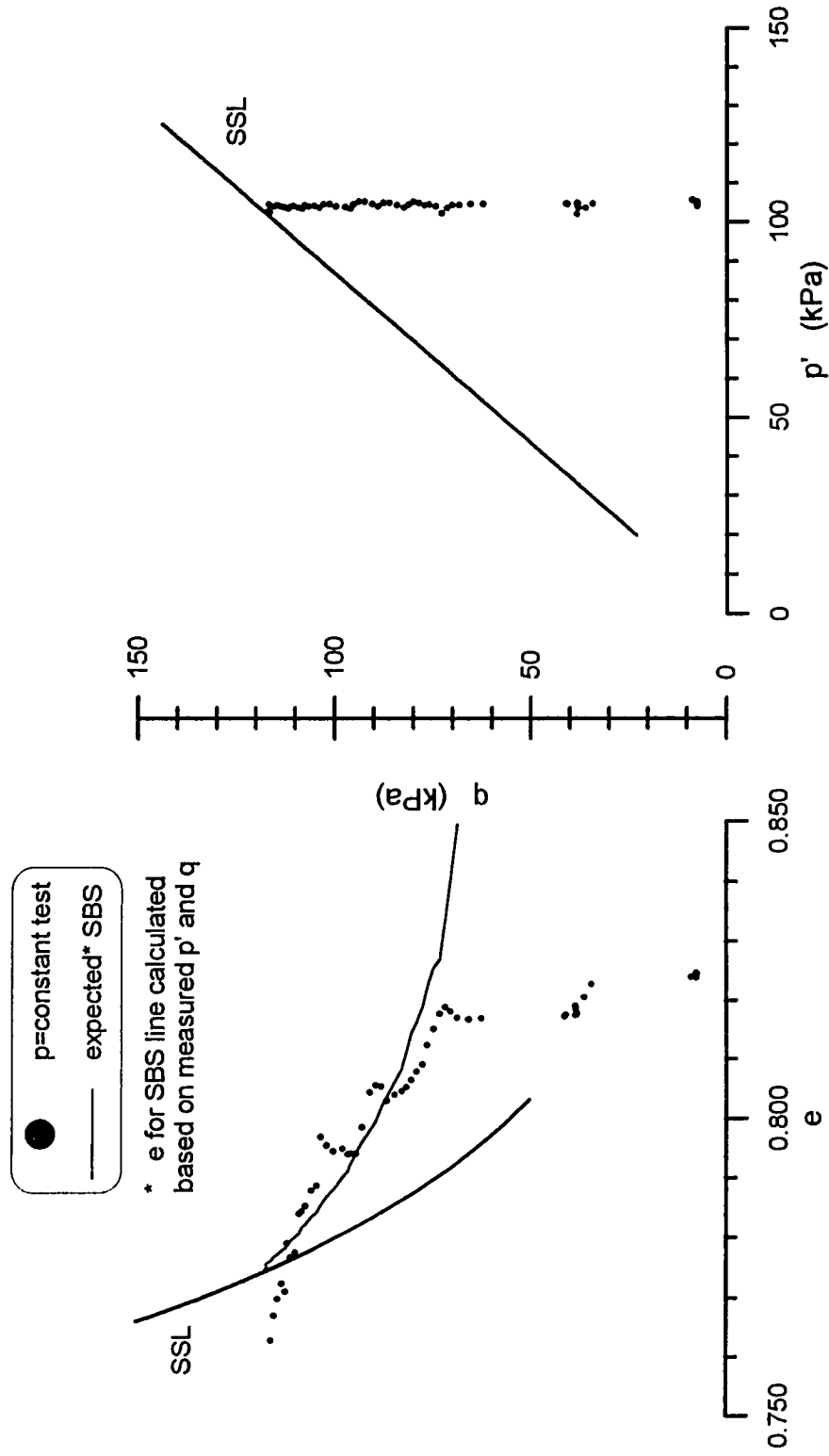


Fig. 3.4 Stress path deflection due to the state boundary surface for the $p = \text{constant}$ test (test #p1)

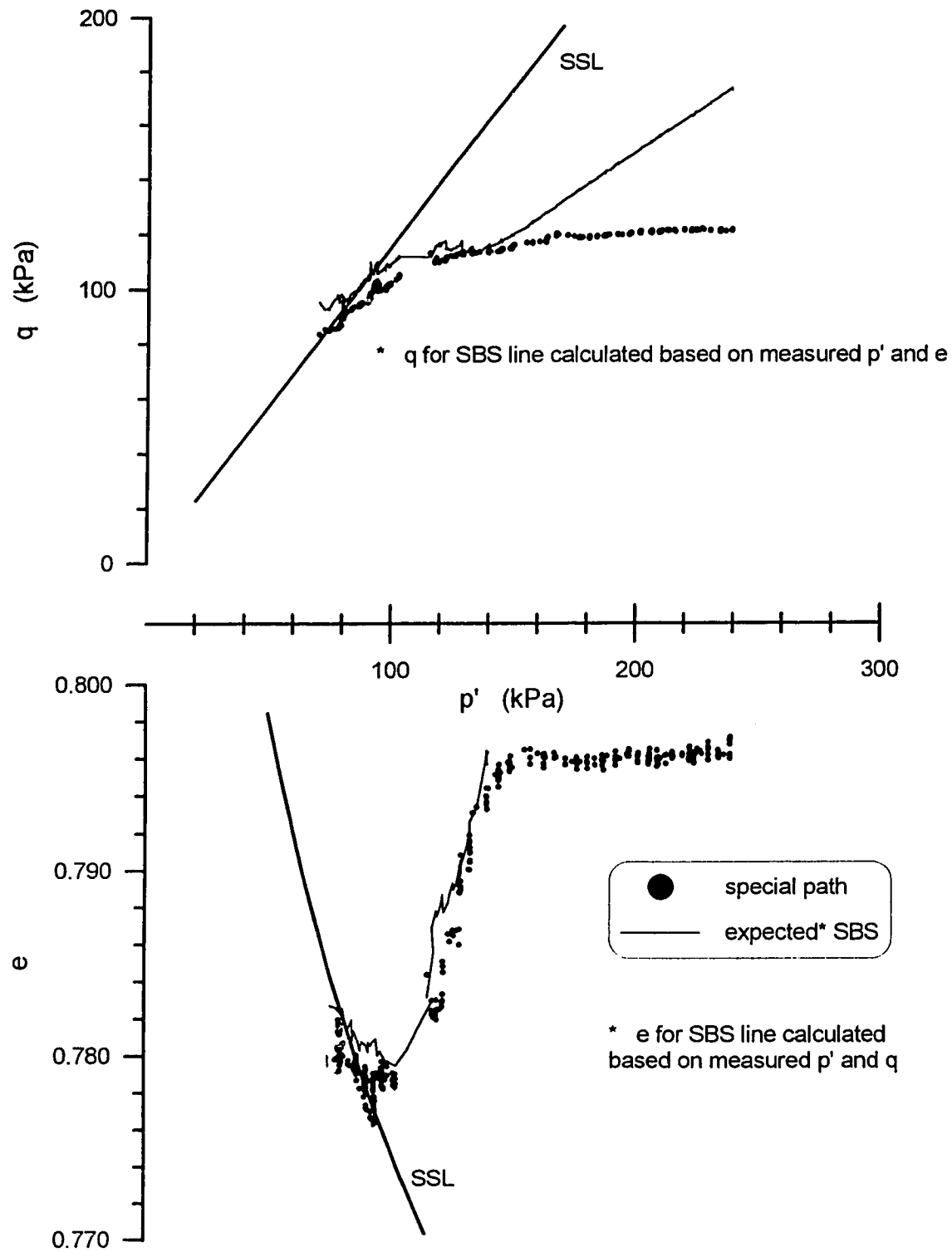


Fig. 3.5 Stress path deflection due to the state boundary surface for the special path test (test #spec)

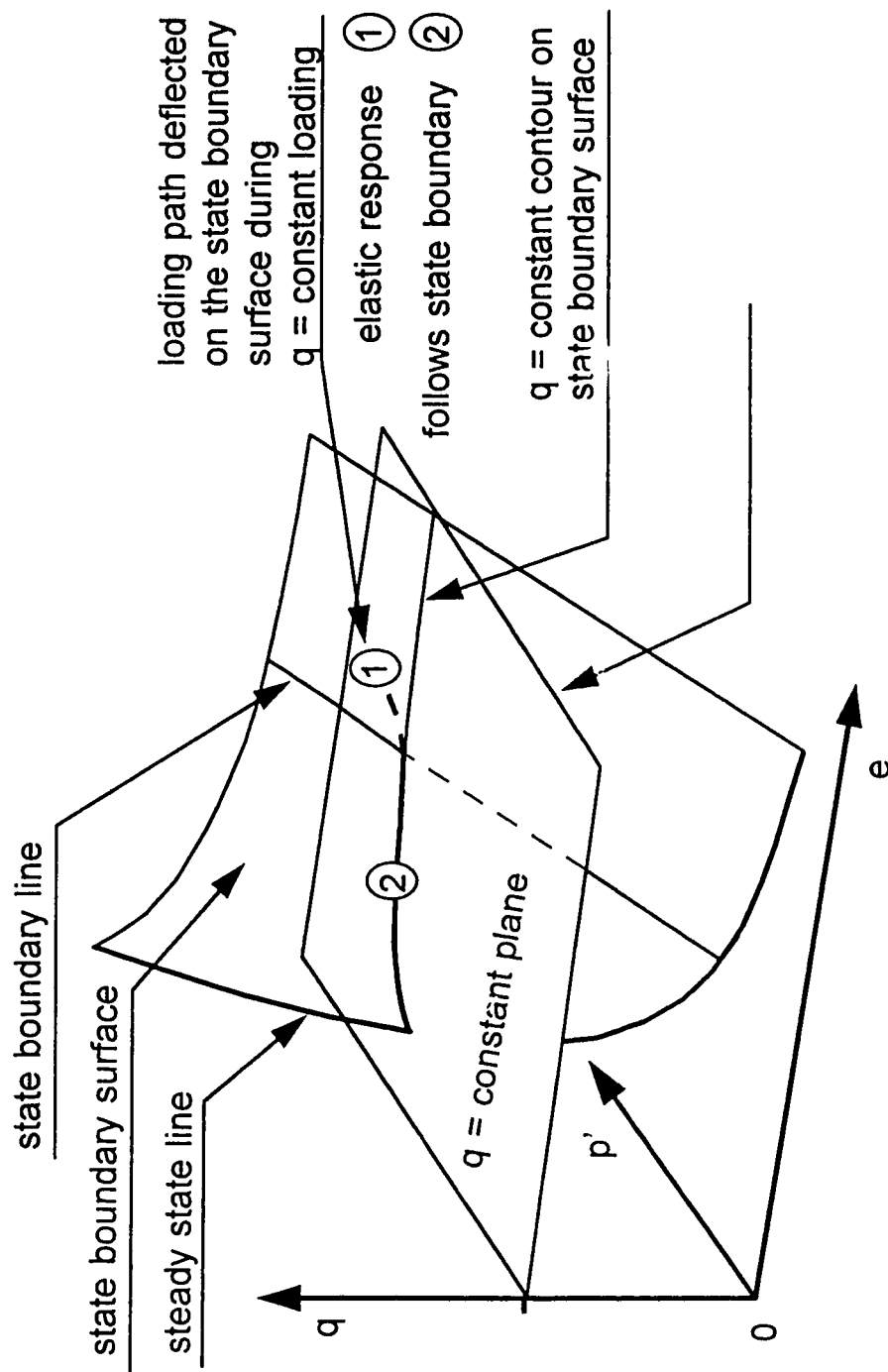


Fig. 3.6 The effect of the state boundary surface on a $q = \text{constant loading path}$

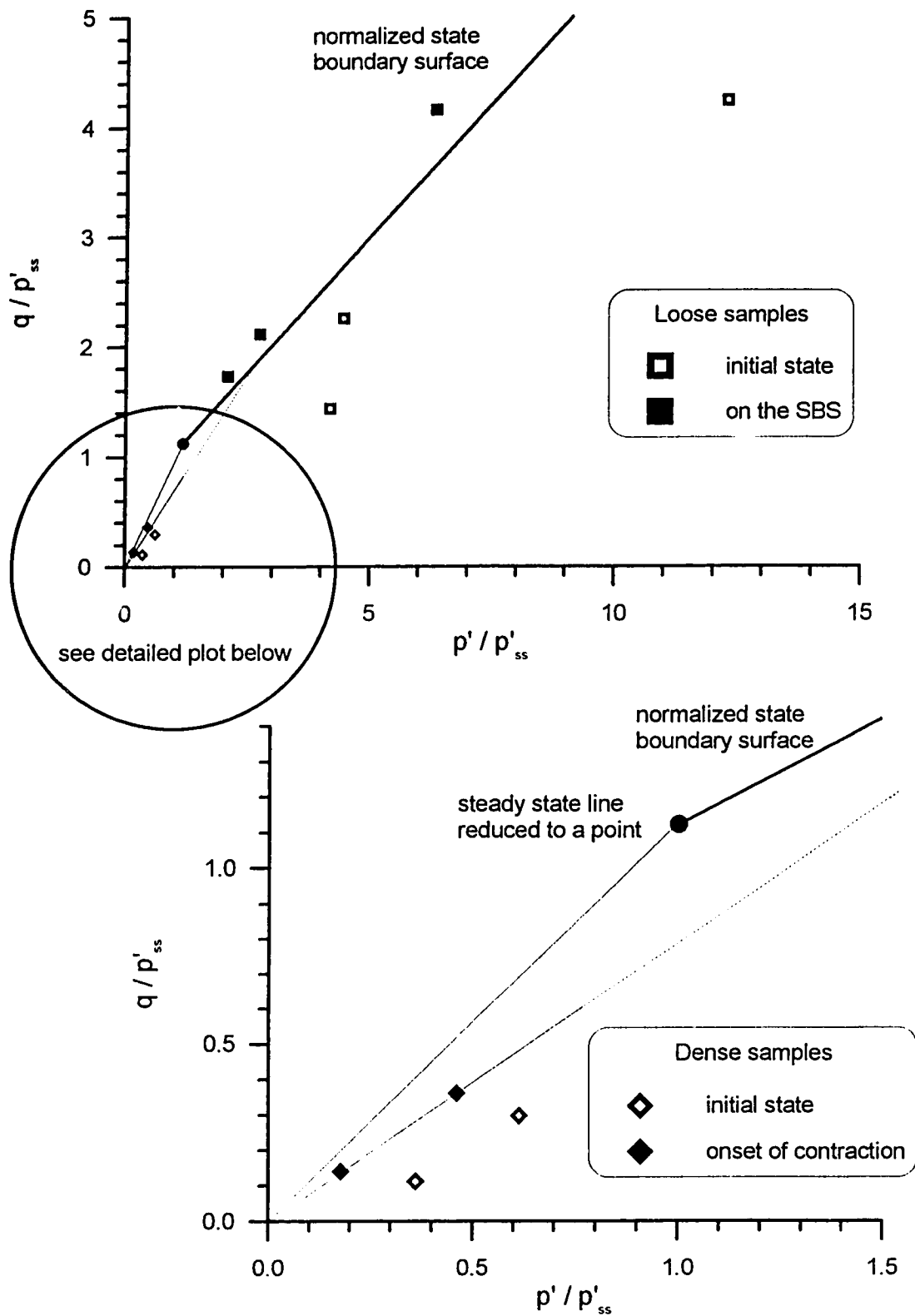


Fig. 3.7 Normalized plot of the state condition of the loose and dense samples (test #9, #14, #spec, #dns1, #dns2)

References

- Alarcon-Guzman, A., Leonards, G. A., and Chameau, J. L. (1988). "Undrained monotonic and cyclic strength of sands." *ASCE Journal of the Geotechnical Engineering Division*, 114(No.10), 1089-1109.
- Casagrande, A. (1936). "Characteristics of cohesionless soils affecting the stability of earth fills." *Journal of the Boston Society of Civil Engineers*, Vol. 23, No. 1, January, 257-276.
- Castro, G. (1969). "Liquefaction of sands". *Harvard Soil Mechanics Series*, No. 81, Harvard University, Cambridge, MA.
- Castro, G., and Poulos, S. J. (1977). "Factors affecting liquefaction and cyclic mobility." *ASCE Journal of the Geotechnical Engineering Division*, 103(GT6), 501-516.
- Dawson, R. F., Morgenstern, N. R., and Gu, W. H. 1992. "*Instability mechanisms initiating flow failures in mountainous mine waste dumps - Phase I.*" Study for Energy, Mines and Resources Canada, DSS contract #23440-0-9198/01-X8G.
- Dawson, R. F., Morgenstern, N. R., and Gu, W. H. 1994. "*Liquefaction flowslides in Western Canadian coal mine waste dumps - Phase II: case histories.*" Study for Energy, Mines and Resources Canada, SSC file # XSG42-00138 (608), SSC contract 23440-2-9151/01-XSG.
- Eckersley, J. (1990). "Instrumented laboratory flowslides." *Geotechnique*, 40(3), 489-502.

- Evans, M. D., Seed, H. B., and Seed, R. B. (1992). "Membrane compliance and liquefaction of sluiced gravel specimens." *ASCE Journal of the Geotechnical Engineering Division*, 118(No.6), 856-867.
- Gu, W. H., Morgenstern, N. R., and Robertson, P. K. (1993). "Progressive failure of The Lower San Fernando Dam." *ASCE Journal of the Geotechnical Engineering Division*, 119(No.2), 333-348.
- Ishihara, K., (1993). "Liquefaction and flow during earthquakes." *The 33rd Rankine Lecture, Géotechnique*, 43(3), 351-415.
- Ishihara, K., Verdugo, R. and Acacio, A. A. (1991). "Characterization of cyclic behavior of sand and post-seismic stability analysis." *9th Asian Regional Conference on Soil Mechanics and Foundation engineering*, Bangkok, Thailand. Vol.2., 17-40.
- Lade, P. V. (1993). "Initiation of static instability in the submarine Nerlerk berm." accepted for *Canadian Geotechnical Journal*, December 1993.
- Roscoe, K. H., Schofield A. N., Wroth C. P. (1958). "On the yielding of soils." *Géotechnique*, 8(1), 22-53
- Robertson, P. K. 1994. "Terminology for soil liquefaction." *Proc. 47th Canadian Geotechnical Conference*, Halifax, in press.
- Sasitharan, S., Robertson, P. K., Sego, D. C. and Morgenstern, N. R. (1993). "Collapse behavior of sand." *Canadian Geotechnical Journal*, 4, 569-577.
- Sasitharan, S., Robertson, P. K., Sego, D. C. and Morgenstern, N. R. (1994). "A state boundary surface for very loose sand and its practical implications." *Canadian Geotechnical Journal*, in press.

- Skopek, P., and Cyre, G. (1994). "Volume change measurement of unsaturated triaxial samples." submitted to *Geotechnical Testing Journal*, in press.
- Skopek, P., Morgenstern, N. R., Robertson, P. K., and Sego, D. C. (1994). "Collapse of dry sand." submitted to *Canadian Geotechnical Journal*, in press.
- Sladen, J. A., D'Hollander, R. D., and Krahn, J. (1985a). "Back analysis of the Nerlerk berm liquefaction slides." *Canadian Geotechnical Journal*, 22, 579-588.
- Sladen, J. A., D'Hollander, R. D., and Krahn, J. (1985b). "The liquefaction of sands, a collapse surface approach." *Canadian Geotechnical Journal*, 22, 564-578.
- Terzaghi, K. (1956). "Varieties of submarine slope failure." *Proc. 8th Texas Conference on Soil Mechanics and Foundation Engineering*, U. Texas, Austin, 1-41.
- Yegian, K. K., Ghahraman, V. G., and Harutiunyan, R. N. (1994). "Liquefaction and embankment failure case histories, 1988 Armenia earthquake." *ASCE Journal of the Geotechnical Engineering Division*, 120(No.3), 581-596.
- Vaid, Y. P., and Chern, J. C. (1985). "Cyclic and monotonic undrained response of saturated sands." *Advances in the Art of Testing Soils Under Cyclic Conditions*, Edited by V. Khosla, ASCE, New York, N. Y., 120-147.

EFFECTIVE STRESS APPROACH TO EVALUATE FLOW LIQUEFACTION¹

INTRODUCTION

Liquefaction flowslides can be triggered both dynamically and statically. Dynamic triggering due to cyclic loading associated with earthquakes has been much studied. Current practice in this regard has been summarized by Marcuson et al. (1992). A correlation between cyclic shear stress and standard penetration resistance (or other correlatable in situ test) is used as the triggering criterion. If liquefaction is triggered, the in situ undrained strength is taken as operational. If the acting shear stresses exceed the undrained resistance, a liquefaction flowslide can ensue, or at least large deformations will result.

Liquefaction flowslides have been observed for which no identifiable source of cyclic loading had been detected. Terzaghi (1956) describes several cases of significant submarine movement where no triggers could be identified. He referred to this phenomenon of sudden liquefaction without presence of cyclic shear stresses as **spontaneous liquefaction**. Such failures of natural or man-made are believed to be instigated by minor stress changes such as groundwater fluctuation or toe erosion, hence essentially by static loading.

¹ A version of this paper has been submitted for publication. Skopek, P., Morgenstern, N. R., and Robertson, P. K. (1994). *Journal of the Geotechnical Engineering Division ASCE*.

The design against statically triggered flowslides in cohesionless soils is quite enigmatic. Conventional limit equilibrium methods have proven to be unreliable. For submarine flowslides at Nerlerk the Factor of Safety was calculated as high as 3 (Lade 1993). Coal mine waste dump failures in the Canadian Rocky Mountains have reached runout distances up to 2.5 kilometers, indicating liquefaction flowslides. They were initially considered safe with Factors of Safety around 1.2 (Dawson et al. 1994). Obviously the concepts embraced in the characterization of very loose materials within classical limit equilibrium methods fail to properly assess the behavior of cohesionless liquefiable materials. Nevertheless, these failures are real and in some instances fatal. Due to the fact that these types of catastrophic failures are restricted to very loose saturated cohesionless materials, these events have not been sufficiently common to attract considerable research attention. However, recently significant progress has been made in understanding the fundamental mechanism of statically triggered flow liquefaction in cohesionless soils.

Sladen et al. (1985) introduced the **collapse surface** concept which defines a locus of state conditions in $p' - q - e$ (mean principle stress - deviatoric stress - void ratio) space at which collapse and weakening of an element, possibly leading to flow liquefaction of the entire body, is initiated during undrained loading. Consequently it was shown that undrained loading is not a prerequisite for collapse to occur. Sasitharan et al. (1993) demonstrated experimentally that a very loose saturated sand can collapse and liquefy under fully drained loading conditions with no excess pore pressure during a triaxial $q = \text{constant}$ stress path. These studies revealed that failure is initiated when the loading path reaches a surface in $p' - q - e$ space, which is an envelope to the post peak portions of the undrained stress paths at different void ratios (Fig. 4.1). They also showed that the state condition for a material cannot exist above this surface, hence such a surface represents a **state boundary**. The collapse surface

constitutes a triggering criterion regardless whether the material element approaches it due to dynamic or static loading.

Current procedures that utilize the collapse surface in flow liquefaction analysis (Gu et al. 1993) assume in common with other liquefaction analyses that once liquefaction is triggered, subsequent deformation is undrained. This is a gross oversimplification of the liquefaction process because it cannot distinguish between fine sand and large boulders. In the latter case, the rate of dissipation of pore pressures could be commensurate with the rate of generation and upon triggering of the liquefaction only volume changes would be generated.

In this sense the question can be asked whether the test results reported by Sasitharan et al. (1993), in which liquefaction developed under fully drained test conditions, revealed material properties or were artifacts of the test. This is best resolved by developing a theory of liquefaction in terms of effective stresses in order to gain insight into the undrained response.

The purpose of this paper is to present experimental data on loose collapsing dry sand in terms of effective stress, and to show how pore pressures developing during flow liquefaction can be computed. This is an important issue in that it allows one to evaluate whether very loose materials will fail drained, partly drained, or undrained after collapse has been triggered. This new theory would allow liquefaction mitigation measures to be designed in a more rational manner than is currently the case.

STATE BOUNDARY SURFACE

Skopek et al. (1994) and Sasitharan et al. (1994) have shown that a state boundary surface exists in $p' - q - e$ space. They concluded that the state boundary surface can be approximated by the following equation:

$$q = \beta * p' + (M - \beta) * \exp\left(\frac{e - \Gamma}{-\lambda}\right) \quad (1)$$

where: p' , q , and e are the mean principle stress, deviatoric stress and void ratio respectively on the state boundary surface, M is the slope of the ultimate steady state line in the $p' - q$ plane, Γ and λ are the parameters defining the ultimate steady state line in $\ln(p') - e$ plane, and β is the approximate slope of the envelope to all undrained stress paths at the same void ratio in the $p' - q$ plane, i.e., constant volume plane (Fig. 4.1).

This equation approximates the state boundary surface as a warped surface composed of straight lines which are an approximate envelope to the post peak portions of undrained stress paths at the same void ratio.

Skopek et al. (1994) showed that the parameters for the state boundary surface for very loose dry Ottawa sand were as follows:

$$M = 1.154 \quad \Gamma = 0.9303 \quad \lambda = 0.0337 \quad \beta = 0.6$$

This state boundary surface was shown to control the behavior of very loose dry Ottawa sand during triaxial $q \cong \text{constant}$ loading. Because there was no generation of pore pressures, the dry sand could not liquefy but could freely deform in order to maintain desired equilibrium. This was manifested as a significant increase of compressibility resulting in a pronounced decrease in void ratio. The change in void ratio allowed the state condition to remain on the state boundary surface, even when the direction of the stress path tried to cross the boundary. Hence, the state boundary surface caused the loading path to deflect and forced the state condition of an element to follow on and along the state boundary surface. The state boundary surface acts as an impenetrable wall for a loading path and causes a distinctly discontinuous behavior of a soil element.

STRUCTURAL CONTRACTION/COLLAPSE

A typical test result reported by Skopek et al. (1994) is shown in Fig. 4.2. This was a triaxial test on very loose dry Ottawa sand where the deviatoric stress (q) was kept constant and the mean effective principle stress (p') was decreased. During the initial stages of the test the sand responded essentially elastically with little or no change in void ratio (e). At a certain point the stress state reached the state boundary surface and a pronounced increase in sand compressibility was observed. Skopek et al. (1994) call this change in void ratio a **structural contraction**. Structural contraction is initiated by a stress ratio increase, hence is stress dependent. However, on detailed inspection of the test results shown in Fig. 4.2, the change in void ratio along the state boundary surface is also associated with several sudden contractions at constant stress ratio, hence a response that is independent of stress. Skopek et al. (1994) named these sudden stress independent time dependent contractions **structural collapse**. Following the structural collapse the soil state condition would drop below the state boundary surface into a more stable elastic region. Figure 4.2 also shows an expanded view of the three structural collapses in terms of void ratio versus time. From Fig. 4.2 it appears that the amount of structural collapse decreases as the soil state condition moves closer to the ultimate steady state line. This decrease in creep deformation occurs even though the stress ratio is increasing. It appears that the strengthening by densification dominates the process and the amount of structural collapse decreases. The phenomenon of structural collapse is a result of the intrinsically unstable state of a very loose sand on the state boundary surface.

MODE OF LIQUEFACTION FAILURE

It was shown that for a body containing very loose saturated granular material to experience flow liquefaction, it is not necessary for the entire volume of the material to liquefy (Gu et al. 1993). Thus, liquefaction can be limited to a relatively thin layer

which acts as a roller bearing and carries unliquefied stable material as suggested by (Casagrande 1936). This mode of failure was demonstrated experimentally by Eckersley (1990) and detected in coal mine waste dump failures in the Rocky Mountains (Dawson et al. 1992).

Several documented case histories provide valuable information on the effect of permeability on failure development. Flowslide failures of the exploration subsea berm in the Beaufort Sea at Nerlerk occurred in sand with an average permeability about $1.6 \cdot 10^{-5}$ m/s but never reached into the underlying sand which had an average permeability one order of magnitude higher of $2.3 \cdot 10^{-4}$ m/s (Lade 1993). Evans et al. (1992) cite several cases histories where liquefaction of gravels and gravelly soils have occurred. In all cases the sand content was at least 40% which must have contributed to the temporary impeded drainage conditions and reduced permeability. Yegian et al. (1994) report cases where a highly permeable silty-gravelly layer ($k \cong 5 \cdot 10^{-1}$ m/s) liquefied but was capped with a practically impermeable 30 - 50 cm thick clayey topsoil. A nearby site where a similar silty-gravelly deposit was topped with extremely permeable gravel layer ($k \cong 3 \cdot 10^1$ m/s) did not liquefy even though it experienced the same ground accelerations. These case histories provide evidence that the resistance against liquefaction is also governed by the ability of a material to dissipate generated pore pressures. The dissipation of excess pore pressures is essentially a consolidation problem and reflects the actual drainage conditions. Hence, if there is a prediction of the amount and rate of excess pore pressures generated during undrained conditions, consolidation theory can calculate the dissipation of these pore pressures under general drainage conditions.

MATHEMATICAL MODELING

Pore pressure generation at the state boundary surface is controlled by the propagation of structural volume changes through the very loose cohesionless

structure. If no pore pressures are dissipated, the state condition follows the constant volume stress path along the state boundary and the element can lose the maximum possible shear resistance, weaken, and the state condition moves directly toward the ultimate steady state at which a continuous deformation at constant volume and stress can be sustained. The weakening of the element can cause adjacent elements to carry the excessive load which can, in turn, generate additional pore pressures due to structural volume changes. On the other hand, if all the pore pressures dissipate as they are generated, fully drained behavior associated with no loss of shear resistance will take place and flow liquefaction is impossible.

By knowing the fully undrained behavior of very loose saturated sand and the equivalent fully drained response of the identical sand along the state boundary the two limiting cases are defined. The difference in behavior is controlled primarily by the different drainage conditions. Hence, the difference in behavior can be fully described by different consolidation properties and treated as a consolidation problem.

Fully undrained behavior of saturated sand produces no volume change. Since there is no pore pressure generation in dry sand the only response to the ongoing loading is the volume change due to structural contraction/collapse. It is possible to relate the undrained pore pressure generation to the fully drained volume change (Martin et al. 1975) using:

$$\Delta u = \frac{\Delta \varepsilon_{vd}}{\frac{1}{E_r} + \frac{n}{K_w}} \quad (2)$$

where: Δu is the pore pressure increment under undrained conditions equivalent to the volumetric strain $\Delta \varepsilon_{vd}$ under drained conditions. E_r is a rebound modulus of the material, n is the porosity and K_w is the bulk modulus of water.

Based on the above comments the following fundamental assumptions will be made in the proposed mathematical modeling:

1. The amount of pore pressure generation will depend on the amount of volume change that occurs on the state boundary surface during structural contraction/collapse.
2. The rate of pore pressure generation will depend on the rate of volume change.
3. The amount of dissipation will depend on the consolidation properties of the material, geometry of the investigated body and on the boundary conditions.

For the mathematical modeling the pore pressures can be generated either during structural contraction or during structural collapse. The structural contraction is caused by the travel along the state boundary and does not contain any information about the rate of volume change needed for the calculation of pore pressure generation. Therefore, for testing the effects of this phenomenon, a range of loading rates will be evaluated. The actual modeling is conducted incrementally. The test input variable is a time increment dt . The load increment is calculated from the loading rate dp'/dt for a given time increment. During each load increment on the state boundary surface a potential volume change is induced in dry material (equation 1). This volume change is converted into a pore pressure increment in an identical saturated material (equation 2). Then the resulting excess pore pressure is dissipated over the same time increment dt , using Terzaghi's consolidation theory:

$$c_v \frac{\partial^2 u}{\partial z^2} = \frac{\partial u}{\partial t} \quad (3)$$

$$c_v = \frac{k * E_{def}}{\gamma_w}$$

where the coefficient of consolidation c_v is calculated based on permeability k , the deformation modulus E_{def} calculated from the slope dp'/de of the loading path in the $p' - e$ plane in Fig. 4.2. and the specific gravity of water γ_w .

Using this model it is possible to calculate the path of state conditions on the state boundary surface during structural contraction. It predicts the amount of loss of shear resistance, i.e., amount of material weakening, and the proximity of the material to the ultimate steady state for a prescribed loading rate.

The structural collapses which can occur on top of structural contraction along the state boundary surface are time dependent. Therefore, they contain information about the rate of volume change. The modeling of the structural collapses is also conducted incrementally. The test input variable is again a time increment dt . Then the volume change during this time increment is determined from the measured structural collapse. This volume change is once again converted into a pore pressure increment in an identical saturated material (equation 2). However, structural collapses are stress independent and the compressibility is infinite, which rules out the application of Terzaghi's consolidation theory. Therefore, a theory considering consolidation of soils under constant effective stress (creep) was adopted (Garlanger 1972):

$$\begin{aligned} \frac{\partial v}{\partial t} &= \frac{k(1+e_0)}{\gamma_w} \frac{\partial^2 u}{\partial z^2} \\ \frac{\partial v}{\partial t} &= \frac{\partial v}{\partial u} \frac{\partial u}{\partial t} + \left(\frac{\partial v}{\partial t} \right)_{creep} \end{aligned} \quad (4)$$

where: k is the permeability, e_0 is the initial void ratio and γ_w is the specific gravity of water.

The magnitude of the residual pore pressures indicate the amount of the material weakening and the proximity of the material to the ultimate steady state.

Detailed calculation algorithm of the effect of structural contraction on the effective stress path during a $q = \text{constant}$ loading

Figure 4.3 presents a schematic diagram of the resulting stress path during partly drained conditions along the state boundary surface. This model is applicable if the direction of a loading path is known. In the case presented, q is assumed constant and p' is decreasing at given rate dp'/dt .

1. During a $q = \text{constant}$ loading an element of soil reaches the state boundary surface (defined by M , Γ , λ , and β); this state condition is fully defined by p' , q , and e at the point on the state boundary surface (sbs) and is controlled by the governing equation (1).
2. A decrement of dp' is applied to the element over a time increment dt , which due to the effect of the state boundary surface produces a change in void ratio d_1e during fully drained conditions.
3. This drained void ratio change d_1e is converted into an equivalent pore pressure increment d_1u which would be generated if the drainage conditions of an identical saturated element were perfectly undrained (equation 2).
4. The time increment dt is available for the pore pressure increment d_1u to dissipate through consolidation to the final excess pore pressure du_f . The amount of dissipation through consolidation is controlled by the actual drainage conditions defined by k , E_{def} , γ_w , and H (length of the drainage path) in equation 3. It was found convenient to solve this differential equation using the marching forward method.
5. The degree of dissipation of the initial pore pressure increment d_1u is the degree of consolidation, which is associated with a certain consolidation ratio and which yields the amount of the actual volume (void ratio) change, $d_1e - de_f$. If all the pore pressures are dissipated the initial, perfectly drained, void ratio change d_1e takes place; if none of the pore pressures are dissipated, no volume change is observed. This calculation step results in a new soil state in

terms of void ratio $e = e_{shs} - (d_1e - de_1)$, $p' = p'_{shs} - (d_1u - du_1)$ and q given by the condition that the state remains on the state boundary surface by equation (1) and an element arrives at point 1 in Fig. 4.3.

6. The second calculation cycle begins and an additional dp' decrement over a time increment dt is applied which results through the above steps 2 and 3 in a new undrained pore pressure increment d_2u . This pore pressure is added to the undissipated pore pressure from the first calculation cycle du_1 and is dissipated as in step 4 over the new time increment dt .
7. The degree of consolidation determines the amount of the volume change which takes place during dissipation. The maximum volume change during this cycle (d_2e) is given by the sum of the void ratio decrement calculated in step 6 and the undissipated volume change accumulated in previous steps (de_1). It is important to realize that if all the pore pressures are dissipated at this point, the value of q reaches its original value as it would if the whole process was perfectly drained. Now the new e , p' , and q can be calculated.

This model calculates the loading path of one element during structural contraction along the state boundary surface. It cannot predict whether a particular soil body will liquefy. However the weakening of such an element certainly triggers stress redistribution within the soil body which may lead to full scale flow liquefaction. It is noted that material weakening is a prerequisite for progressive propagation of flow liquefaction.

Detailed calculation algorithm of the effect of structural collapse on pore pressure generation

The calculation of the pore pressure generation is very similar but simpler than the calculation due to the effects of structural contraction. However, the calculation must be performed with measured structural collapses which provide the information about the rate of volume change is available.

1. The data for a structural collapse are selected $e = f(t)$ (Fig. 4.2).
2. For a selected time increment the void ratio change is calculated.
3. This perfectly drained void ratio change is converted into the equivalent undrained pore pressure generation (equation 2).
4. For the same time increment as above the pore pressure dissipation for real drainage conditions is calculated using equation 4. It was found convenient to solve this differential equation using a modified marching forward method described in detail by Garlanger (1972).
5. The calculation cycle starts again in step 2 with the next time increment and the pore pressures are accumulated.
6. Ultimately the largest pore pressure generated during a collapse is a measure of the loss of shear resistance.

This model calculates the resulting pore pressures during one structural collapse. It gives a measure of material weakening within one element. Similar to the structural contraction model, the weakening of such an element is capable of causing stress redistribution within the soil body which could result in full scale flow liquefaction.

RESULTS

The proposed mathematical modeling attempts to explain the known behavior of very loose saturated sand during a triaxial $q = \text{constant}$ test. Sasitharan et al. (1993) tested 120 mm high triaxial samples of very loose saturated Ottawa sand with open drainage from both ends. These samples collapsed vigorously in undrained manner when liquefied upon reaching the state boundary surface. Ottawa sand is expected to have a permeability according to Hazen's formula in the order of $1 \cdot 10^{-5}$ m/s. Figure 4.4 presents a series of lines at different permeabilities to illustrate the effect of loading rate during structural contraction on an element of sand with the drainage path $H = 60$ mm. A measure of weakening is expressed in terms of the ratio between the loss of shear strength during the calculated loading path and the maximum possible loss of

shear strength (0 = fully drained, 1 = fully undrained) for a range of permeabilities. From Fig. 4.4 it appears that only loading rates well in excess of 1 kPa/s are capable of generating significant pore pressures due to structural contraction. The average estimated loading rate in the test by Sasitharan et al. (1993) was 0.2 kPa/s. However, it is known that loading was applied in increments and therefore the actual loading rate during an increment could have been much higher. Figure 4.5 shows the calculated stress paths and void ratio change during structural contraction for a range of loading rates for the material with permeability $1 \cdot 10^{-6}$ m/s for the test reported by Sasitharan et al. (1993).

The analysis of the effect of structural collapse (#2 from Fig. 4.2) on pore pressure generation is shown in Fig. 4.6. The amount of maximum pore pressure generated is expressed in a normalized form with respect to the initial mean effective principle stress for a range of layer thicknesses and permeabilities. It is noted that the pore pressure buildup during the structural collapse first accelerates and later decelerates as the volume change rate decreases to zero. The maximum pore pressure which is built up during this event controls the amount of weakening and stress redistribution. The model calculation neglects any pore pressure, which may have been generated along the loading path prior the structural collapse by structural contraction. Hence, the calculated pore pressure acts on top of any previously generated pore pressure and contributes further to the undrained weakening of an element.

From Fig. 4.6 it appears that significant pore pressures are generated in 120 mm high specimens drained from both ends in soils with permeabilities about $1 \cdot 10^{-6}$ m/s, which is less than the expected permeability of Ottawa sand. It seems that according to this model the tests reported by Sasitharan's et al. (1993) were just on the borderline between liquefiable (undrained) and non-liquefiable (drained). The temporary excess pore pressures during incremental loading and possible temporary

impeded flow in the triaxial drainage system due to delayed hardware response time may have played a significant role and caused the observed vigorous undrained liquefaction failure. These comments require additional experimental investigation.

Application of the proposed models to in situ soil profiles reveals some interesting points. Loading rates in nature cannot reasonably exceed 0.0003 kPa/s (10 cm water table rise / hour). A loading rate of 1 kPa/s represents the rate of raising water table of approximately 360 m/hour which appears hardly possible. It is shown in Fig. 4.4 that the loading rate 0.0003 kPa/s will not generate any pore pressures for a 60 mm drainage path. Even for significantly longer drainage paths at this loading rate the pore pressure generation is not sufficient to establish considerable material weakening. This implies, that only in special cases of rapid loading associated with some external activity (blast, dumping, extremely high construction rate), i.e., loading commonly considered as undrained, could structural contraction itself produce sufficient pore pressure. The experience from oilsand tailings construction (Plewes et al. 1988) indicates that the large volumes of loose subaqueous tailings up to 15 meters thick are susceptible to flowslides during intense seasonal construction of 30 - 40 cm / day (0.0002 kPa/s)

The state of an element during the structural contraction on the state boundary surface is intrinsically unstable and structural collapses can be initiated. Figure 4.6 illustrates that if the structural collapse is initiated in a layer of liquefiable material only 1 to 2 meters thick, large pore pressures can be generated. The total thickness of the failing mass in the Nerlerk failures (Sladen et al. 1985a) varied between 5 to 12 meters and the average permeability was lower than $1 \cdot 10^{-4}$ m (Sladen 1993). Figure 4.6 clearly predicts that extremely large pore pressures would be generated in this case. It is also reasonable to expect that weakening due to one structural collapse can instantaneously trigger additional collapse which can result in further pore pressure elevation.

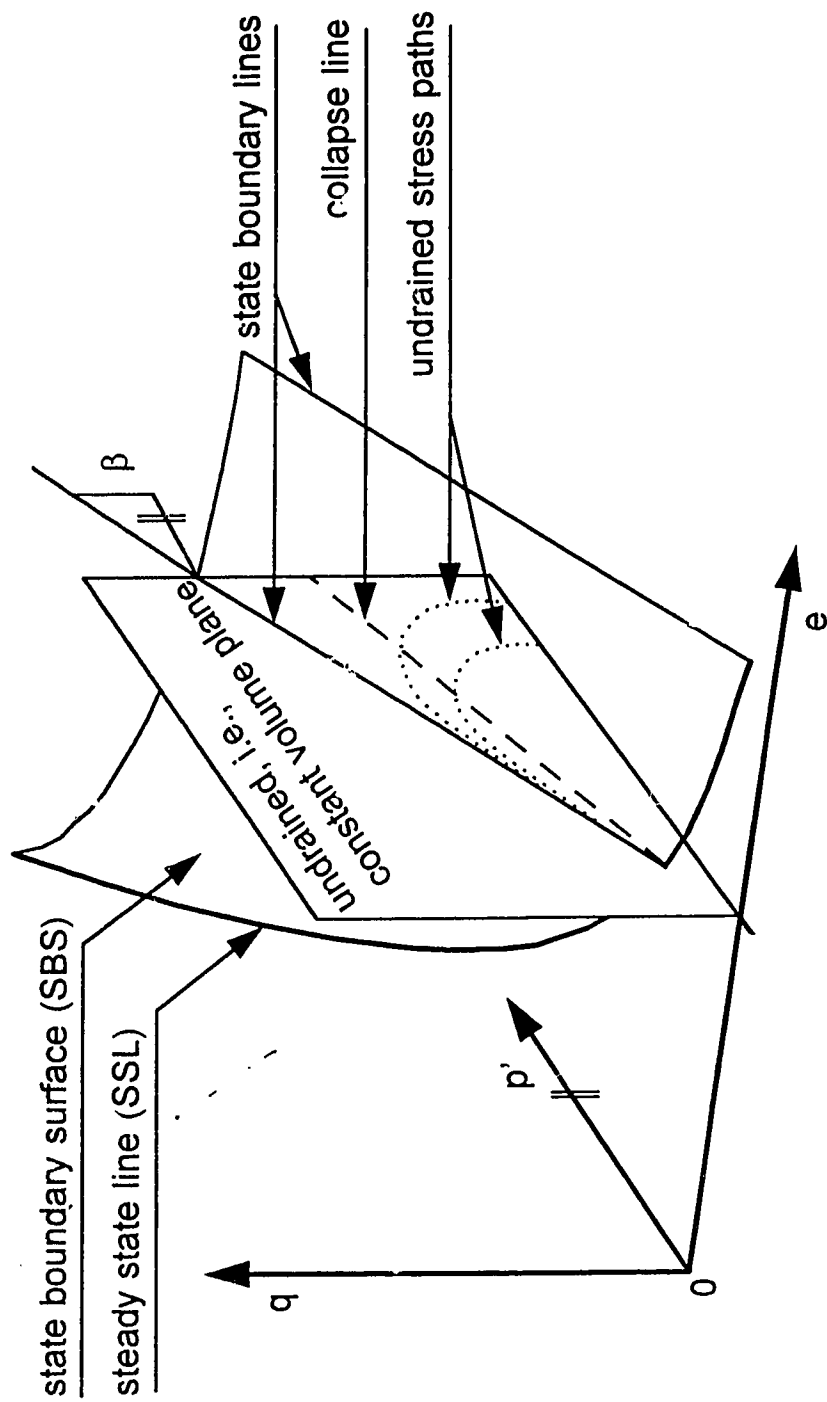
Superposition of the two phenomena, i.e., structural contraction and collapse appears to explain the mechanism of statically triggered flow liquefaction. The travel of an element along the state boundary surface initiates structural contraction, which can generate some pore pressure but primarily renders the state of the sand intrinsically unstable so that structural collapse associated with large pore pressure generation can be triggered. This apparently accounts for spontaneous liquefaction (Terzaghi 1956). The structural collapse phenomenon appears to be more important. In nature the effect of pore pressure generation due to structural contraction can be eliminated by slow loading rates. However, in the laboratory the loading rates have to be monitored carefully, since they can easily reach levels capable of generating considerable pore pressures due to structural contraction and trigger sufficient weakening which would be augmented further by initiating structural collapses.

CONCLUSIONS

1. A state boundary surface has been presented that provides a constitutive relation between volume change and stress change in terms of the effective stress during the collapse of very loose sand. It has been shown that material instabilities exist on the state boundary surface that manifest themselves as increments of volumetric creep. In this paper both the contraction along the state boundary surface and the structural collapse phenomena have been incorporated into a simple theory of pore pressure generation associated with liquefaction. This provides a theory based on effective stress to explain flow liquefaction.
2. Structural contraction enhances pore pressure generation and the degree to which the pore pressures dissipate is a function of external loading rate. A sufficiently slow loading rate will never produce any excess pore pressures and the soil will remain stable. It appears that common “natural” loading

rates do not have the potential for initiating significant weakening needed to develop flow liquefaction.

3. Structural collapse due to its vigorous nature generates large pore pressures which may not be dissipated over the short duration of the collapse. Hence, the structural collapse can produce significant weakening which can result in triggering additional collapse which could further elevate the pore pressures and promote material weakening. The magnitude of generated pore pressures is controlled by the amount of contraction, i.e., a structural collapse must produce sufficient volume change. Hence, a material which does not exhibit sufficient contraction during a structural collapse or does not exhibit structural collapse at all may not be susceptible to static liquefaction under “natural” loading rates even though it still exhibits weakening during undrained loading.
4. Higher loading rates result in more pronounced pore pressure generation and weakening due to structural contraction. This may distort the results of laboratory tests with incremental load control when the actual temporary loading rate can be much higher than acceptable “natural” or construction loading rates. Therefore, very slow triaxial $q = \text{constant}$ tests are needed to separate thoroughly the effect of structural collapse from the effect of structural contraction.
5. The effective stress model presented here incorporates permeability, compressibility and drainage path for analysis of flow liquefaction. It can be applied to numerical evaluation of structures or formations susceptible to flow liquefaction under circumstances where liquefaction mitigating measures are being developed.



Note: collapse line is BELOW the state boundary line in the shown undrained plane; collapse surface pertaining to this collapse line is NOT shown on this figure

Fig. 4.1 Definition of the elements of state boundary surface

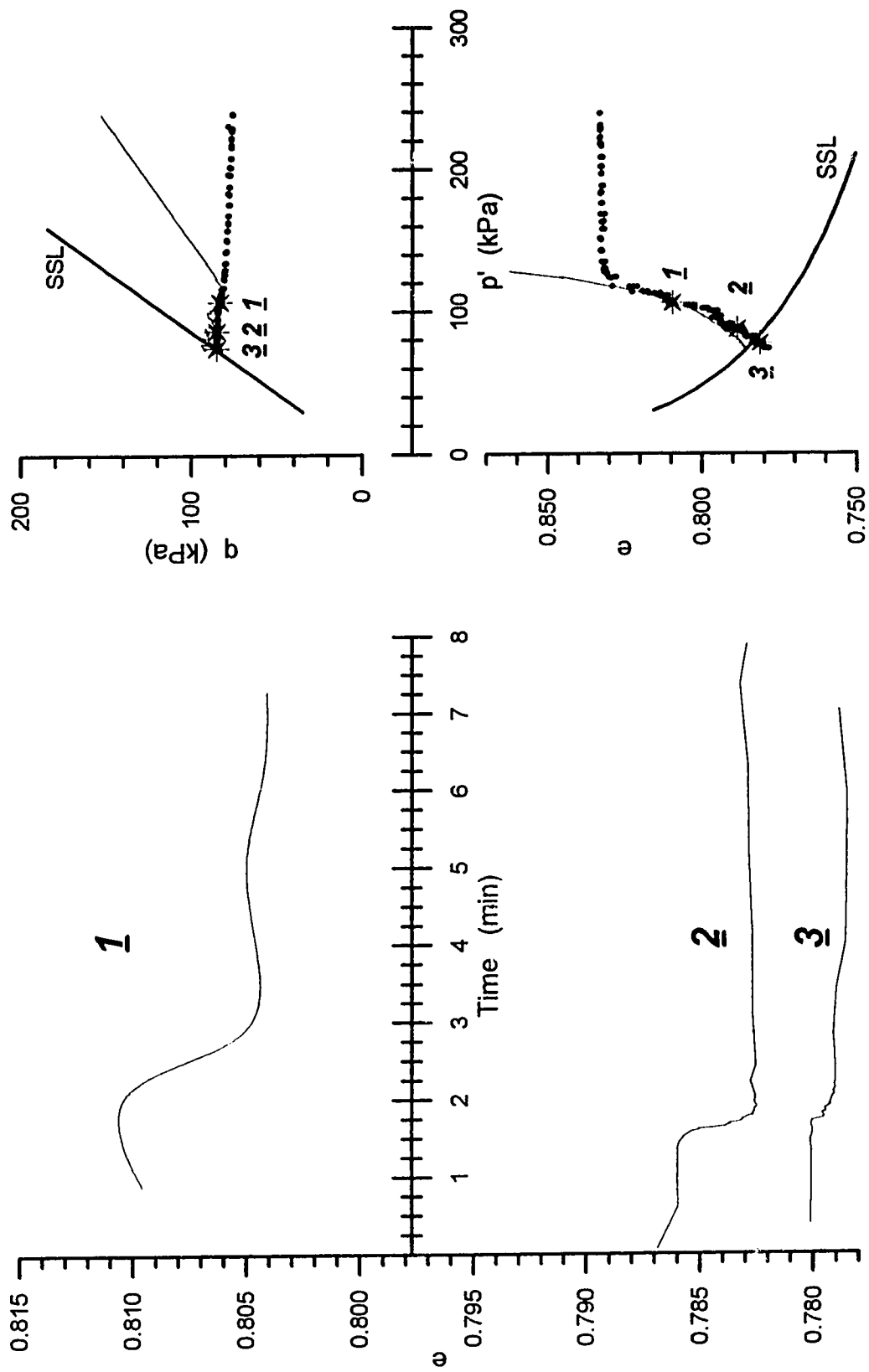


Fig. 4.2 Distribution of structural collapses during a typical $q = \text{constant}$ test (test #9)

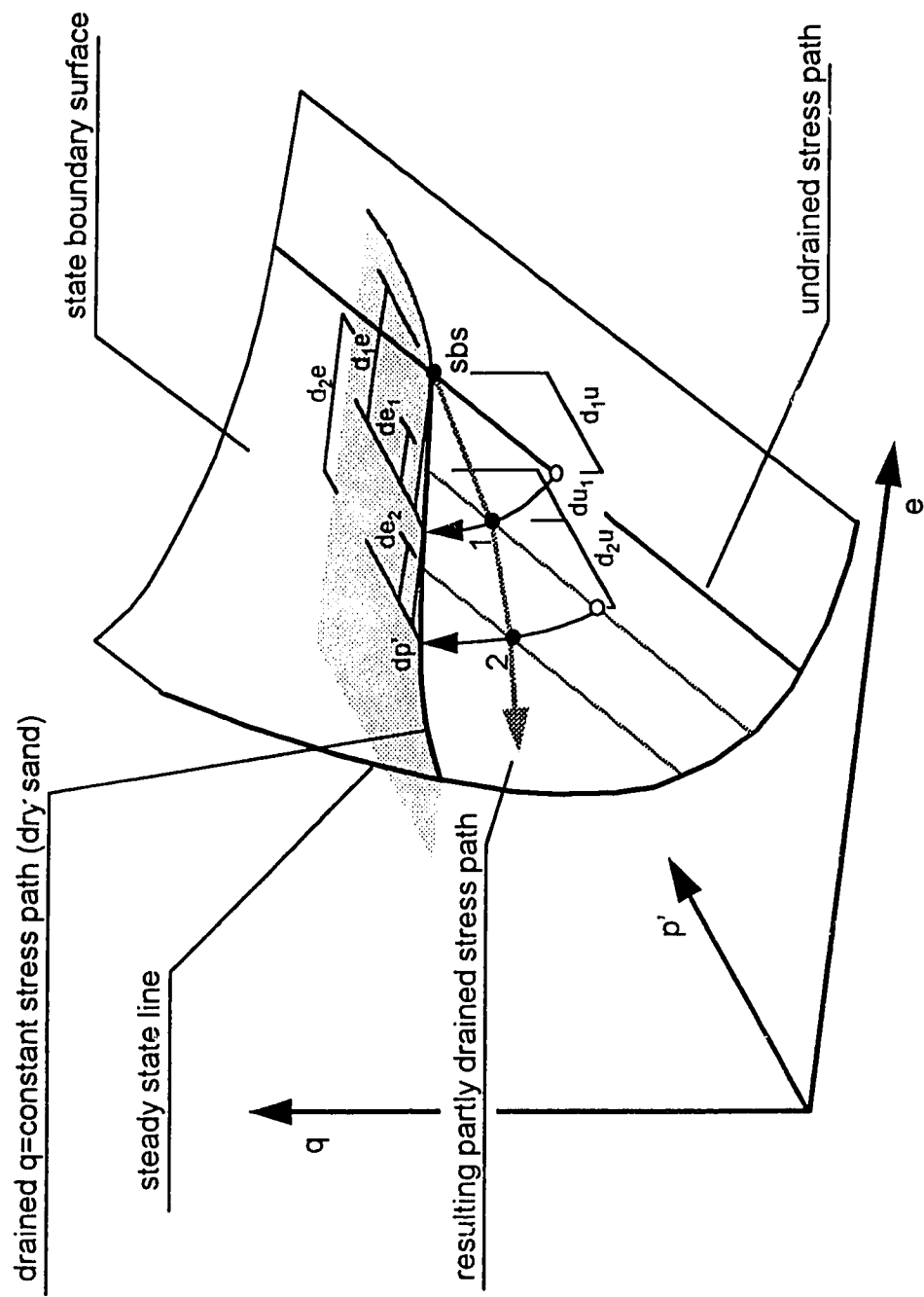


Fig. 4.3 Elements of mathematical model for the effective stress path during structural contraction

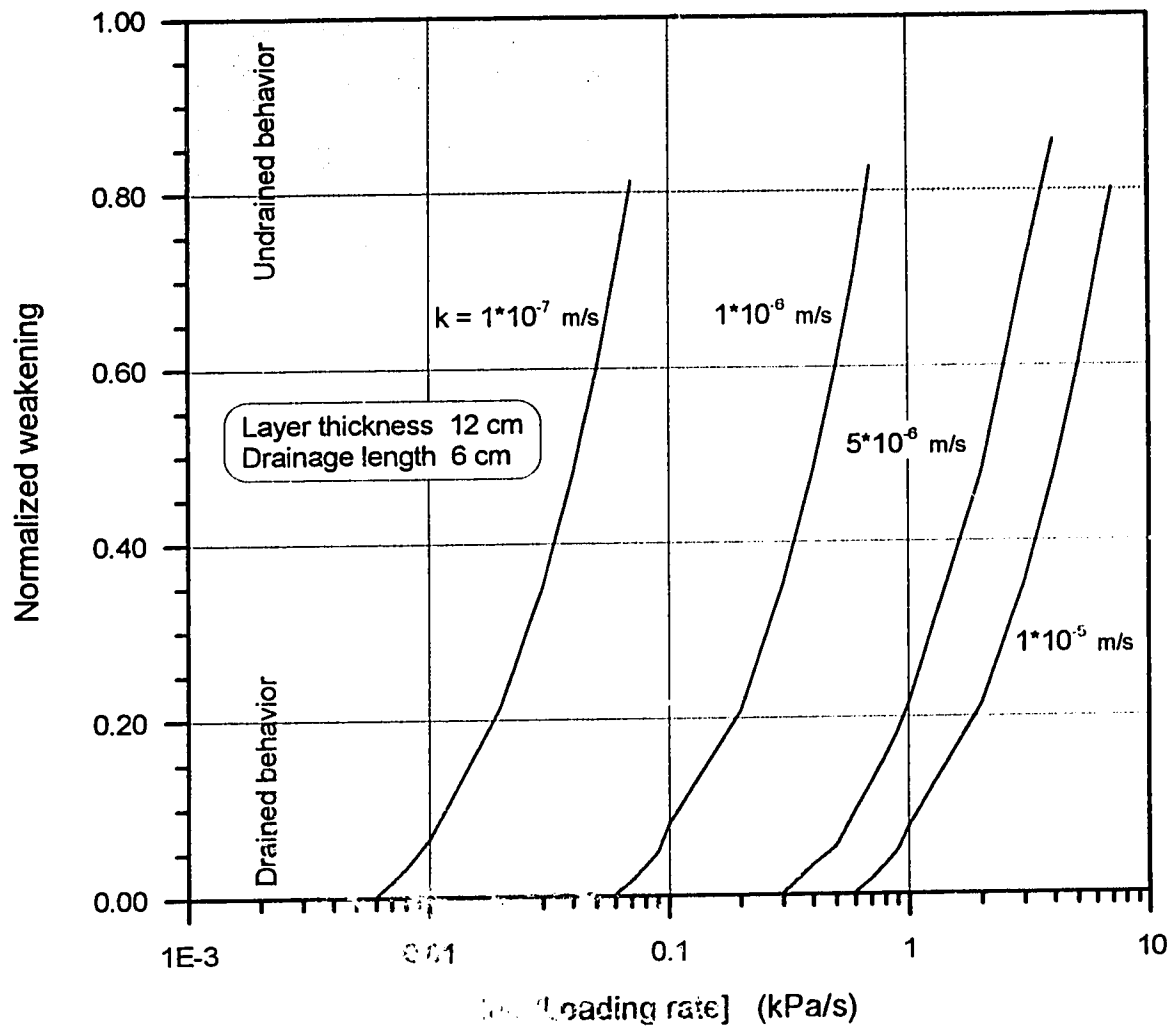


Fig. 4.4 Calculated transition between drained and undrained behavior during structural contraction

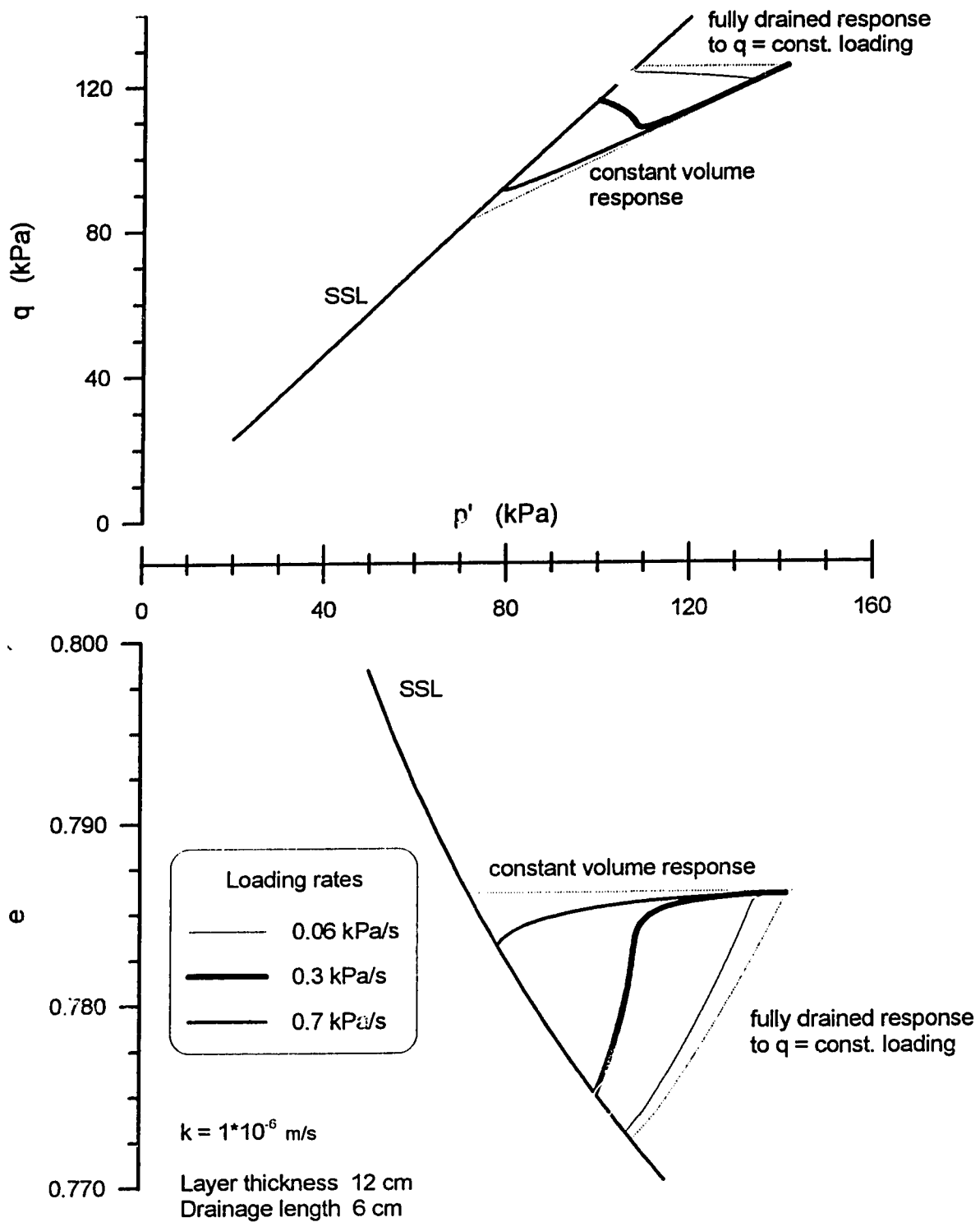


Fig. 4.5 Calculated effective stress path and contraction during structural contraction

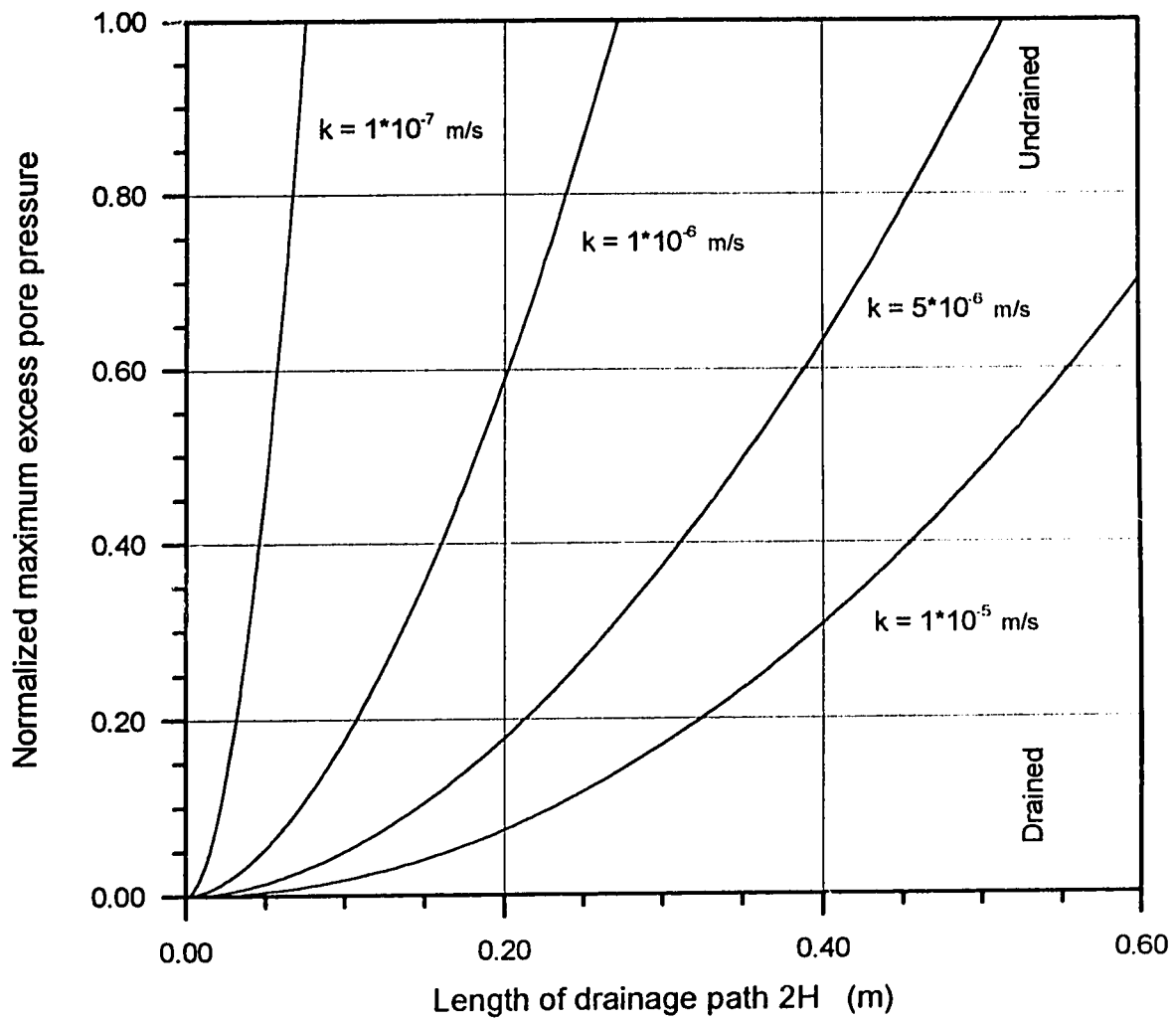


Fig. 4.6 Calculated maximum pore pressure generation during one structural collapse

REFERENCES

- Alarcon-Guzman, A., Leonards, G. A., and Chameau, J. L. (1988). "Undrained monotonic and cyclic strength of sands." *ASCE Journal of the Geotechnical Engineering Division*, 114(No.10), 1089-1109.
- Casagrande, A. (1936). "Characteristics of cohesionless soils affecting the stability of earth fills." *Journal of the Boston Society of Civil Engineers*, Vol. 23, No. 1, January, 257-276.
- Dawson, R. F., Morgenstern, N. R., and Gu, W. H. 1992. "Instability mechanisms initiating flow failures in mountainous mine waste dumps - Phase I." *Study for Energy, Mines and Resources Canada*, DSS contract #23440-0-9198/01-X8G.
- Dawson, R. F., Morgenstern, N. R., and Gu, W. H. 1994. "Liquefaction flowslides in Western Canadian coal mine waste dumps - Phase II: case histories." *Study for Energy, Mines and Resources Canada*, SSC file # XSG42-00138 (608), SSC contract 23440-2-9151/01-XSG.
- Eckersley, J. (1990). "Instrumented laboratory flowslides." *Géotechnique*, 40(3), 489-502.
- Evans, M. D., Seed, H. B., and Seed, R. B. (1992). "Membrane compliance and liquefaction of sluiced gravel specimens." *ASCE Journal of the Geotechnical Engineering Division*, 118(No.6), 856-867.
- Garlanger, J. E. (1972). "The consolidation of soils exhibiting creep under constant effective stress." *Géotechnique*, 22(1), 71-78.

- Gu, W. H., Morgenstern, N. R., and Robertson, P. K. (1993). "Progressive failure of The Lower San Fernando Dam." *ASCE Journal of the Geotechnical Engineering Division*, 119(No.2), 333-348.
- Lade, P. V. (1993). "Initiation of static instability in the submarine Nerlerk berm." *Canadian Geotechnical Journal*, 30(6), 895-904.
- Marcuson, III, W. F., Hynes, M. E. and Franklin, A. G. (1992). "Seismic stability and permanent deformation analyses: the last twenty five years" *Proc. of a Specialty Conference Stability and Performance of Slopes and Embankments II*, Vol. 1, edited by R. B. Seed and R. W. Boulanger, published by ASCE New York, 552-592.
- Martin, G. R., Finn, L. W. D. and Seed, B. H. (1975). "Fundamentals of liquefaction under cyclic loading." *ASCE Journal of the Geotechnical Engineering Division*, 101(No.GT5), 423-438.
- Plewes, H. D., O'Neil, G. D., McRoberts, E. C. and Chan, W. K. (1988) "Liquefaction consideration for Suncor tailings ponds." *Proc. Canadian Dam Safety Conference*, Calgary.
- Sasitharan, S., Robertson, P. K., Sego, D. C. and Morgenstern, N. R. (1993). "Collapse behavior of sand." *Canadian Geotechnical Journal*, 30(4), 569-577.
- Sasitharan, S., Robertson, P. K., Sego, D. C. and Morgenstern, N. R. (1994). "A state boundary surface for very loose sand and its practical implications." *Canadian Geotechnical Journal*, in press.
- Skopek, P., and Cyre, G. (1994). "A resistance wire transducer for circumferential strain measurement in triaxial test." *Geotechnical Testing Journal*, in press.

Skopek, P., Morgenstern, N. R., Robertson, P. K., and Sego, D. C. (1994).

"Collapse of dry sand." *Canadian Geotechnical Journal*, in press.

Skopek, P., Morgenstern, N. R., and Robertson, P. K., (1994). "State boundary surface for very loose sand." *ASCE Journal of the Geotechnical Engineering Division*, under review.

Sladen, J. A., D'Hollander, R. D., and Krahn, J. (1985b). "The liquefaction of sands, a collapse surface approach." *Canadian Geotechnical Journal*, 22, 564-578.

Terzaghi, K. (1956). "The submarine slope failures." *Proc. 8th Texas Conference on Soil Mechanics and Foundation Engineering*, U. Texas, Austin, 1-41.

Yegian, K. K., Ghahraman, V. G., and Harutiunyan, R. N. (1994). "Liquefaction and embankment failure case histories, 1988 Armenia earthquake." *ASCE Journal of the Geotechnical Engineering Division*, 120(No.3), 581-596.

A RESISTANCE WIRE TRANSDUCER FOR CIRCUMFERENTIAL STRAIN MEASUREMENT IN TRIAXIAL TESTS¹

INTRODUCTION

Tracking of local strains in a triaxial specimen has always been a difficult challenge. In our study on collapsing sand, the task was further complicated by the fact that the strains were occurring extremely rapidly, which required a stable fast response measurement transducer and a high speed (up to 30 times per second) data acquisition system. The measured deformations were later used for calculation of volume changes of unsaturated specimens. Hence, during a test the changes in specimen dimensions, namely axial and circumferential deformations, were measured directly.

Measuring of axial deformation is simple and is routinely conducted during any triaxial test usually with commercially available Linear Voltage Displacement Transducers (LVDT). Measurement of circumferential or lateral deformations is more difficult. The few commercially available devices are usually designed for somewhat specific conditions and have considerable restrictions (working range, size, method of data acquisition). This note presents a design of a transducer for measurement of circumferential deformations of a specimen inside a triaxial cell.

¹ A version of this paper has been accepted for publication. Skopcek, P., and Cyre, G. P. (1994). *Geotechnical Testing Journal*.

PROPOSED METHOD

In order to provide acceptable results, the transducer had to satisfy the following criteria:

- 1/ to be capable of measuring large circumferential deformations of up to 30 mm corresponding to 10 mm diameter change
- 2/ to be small enough to fit into the cell and measure at several locations along the specimen height
- 3/ to be stable for long duration
- 4/ to be accurate during rapid deformation changes and lend itself to high speed automatic data acquisition
- 5/ not to load or restrain the specimen
- 6/ not to be affected by changing cell pressure

Several methods for direct measurement of lateral deformations are found in the literature. They are, for example, the application of Hall Effect sensors is described by Clayton et al. (1989), proximity sensors by Hird and Yung (1989) or strain gage collars by Kolymbas and Wu (1989).

It was found that the existing mechanisms for measurement of lateral deformations, while being quite accurate, were usually either too large or the working range was unacceptably limited. Because of these limitations it was decided to pursue the development of a transducer specific to our requirements. It appeared that a solution with direct measurement of circumferential changes using a resistance wire wound freely around the specimen was best suited for our purposes. It was quite easy to accommodate several of these **resistance wire transducers** along the height of the specimen and so obtain an accurate measurement of its changing circumference. A similar idea to the proposed system was used for measuring small lateral strains of rock specimens by Attinger and Köppel (1983). This system was based on the

principle of the change of electrical resistance during straining of a fixed wrapped resistance wire.

The main component of the resistance wire transducer is a high resistance KARMA wire. The diameter of this wire is 0.063 mm and it is supplied by the firm British Driver-Harris Co. Ltd., Stockport (GB). The specified resistance of the wire is 390 Ω /m. The wire is wound once around the specimen (Fig. 5.1 and Fig. 5.2). One end is fixed on one of the two gold plated pins, i.e., pins virtually without any electrical impedance, fixed in the plastic plate. The plate is positioned on the side of the specimen. The wire goes around the specimen, back to the plate, winds freely around the second gold plated pin and tangentially turns back and hangs over a small nonconductive cantilever. This end of the wire is tensioned by a 20 gram weight. The load keeps the wire tight around the specimen and is sufficiently small that the wire does not cut into the membrane and still allows free movement as the specimen deforms. Also the plastic plate does not require any fixing to the specimen membrane because the tension in the wire is sufficient to keep the whole system in place.

The resistance wire transducer is an active arm of a Wheatstone Bridge (Fig. 5.3). The bridge completion is accomplished by using precision resistors. The bridge is excited by 4 Volts in order to optimize the output to the data acquisition system. Excessive excitation could result in heating of the wire, thus damaging the membrane. As the specimen deforms the length of the wire between two fixed points on the specimen circumference, i.e., between the two gold plated pins, increases. This produces, due to the change of resistance, a change in the voltage differential signal output. The signal is amplified 50 times and recorded by the data acquisition system along with all other monitored data and timer information.

The calibration of the transducer was conducted using a micrometer and a calibration setup shown in Fig. 5.4. The calibration data of several resistance wire transducers is compiled in Fig. 5.5. It should be noted that the calibration is unique to

the system rather than to the individual transducer. Additional testing conducted over a duration of two weeks showed that longer term stability was not a concern. The accuracy of the resistance wire transducer is similar to commercially available rectilinear potentiometers. The resistance wire transducer has high output linearity, low noise problems and virtually infinitive resolution, which is controlled essentially only by the quality of the data acquisition system. The calibration curve indicates that the accuracy is about 0.01 % of full scale output, hence the transducer can be used for measurement of small strains. Linearity was established by analysis using the least squares method. The coefficient of determination (r^2) combined for all calibration sets was 0.999. It was found that the resistance wire transducer is not affected by the cell pressure and can be used even for high stress ranges. The effects of temperature change were not considered after testing showed that the temperature sensitivity was less than 0.005 %/°C. This value is similar to other rectilinear potentiometers. The transducers were continuously excited hence any heating from excitation was not a factor.

The effective working range of the resistance wire transducer for measurement of lateral deformations of a triaxial specimen is basically controlled by the height position of the supportive cantilever. As the specimen deforms the tension weight goes up and eventually is stopped on the cantilever. Therefore, the distance between the initial position of the weight and the supportive cantilever also controls the amount of measurable deformation. In the testing program circumference changes up to 34 mm were measured.

As a further check of reliability of the resistance wire transducer a graduated grid paper tape (girth belt) was wrapped around the specimen. Visual readings were taken through the transparent plexiglass wall of the triaxial cell at times when deformations were stabilized or sufficiently slow so that it was possible to synchronize them to the computerized data acquisition system.

An additional advantage of the resistance wire transducer in the determination of lateral deformations is the logical averaging of strains across the whole cross-sectional area of the specimen. It averages out any strain concentration within the appropriate horizontal cross-section. Average diameter deformations can be easily calculated using the following formula $\Delta D = \Delta C / \pi$, where ΔD is the diameter increment (calculated) and ΔC is the circumference increment (measured). This approach virtually increases the accuracy of the measurement over a direct lateral deformation measurement by the factor π .

The transducer also allows for the measurement of decreasing as well as increasing circumference. The tension load keeps the wire stretched at all times. Circumferential contraction was successfully measured during the initial application of the cell pressure during triaxial tests. For measurement of contractive strains the membrane has to be smooth and free of wrinkles. Irregularities in the membrane can lock the wire and thus obstruct the necessary free movement around the gold plated pin. In circumferential extension this “locking” of the wire does not occur even when wrinkles develop because the movement is ensured by the strength of the wire.

Due to the conductive nature of the resistance wire transducer, compressed air instead of water or oil was used as the cell pressure medium. Using air as the cell medium introduced a small but tolerable inertia in cell pressure control.

APPLICATION

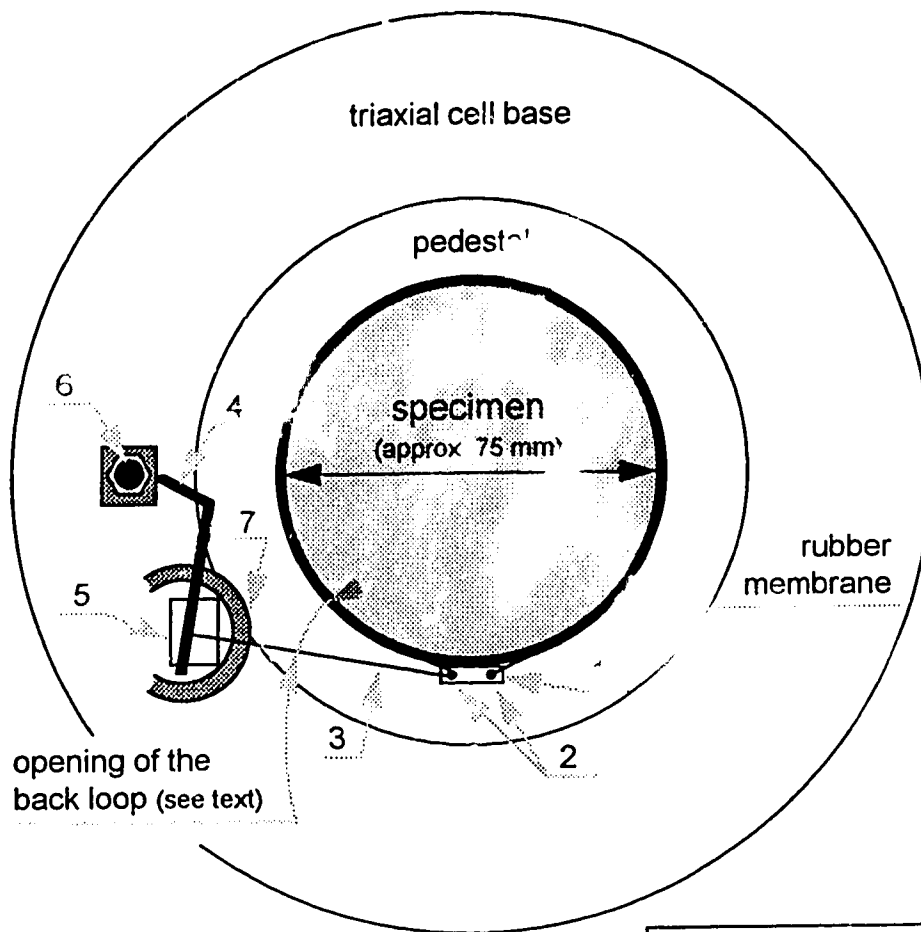
The resistance wire transducers are mounted before the triaxial cell is assembled when the specimen is sufficiently stiff to be self-supportive or when a vacuum is applied to supply the necessary stiffness. The resistance wire transducers have to be aligned horizontally to maintain the shortest path as possible between the pins. One transducer requires a band about 2.5 cm high on the circumference of the specimen to be properly mounted, hence three transducers can be easily fixed on a 10 cm high

specimen. The height of the tension weight above the base has to be properly adjusted so the seating of transducers and/or consolidation of the specimen would not result in excessive lowering of tension weights to the point of contacting the triaxial base. The opening of the back loop (the horizontal distance between the membrane and the arm of the wire going towards the supportive cantilever after turning around the gold plated pin (Fig. 5.1)) has to be sufficient to avoid an electrical short with the returning arm of the transducer or contact between the wire and the membrane as the specimen bulges. After the transducers are in place, the guide cylinders for the weights are positioned to prevent swinging of the weights during the test.

During a test the volume of the specimen at any recording time is calculated after a deformed cross-section is established using the circumference change and axial deformation reading. The volume is calculated by integration of the deformed cross-section. Typical results of a test with the volume change converted to void ratio are presented in Fig. 5.6.

SUMMARY

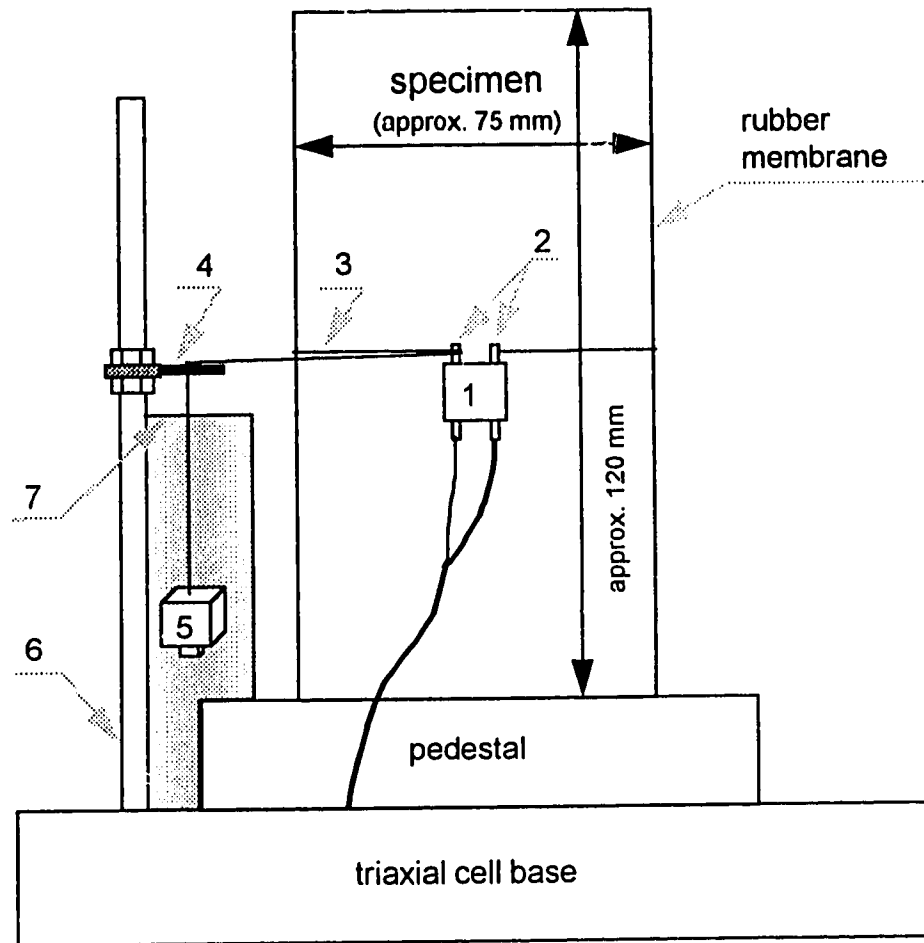
The proposed measuring system has proved acceptable and produced reliable readings of circumferential deformations which can be easily converted into lateral deformations. The resistance wire transducer is a simple device whose principle can be used for a broad spectrum of analogous laboratory applications. The principle of the resistance wire transducer is similar to commercially available rectilinear potentiometers. This category of devices has virtually an infinitive resolution, which is controlled essentially only by the quality of the data acquisition system. Therefore, they can be used for measurement of small strains. The resistance wire transducers are especially useful under conditions where space restrictions apply. It also appears that they are not affected by the cell pressure and can be used even for extreme confining stress ranges.



NOT TO EXACT SCALE !

- | | |
|---|-----------------------|
| 1 | plastic plate |
| 2 | gold plated pins |
| 3 | resistance wire |
| 4 | supporting cantiliver |
| 5 | 20 g tension load |
| 6 | post |
| 7 | guide cylinder |

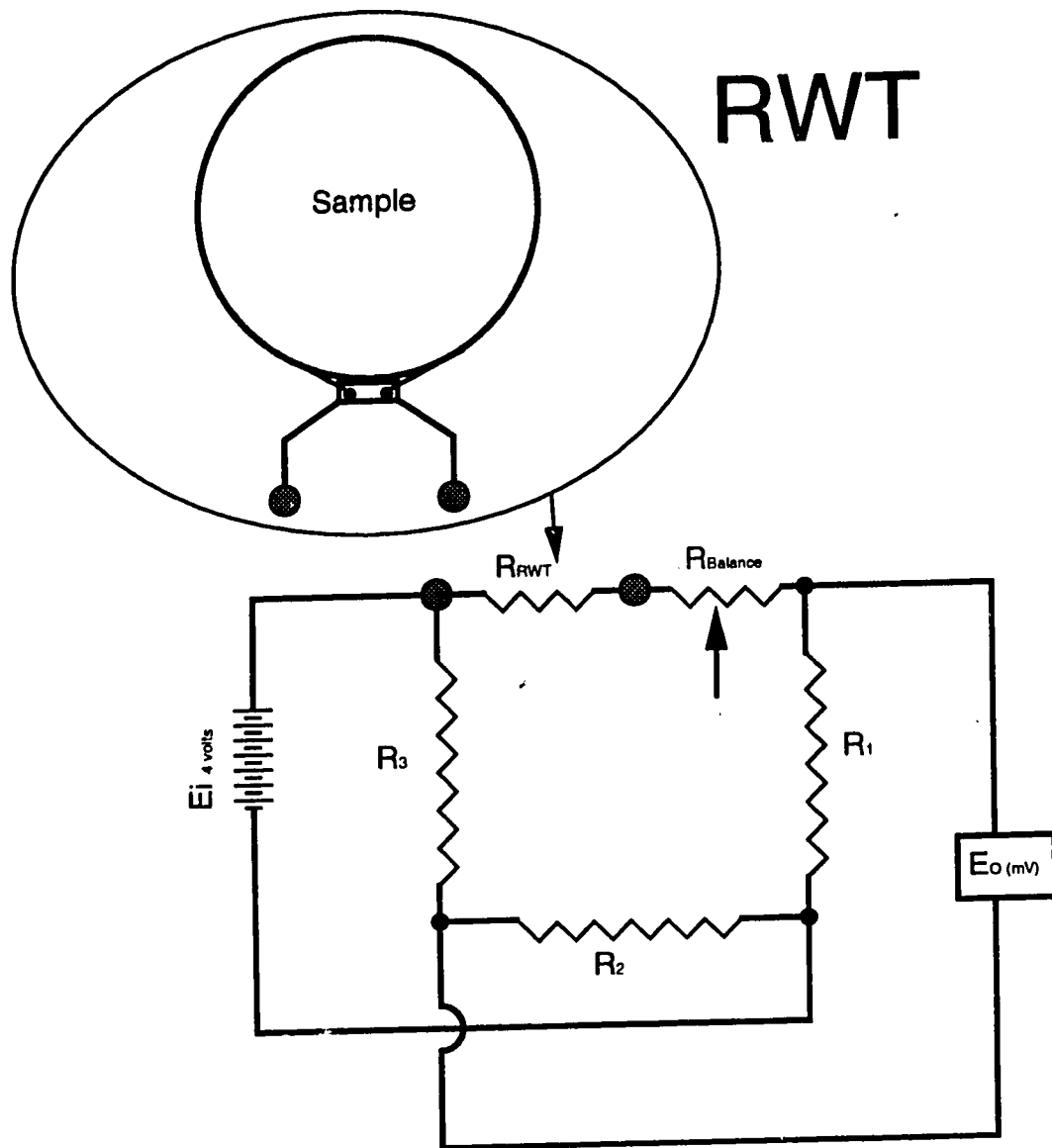
Fig. 5.1 Top view of the resistance wire transducer assembly



See legend for Fig. 5.1

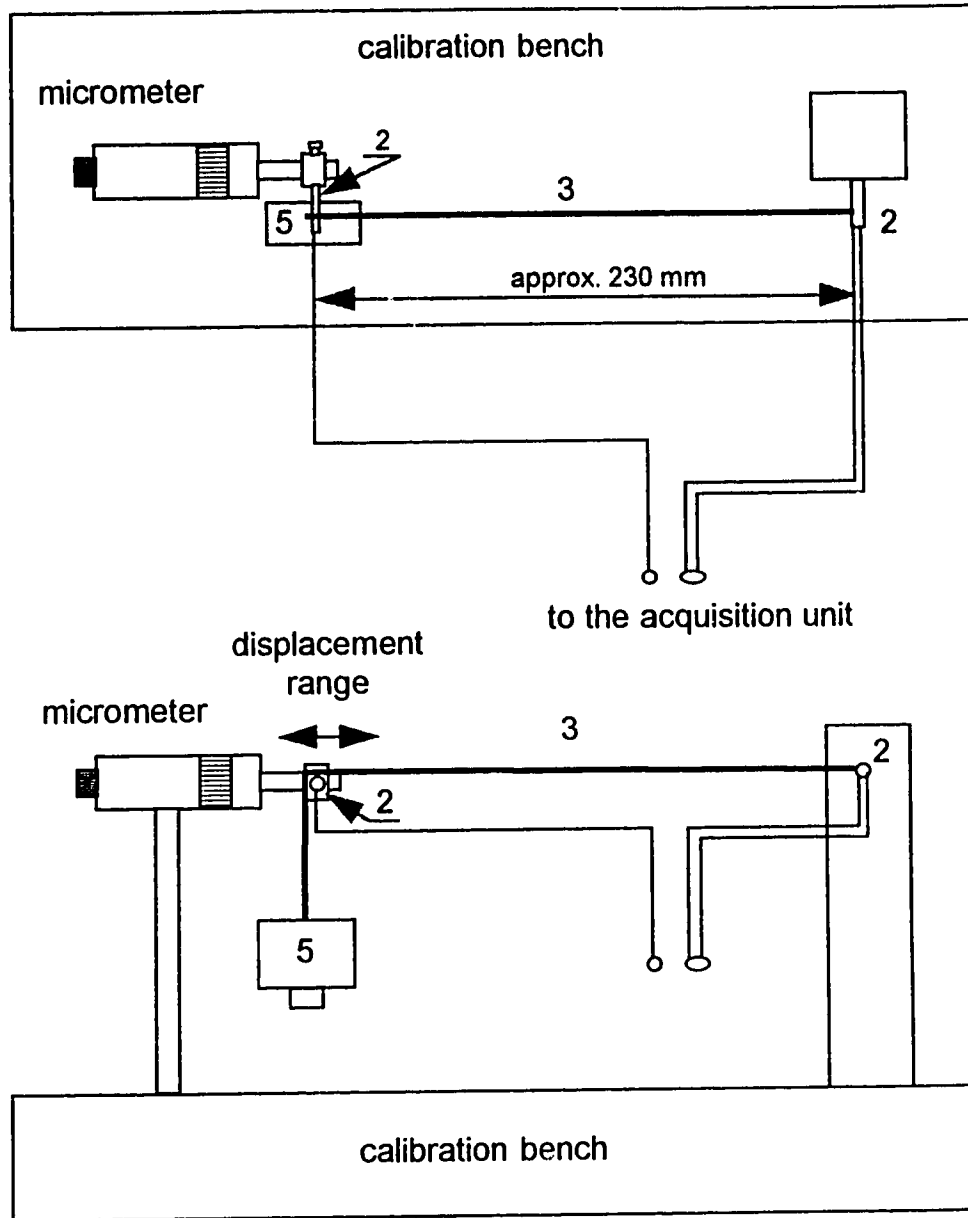
NOT TO EXACT SCALE !

Fig. 5.2 Front view of the resistance wire transducer assembly



E_o - Output Voltage (mV)
 E_i - Excitation (Volts)
 $R_{\#}$ - Precision Resistors
 $R_{Balance}$ - Balancing Potentiometer
 R_{WT} - Resistance Wire Transducer

Fig. 5.3 Wheatstone Bridge schematic for the resistance wire transducer



See legend for Fig. 1

Fig. 5.4 Calibration setup for the resistance wire transducer

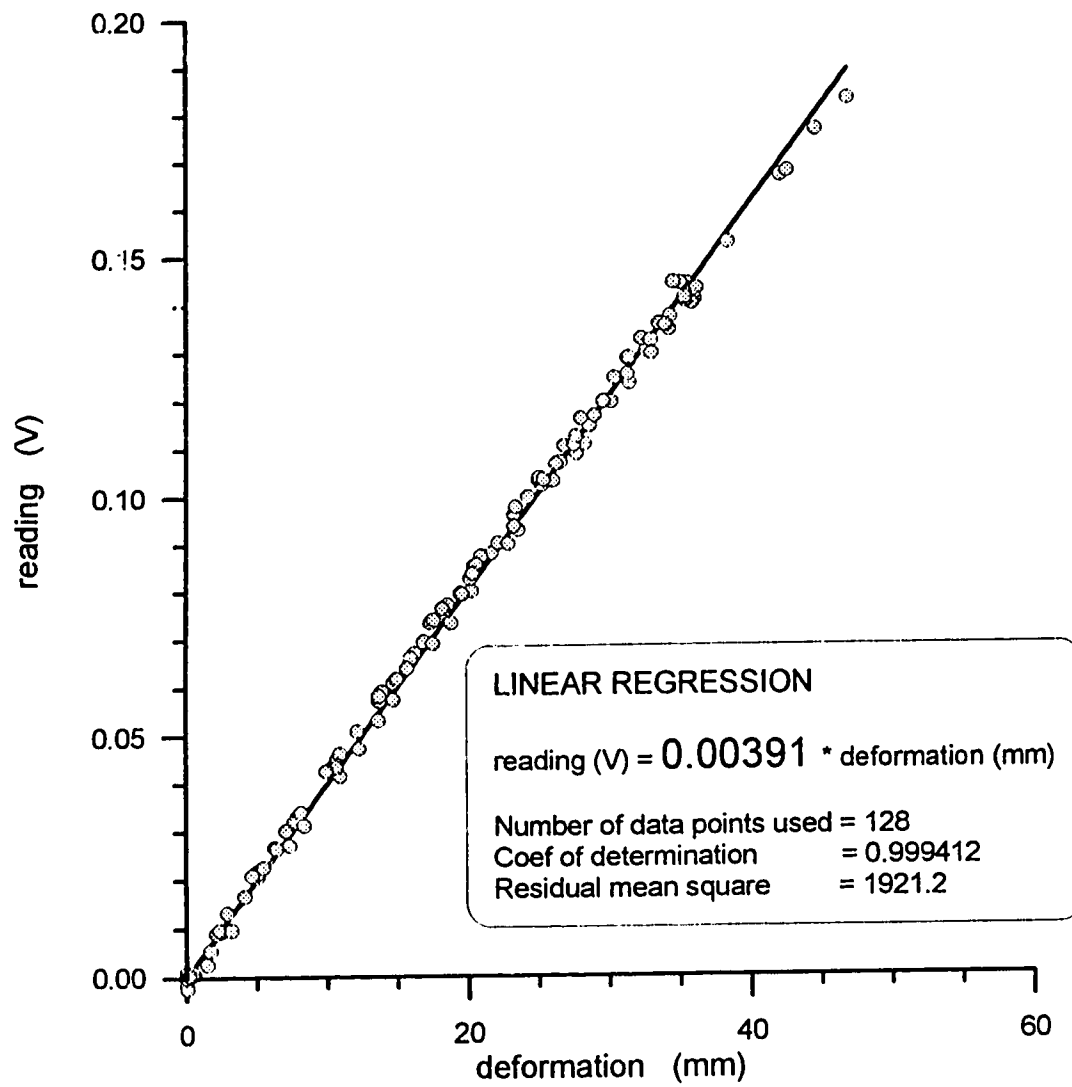


Fig. 5.5 Calibration for resistance wire transducer

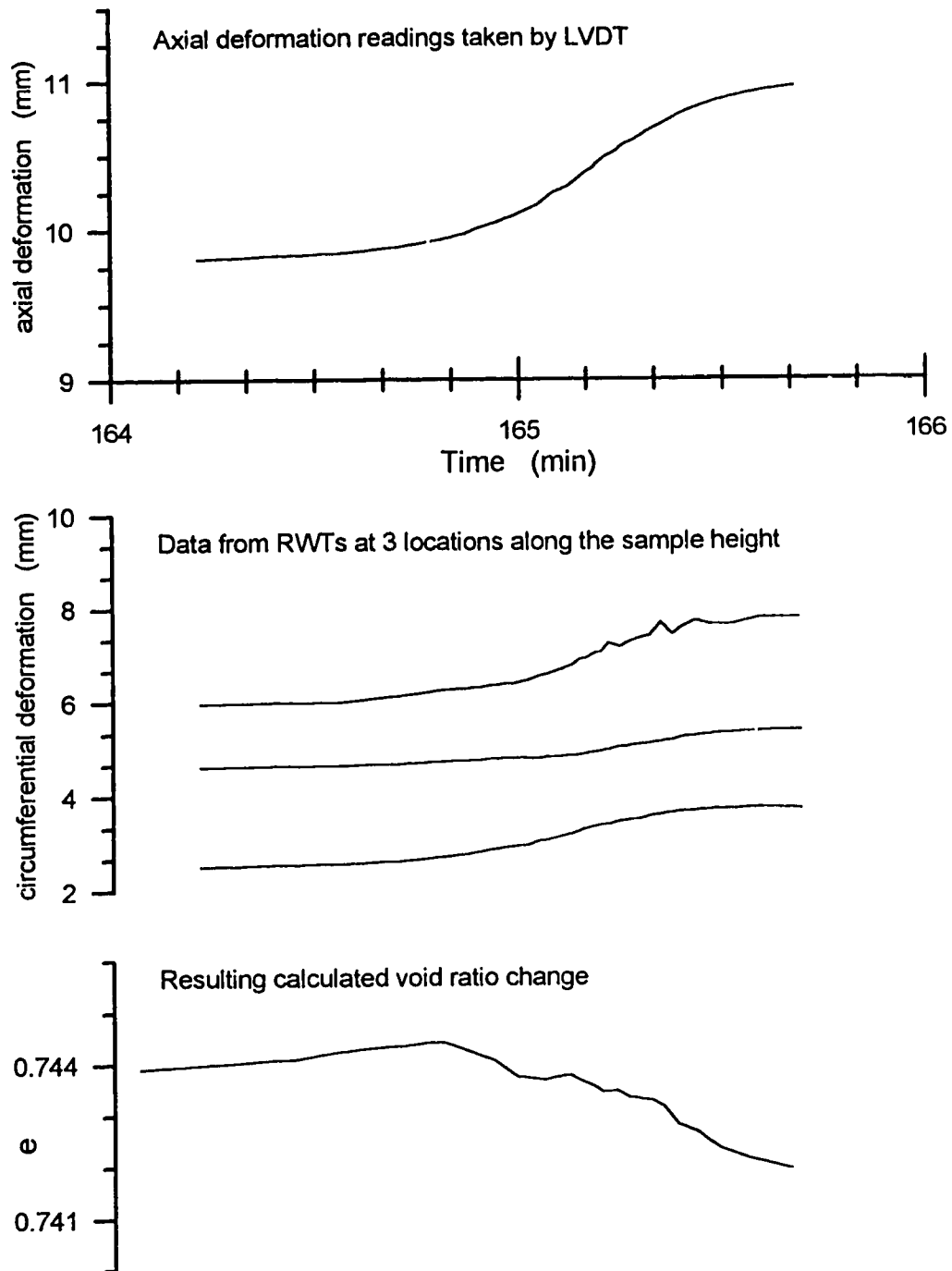


Fig. 5.6 Typical axial and circumferential deformation record during a test and associated calculated void ratio

REFERENCES

- Attinger, R. O. and Köppel, J. (1983). "A new method to measure lateral strain in uniaxial and triaxial compression tests." *Rock Mechanics and Rock Engineering*, 16(No.1), 73-78.
- Clayton, C. R. I., Khatrush, S. A., Bica, A. V. D. and Sidique, A. (1989). "The use of Hall Effect semiconductors in geotechnical instrumentation." *Geotechnical Testing Journal*, GTJODJ, 12(No.1), 69-76.
- Hird, C. C. and Yung, P. C. Y. (1989). "The use of proximity transducers for local strain measurements in triaxial tests." *Geotechnical Testing Journal*, GTJODJ, 12(No.4), 292-296.
- Kolymbas, D. and Wu, W. (1989). "A device for lateral strain measurement in triaxial tests with unsaturated specimens." *Geotechnical Testing Journal*, GTJODJ, 12(No.3), 227-229.

SUMMARY AND CONCLUSIONS

The detailed objectives of this study were to investigate:

1. the behavior of a very loose dry sand during a $q = \text{constant}$ triaxial stress path which was shown to initiate flow liquefaction in the same very loose saturated sand.
2. the validity of the state boundary surface concept for very loose dry sand. This was accomplished by testing the material under a variety of different triaxial stress paths.
3. the fundamental mechanisms controlling flow liquefaction in order to present a theory in terms of effective stresses for evaluating flow liquefaction.

The behavior of very loose dry Ottawa sand during a $q = \text{constant}$ triaxial stress path is discussed in Chapter 2. It is shown that dry sand experiences several distinct stages during such a stress path. First it behaves almost elastically with very small volume change. At a certain point the response changes, the sand becomes increasingly compressible and the loading path in a $p' - e$ plane is deflected and after a short transition stage establishes a new direction towards the ultimate steady state. This stage of high compressibility was named structural contraction. It is shown in Chapter 3 that structural contraction occurs on the state boundary surface which acts as an impenetrable wall for the loading path and forces the state condition to follow along this surface. During structural contraction during a $q = \text{constant}$ stress path test the sand is unstable and structural collapses can arise, i.e., rapid stress independent contractive events. The stress state for the element of soil then drops from the state boundary surface into an essentially elastic domain below. During further loading the soil element initially behaves almost elastically until it again reaches the state boundary

surface. The tests carried out in this study have demonstrated that the onset of structural contraction is associated with attaining the state boundary surface and the following structural collapses occur at mobilized effective friction angles well below the ultimate steady state friction angle. It is shown in Chapter 3 that the state boundary surface also controls and deflects the loading path of very loose dry Ottawa sand during triaxial compression test, $p' = \text{constant}$ tests and a special loading path test with limited allowed strains. A unique mathematical formulation of the state boundary surface based on the formulation presented for very loose saturated sand is derived for very loose dry sand.

Two tests on medium dense dry Ottawa sand presented in Chapter 3 exhibited a temporary minor contraction before dilating towards the ultimate steady state. It appears that this phenomenon agrees well with the observations on the so called instability line (Lade 1993) or critical stress ratio line (Vaid and Chern 1985) during undrained tests on saturated sand where the sand temporarily loses a portion of its shear strength and develops a so called quasi steady state. The existence of this effect for medium dense dry sand can provide some insight into the fundamental mechanism of the quasi steady state. However, more testing on dry samples is needed to justify this claim.

Chapter 4 draws on the observations made during the triaxial laboratory testing program and formulates an effective stress based theory for the evaluation of flow liquefaction. It is recognized that the volume changes in dry material controlled by the structural contraction on the state boundary surface and volume changes occurring during structural collapse are inhibited by the presence of pore fluid in an identical saturated material. The measure of the resistance against this volume change is controlled by the rate at which the pore fluid can escape from the material, hence by drainage conditions.

Current procedures that utilize the collapse surface in flow liquefaction analysis assume in common with other liquefaction analyses that once liquefaction is triggered, subsequent deformation is undrained. This is obviously a gross over-simplification of the liquefaction process because it cannot distinguish between a soil composed of either fine sand or large boulders. In the latter case, the rate of dissipation of pore pressures could be commensurate with the rate of pore pressure generation and upon triggering of liquefaction only volume changes would be generated.

The proposed theory links the volume changes in a fully drained material with the pore pressure generation in an identical saturated undrained material. Such generated pore pressures are then dissipated according to a consolidation theory, which introduces the actual drainage conditions in terms of the permeability and the length of the drainage path. It is concluded that structural contraction along the state boundary surface for “natural” loading rates does not have the potential for producing large pore pressures necessary for initiating material weakening, stress redistribution and progressive propagation of collapse. However, the experience from Suncor tailings pond construction (Plewes et al. 1988) indicates that large volumes of loose subaqueous tailings are susceptible to flowslides during intense seasonal construction representing an increased loading rate.

Results based on the measured structural collapses calculated using the proposed theory indicate that large pore pressures are generated in the soil even for relatively short drainage paths and high permeabilities. Significant weakening can be produced which can result in triggering another collapse which would further elevate the pore pressures and boost material weakening. The magnitude of generated pore pressures is also controlled by the amount of contraction, i.e., a structural collapse must produce sufficient volume change. That implies that a limiting criterion can be based on the amount of contraction. The material which does not exhibit sufficient contraction during a structural collapse or does not exhibit structural collapse at all may not be

susceptible to flow liquefaction under “natural” loading rates even though it still exhibits weakening during triaxial undrained loading.

The presented theory for evaluation of liquefaction is considered to embrace most of the important factors controlling liquefaction, i.e., permeability, compressibility, and drainage path. It is capable of assessing the influence of specific drainage conditions and can be applied to numerical evaluation of structures or formations susceptible to liquefaction under circumstances where liquefaction mitigating measures are being developed.

RECOMMENDATIONS FOR FUTURE WORK

The author is aware of the fact that this study deals with a field which is relatively unresearched and therefore there is considerable additional work to be undertaken. Testing of dry material eliminates any affects of the pore media and discloses only the genuine material response. The biggest obstacle associated with this type of testing is the monitoring of volume changes. However, this study presents a very reasonable and flexible solution to this problem in Chapter 5.

The recommendations for the future work can be divided into several categories:

The first category are topics associated with the state boundary surface. It is necessary to investigate the relationship between the saturated and dry state boundary surface. It may be expected that these surfaces will be different due to the lubricating effects of the pore fluid and other factors. For the constitutive modeling it is necessary to investigate the actual shape of the state boundary surface (high stresses, etc.), which is here approximated as a warped surface, in order to obtain information about any change in curvature and other possible limiting surface geometry. There is also the issue related to the intrinsic instability of the material on the state boundary surface. Therefore, long term tests to study creep effects on the state boundary

surface are desired to gain some insight into the spontaneous trigger of flow liquefaction. In addition many other stress paths merit investigation.

The second category deals with topics associated with structural collapse. It has been shown, that structural collapses take place during triaxial $q \cong \text{constant}$ loading on the state boundary surface. However, no collapses were recorded during a conventional triaxial compression test. Hence, a variety of different load controlled triaxial stress paths should be applied to a “ $q = \text{constant}$ collapsible” material in order to define the stress path directions associated with structural collapses.

The third category relates to tests in extension and cyclic tests on very loose dry sand. These tests would be valuable in order to extend the state boundary surface concept as a general concept governing the behavior of loose granular materials. The two tests on medium dense dilatant sand carried out in this study suggest that the temporary instability commonly described in the literature during undrained triaxial testing for both conventional and cyclic loading can be a result of the material response. In general it appears that the concept of testing the dry material offers a great potential of discerning the true material properties from phenomena controlled by externally imposed drainage conditions.

The fourth category deals with the extension of the above to a broad spectrum of natural materials. Ottawa sand is an excellent starting material, however, it will be important to test other natural and man-made materials to gain more experience with all the facets of the presented study.

The fifth category relates to the application of the presented effective stress based theory of liquefaction evaluation to a numerical model. This theory provides an extension to the currently available strain softening models which commonly assume undrained behavior once material weakening is initiated. However, most of the above mentioned issues should be addressed before this endeavor can be undertaken.

The presented attempts to explain the intriguing phenomenon of flow liquefaction in a very reasonable and sensible way. Moreover, it suggests a way of handling the peculiarity of soil mechanics called the effective stresses. The research was driven by well established soil mechanics axioms as well as by geotechnical common sense. However, as it is commonly the case, at the end there are more questions than at the beginning. Nonetheless, now we know, which questions need to be addressed.

REFERENCES

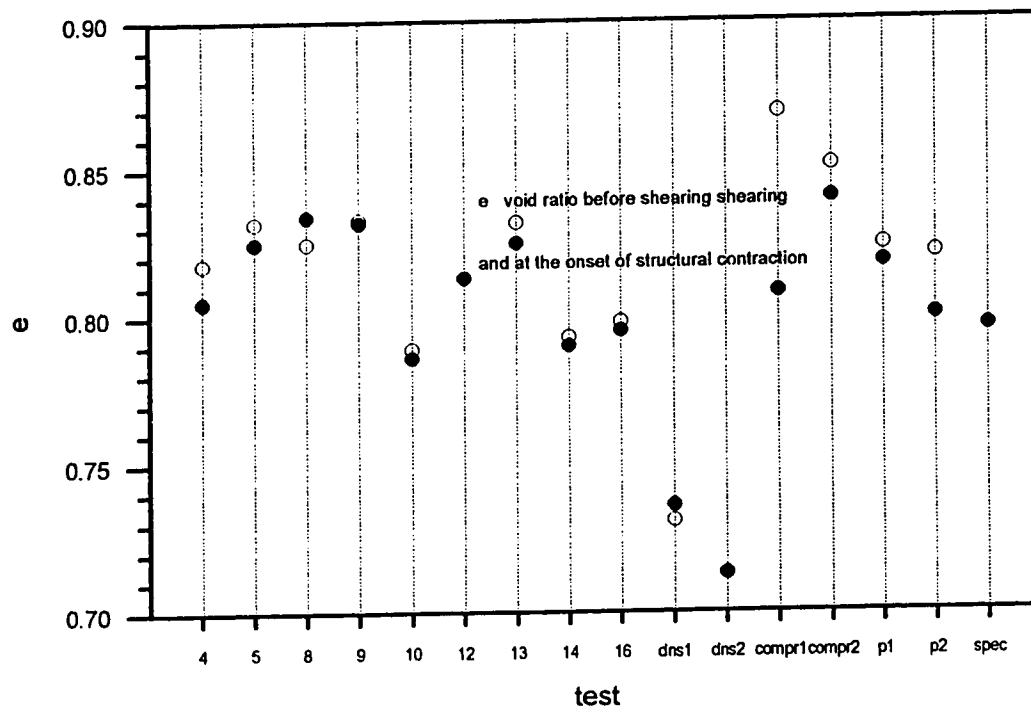
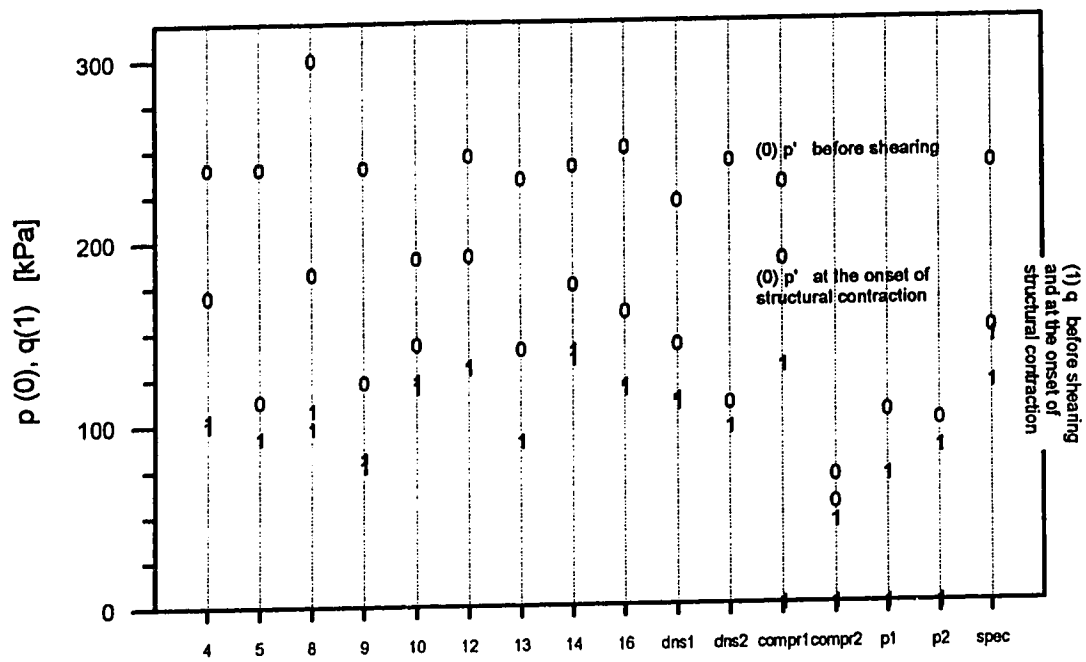
- Lade, P. V. (1993). "Initiation of static instability in the submarine Nerlerk berm." *Canadian Geotechnical Journal*, 30(6), 895-904.
- Plewes, H. D., O'Neil, G. D., McRoberts, E. C. and Chan, W. K. (1988)
"Liquefaction consideration for Suncor tailings ponds." *Proc. Canadian Dam Safety Conference*, Calgary.
- Vaid, V. P., and Chern, J. C. (1985). "Cyclic and monotonic undrained response of saturated sands." *Advances in the Art of Testing Soils Under Cyclic Conditions*, Edited by V. Khosla, ASCE, New York, N. Y., 120-147.

APPENDIX I Summary of Test Characteristics

Summary of tests

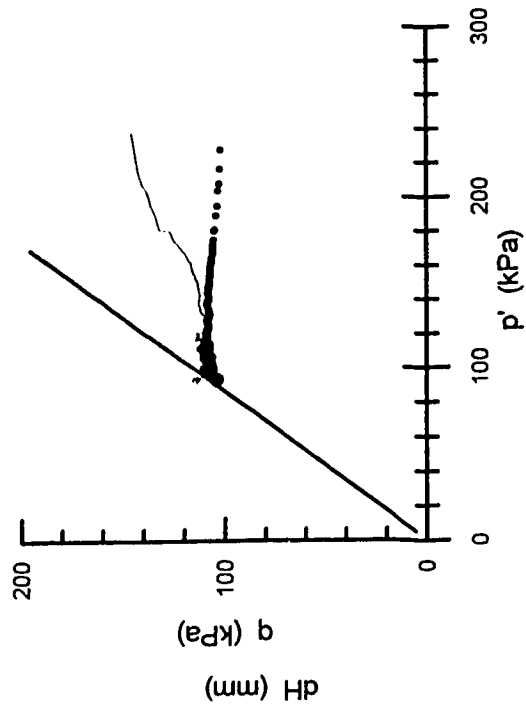
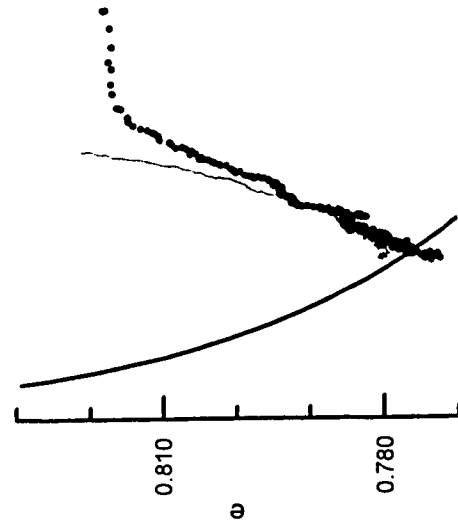
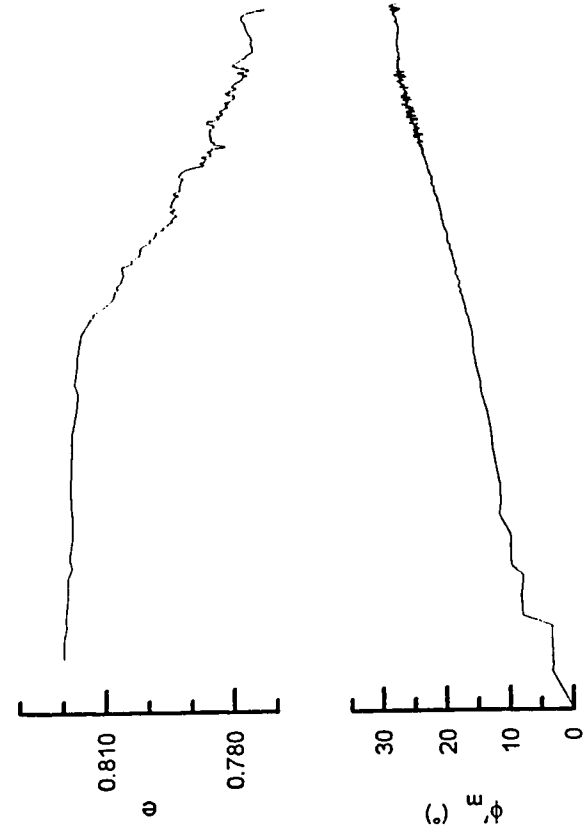
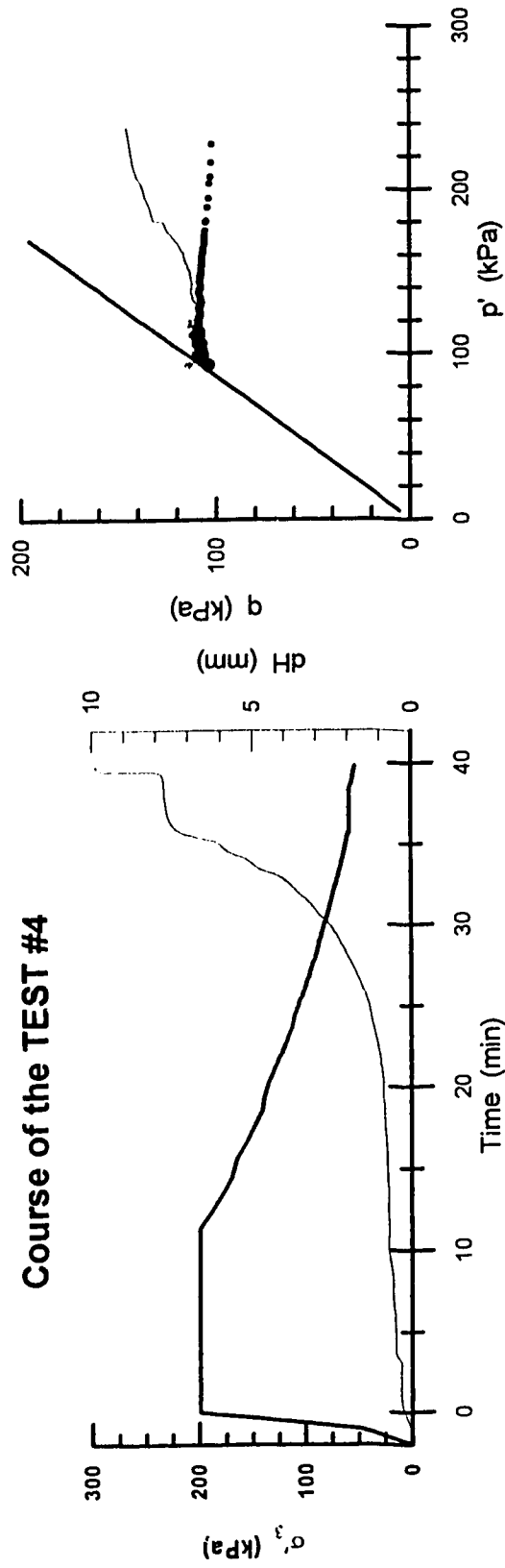
test #	preparation		after consolidation, before shearing			onset of structural contraction			
	e_{prep}	m.c. (%)	p'_{init} (kPa)	q_{init} (kPa)	e_{init}	p'_{brk} (kPa)	q_{brk} (kPa)	ϕ'_{brk}	e_{brk}
4	0.821	3.57	240	100	0.818	170	103	16.0	0.805
5	0.834	4.14	240	93	0.832	113	93	21.2	0.825
8	0.840	3.31	300	98	0.825	182	108	15.7	0.834
9	0.850	2.54	240	77	0.833	123	81	17.3	0.832
10	0.814	2.74	190	120	0.789	143	123	22.1	0.786
12	0.841	2.51	246	130	0.813	191	131	17.9	0.813
13	0.835	2.58	233	90	0.832	140	90	16.9	0.825
14	0.800	2.49	240	135	0.793	175	139	20.5	0.790
16	0.810	2.49	250	118	0.798	160	120	19.5	0.795
dns1	0.709	0.00	220	110	0.731	142	112	20.4	0.736
dns2	0.738	2.49	242	97	0.713	110	97	22.6	0.713
compr1	0.869	3.00	188	0	0.869	230	130	15.0	0.808
compr2	0.851	2.72	55	0	0.851	70	45	16.9	0.840
p1	0.838	2.70	105	0	0.824	105	70	17.5	0.818
p2	0.823	2.00	100	0	0.821	100	85	21.9	0.800
spec	0.820	2.42	240	120	0.796	150	145	24.6	0.796

State boundary surface parameters	
Γ	0.930261
λ	0.0337
M	1.15427
β	0.6



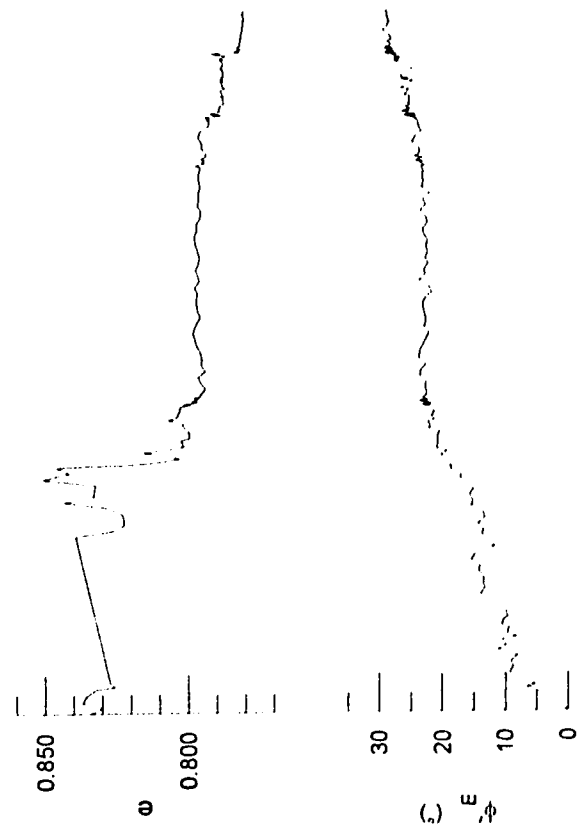
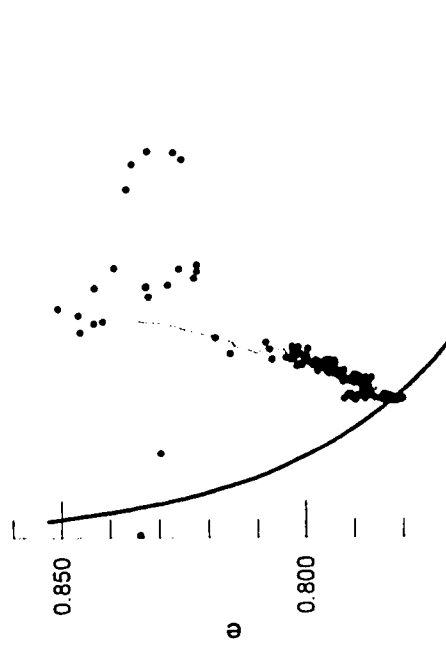
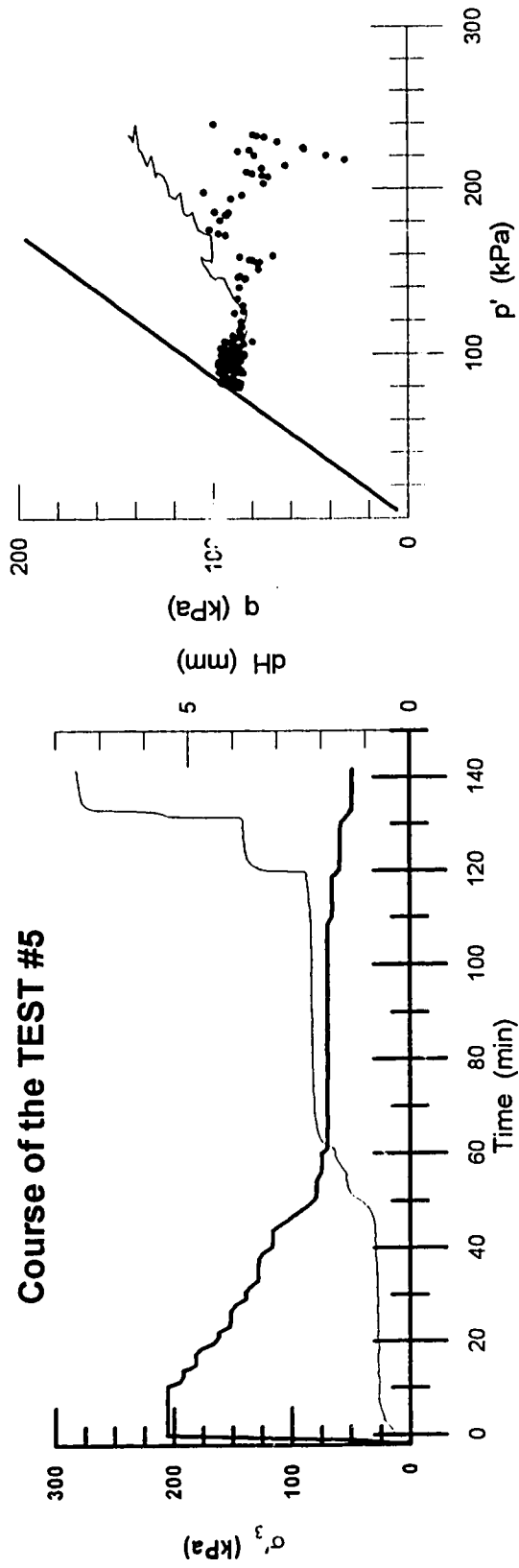
APPENDIX II Course of the tests

Course of the TEST #4

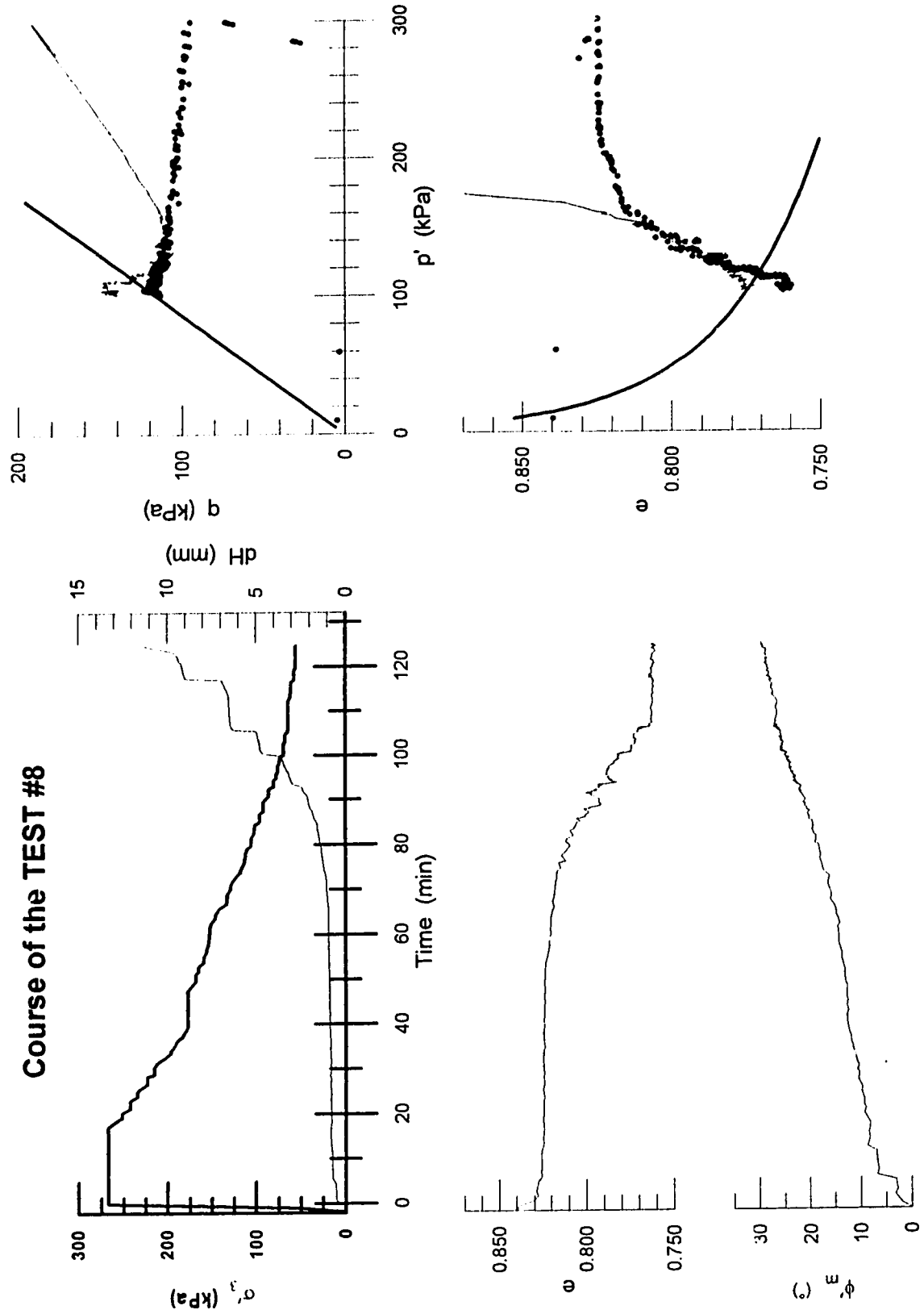


Remark: Relatively fast shearing evoking pronounced structural contraction

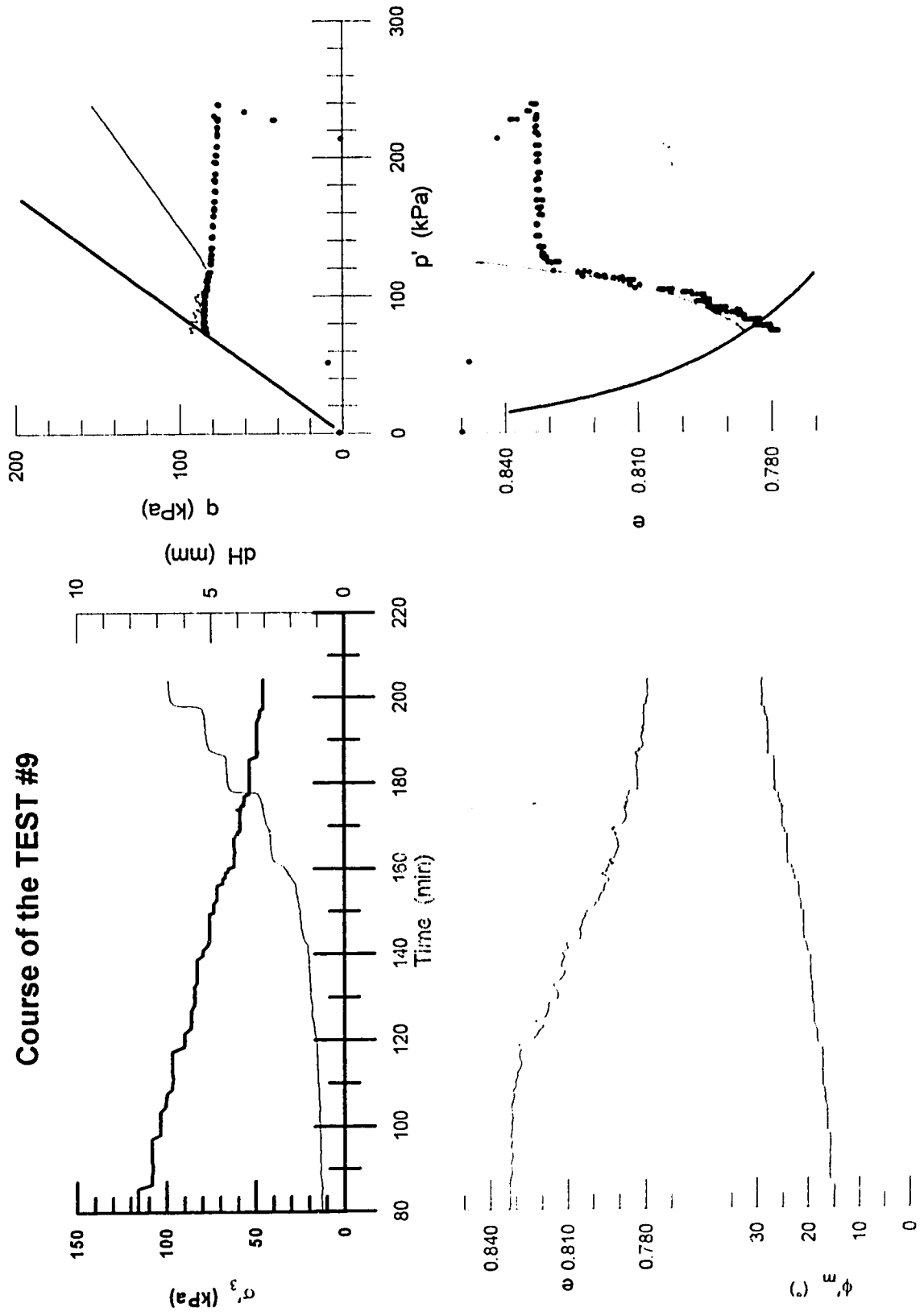
Course of the TEST #5



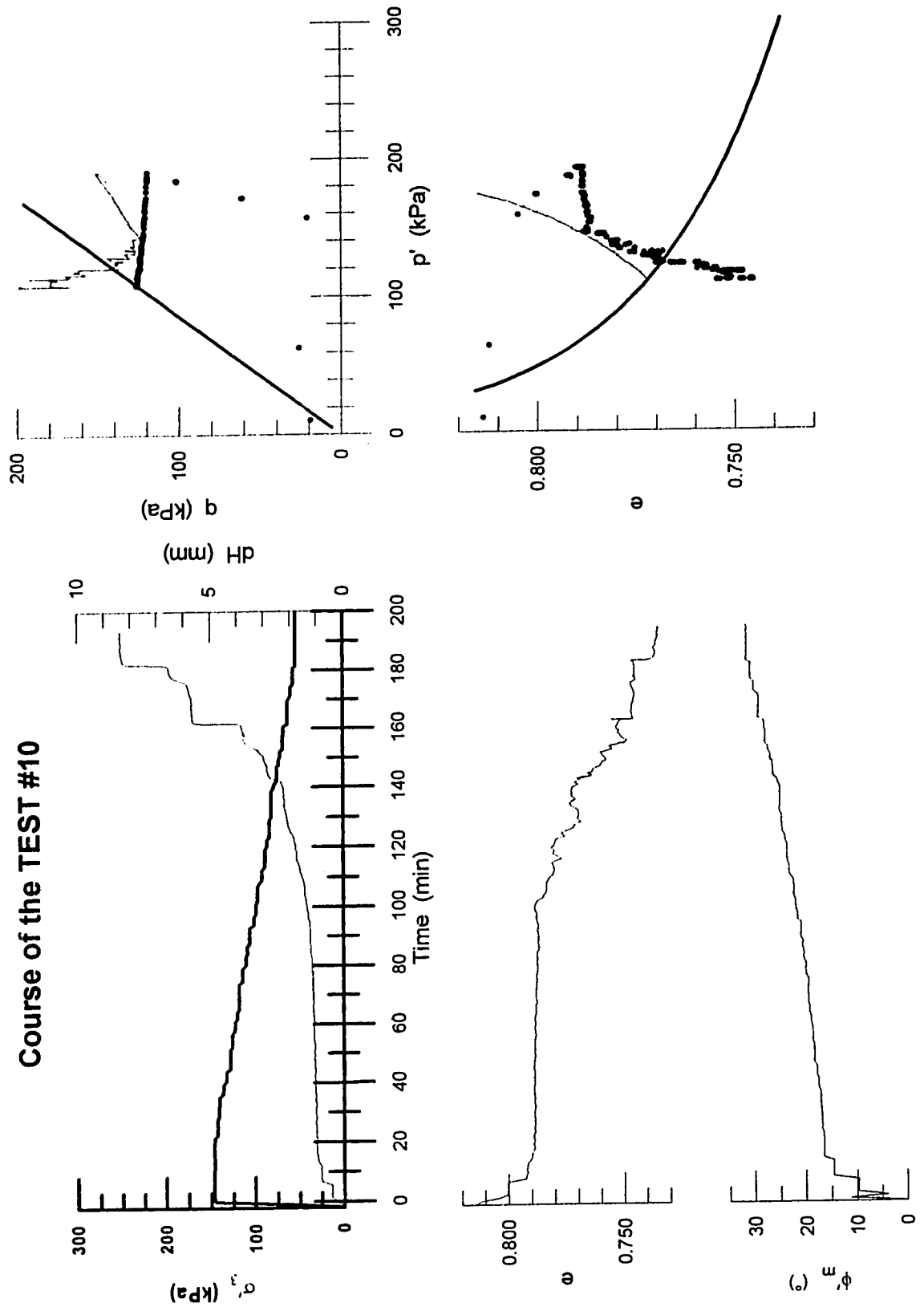
Course of the TEST #8



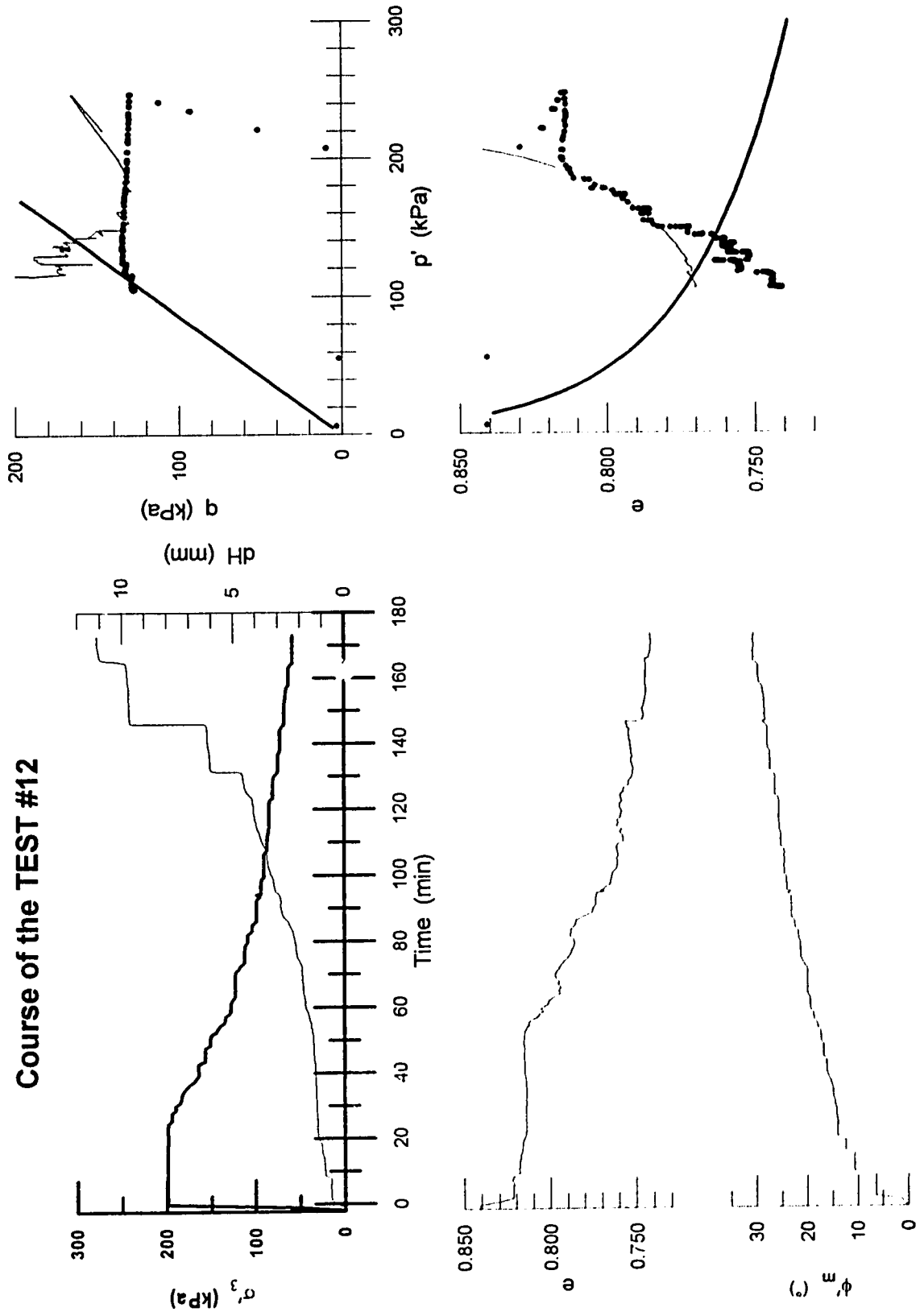
Course of the TEST #9



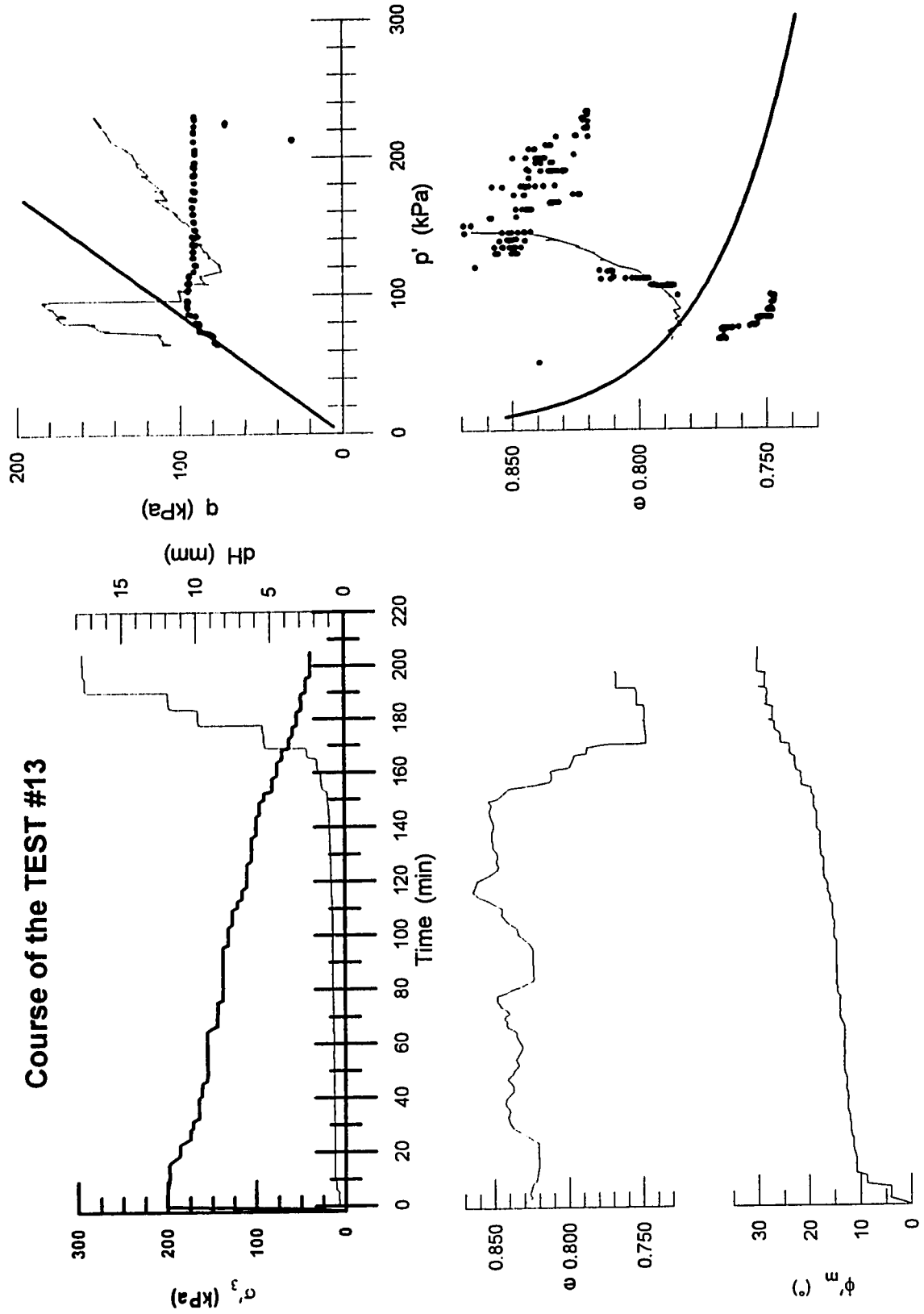
Course of the TEST #10



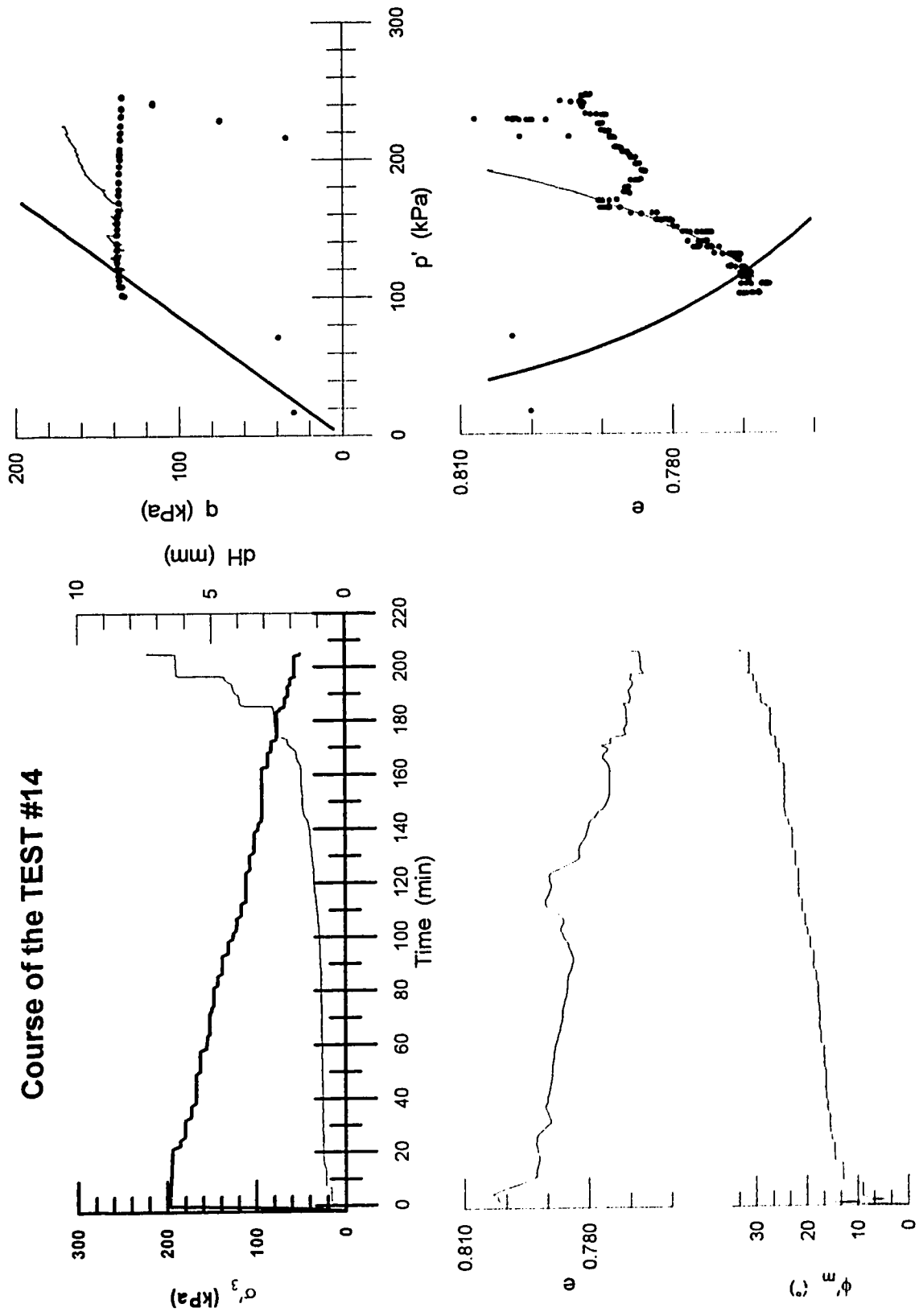
Course of the TEST #12



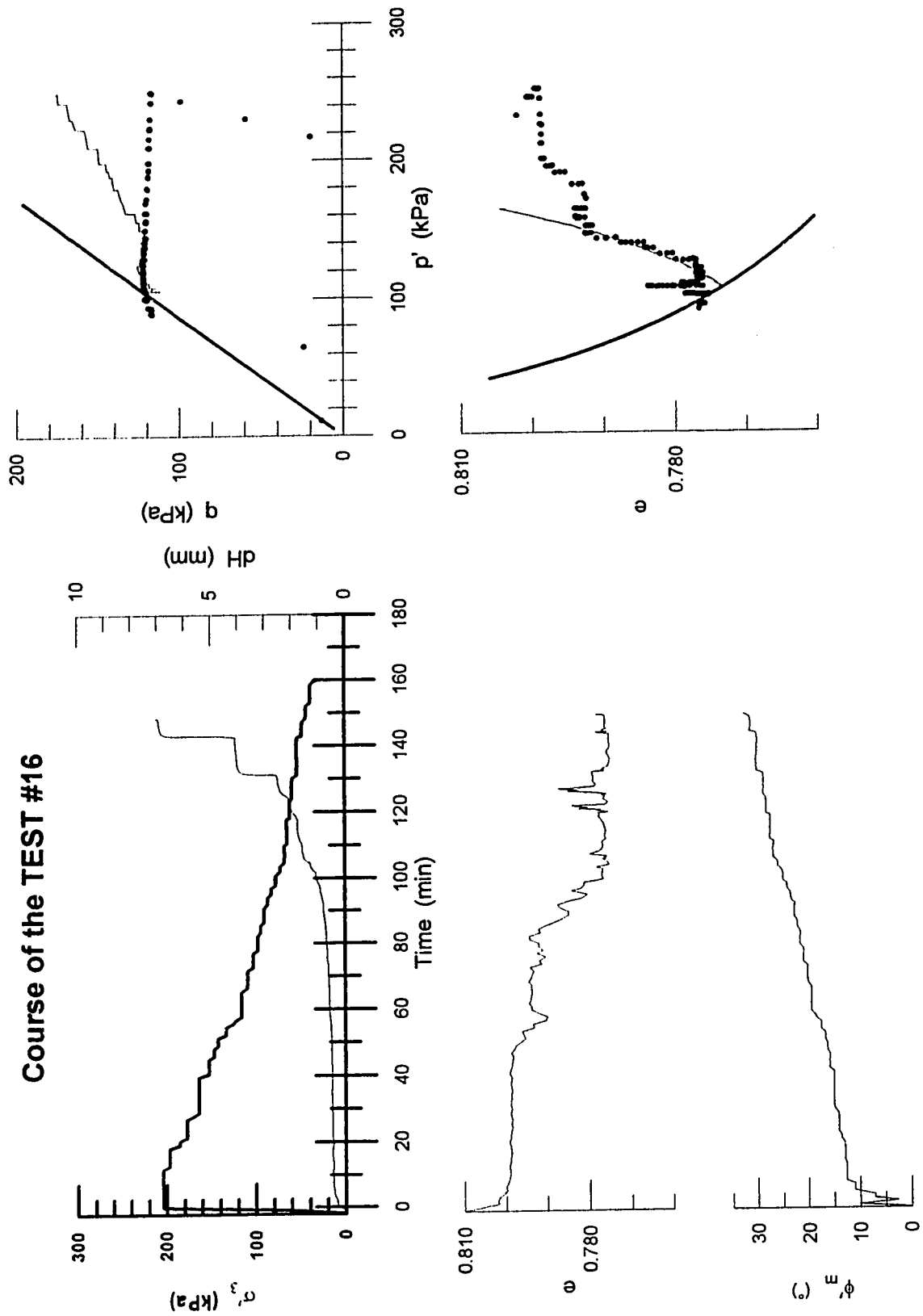
Course of the TEST #13



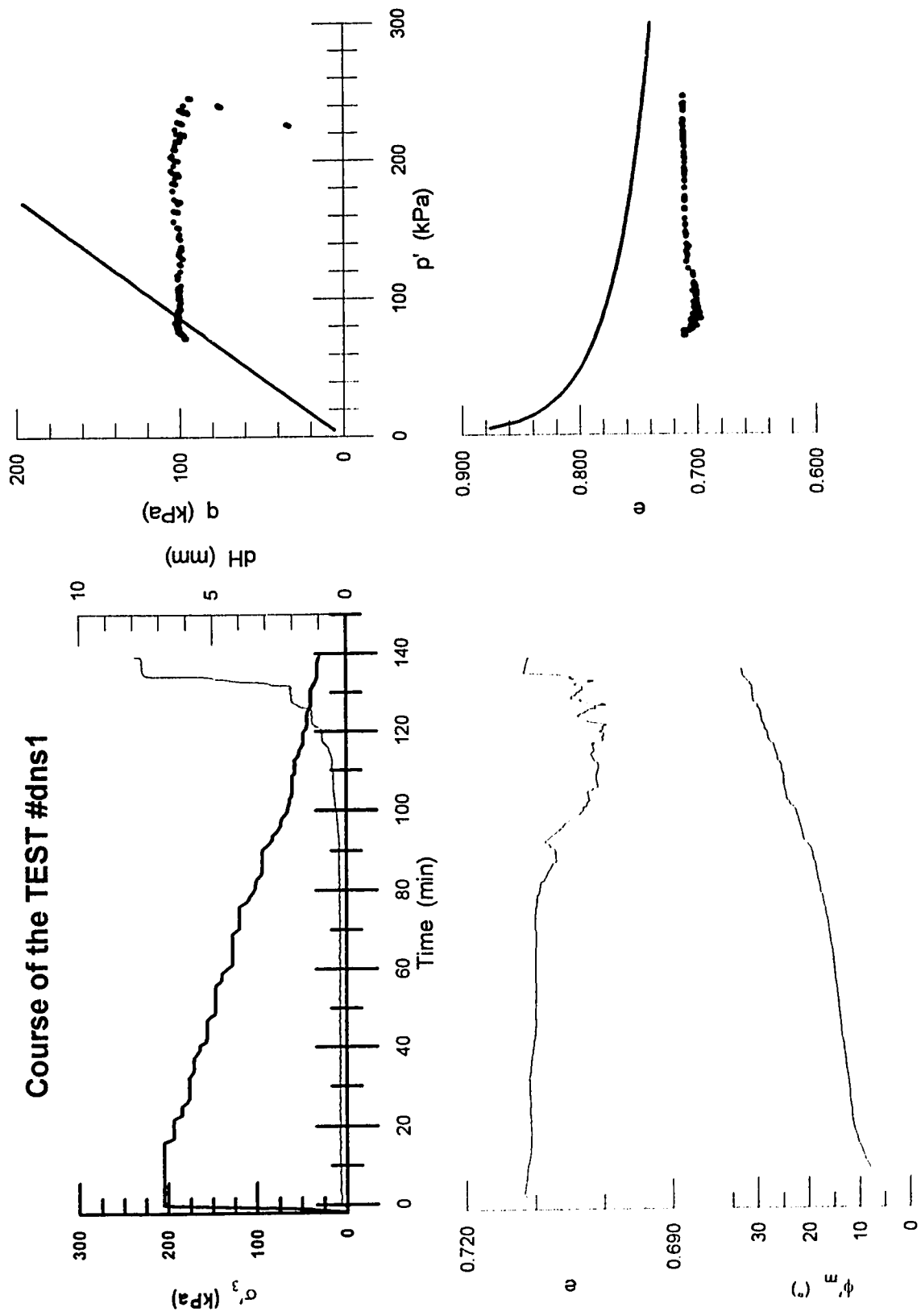
Course of the TEST #14



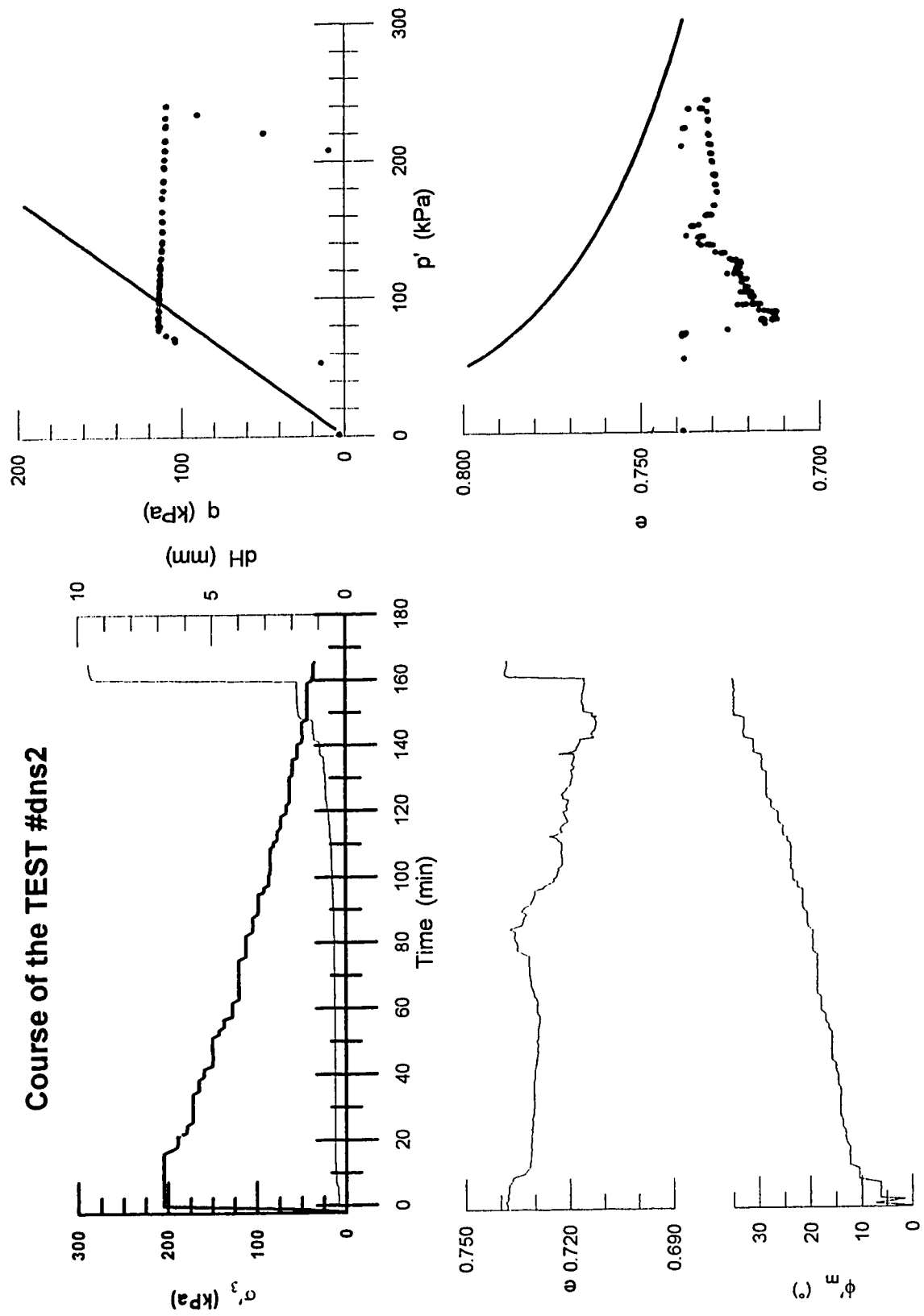
Course of the TEST #16



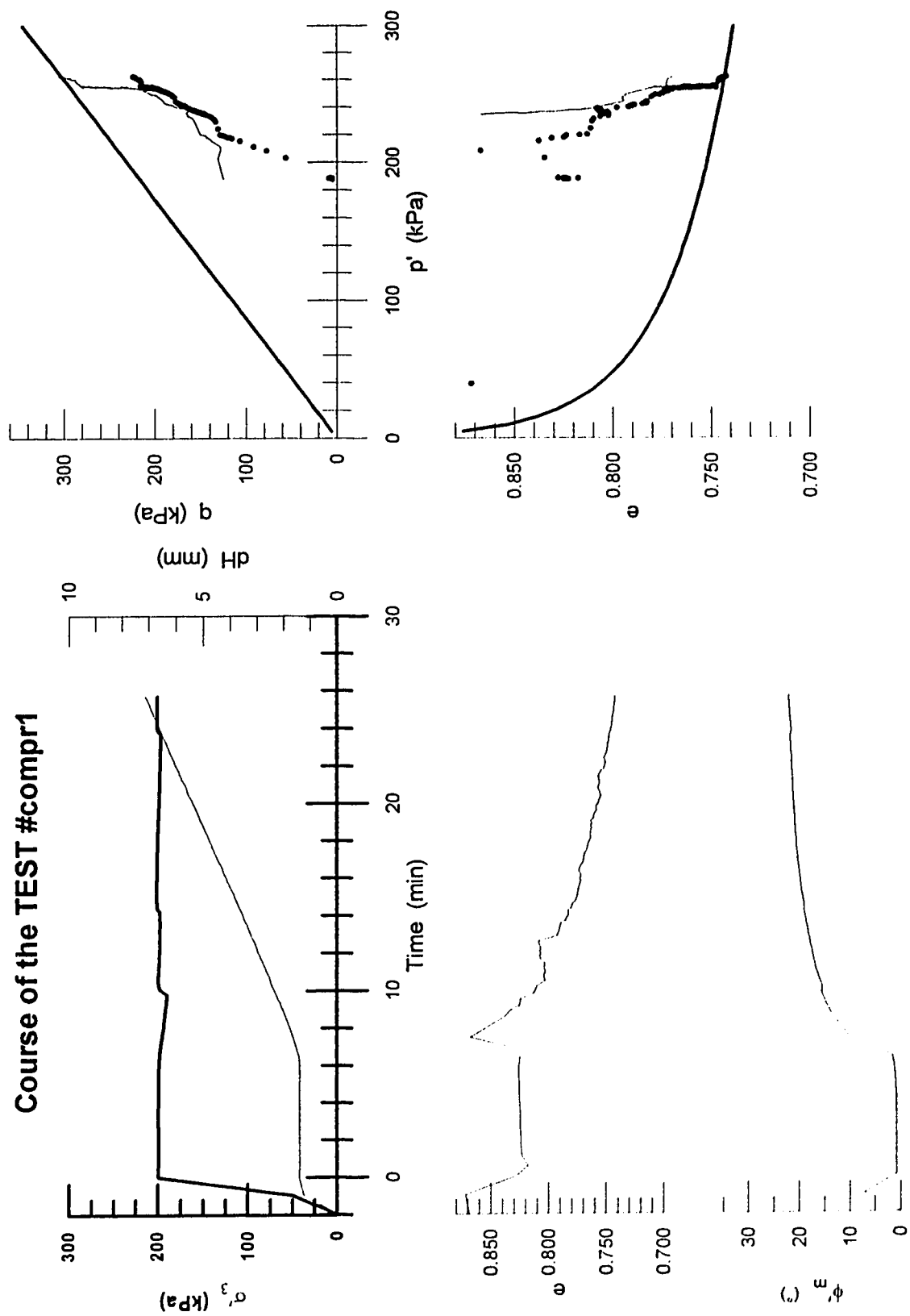
Course of the TEST #dns1



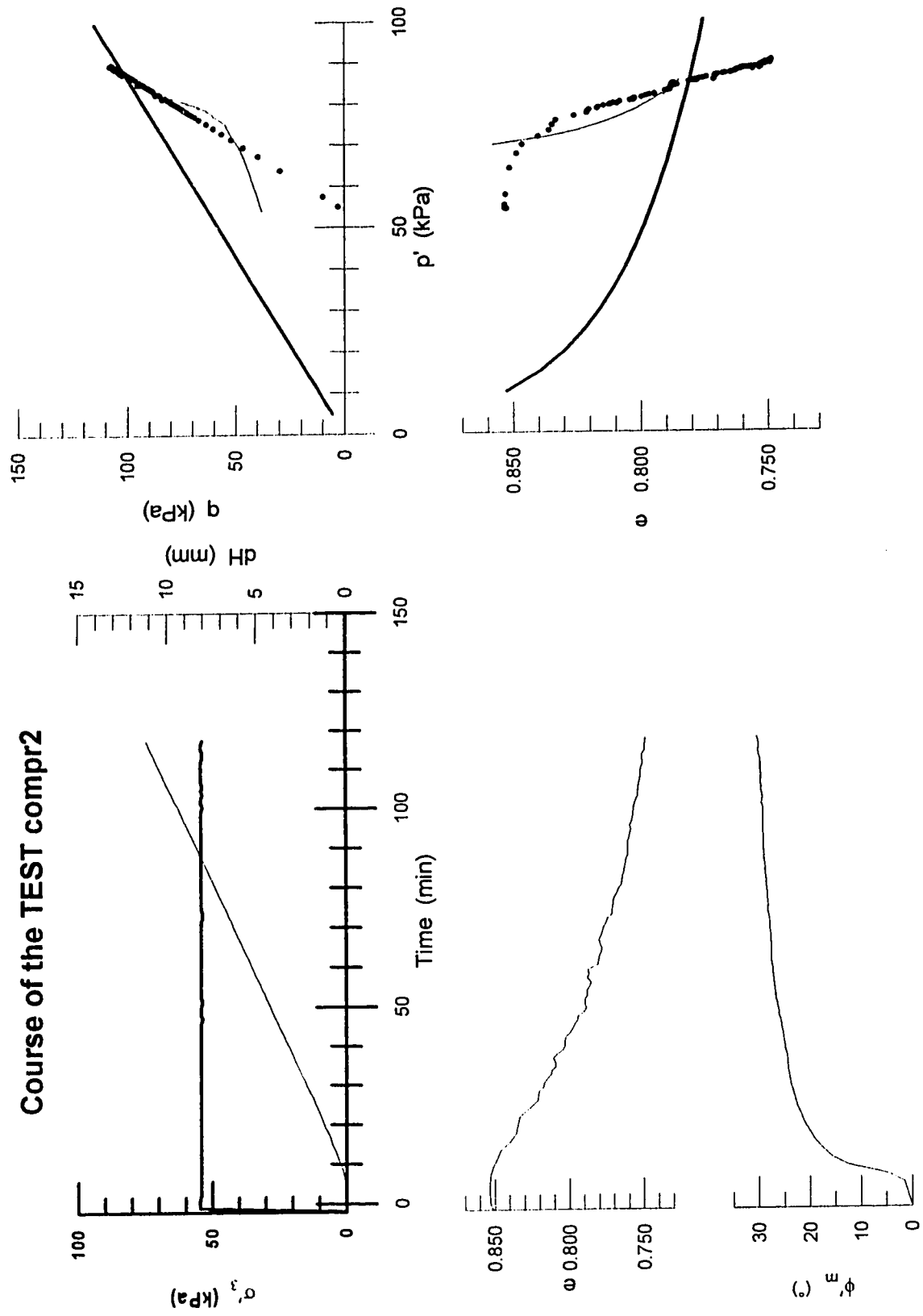
Course of the TEST #dns2



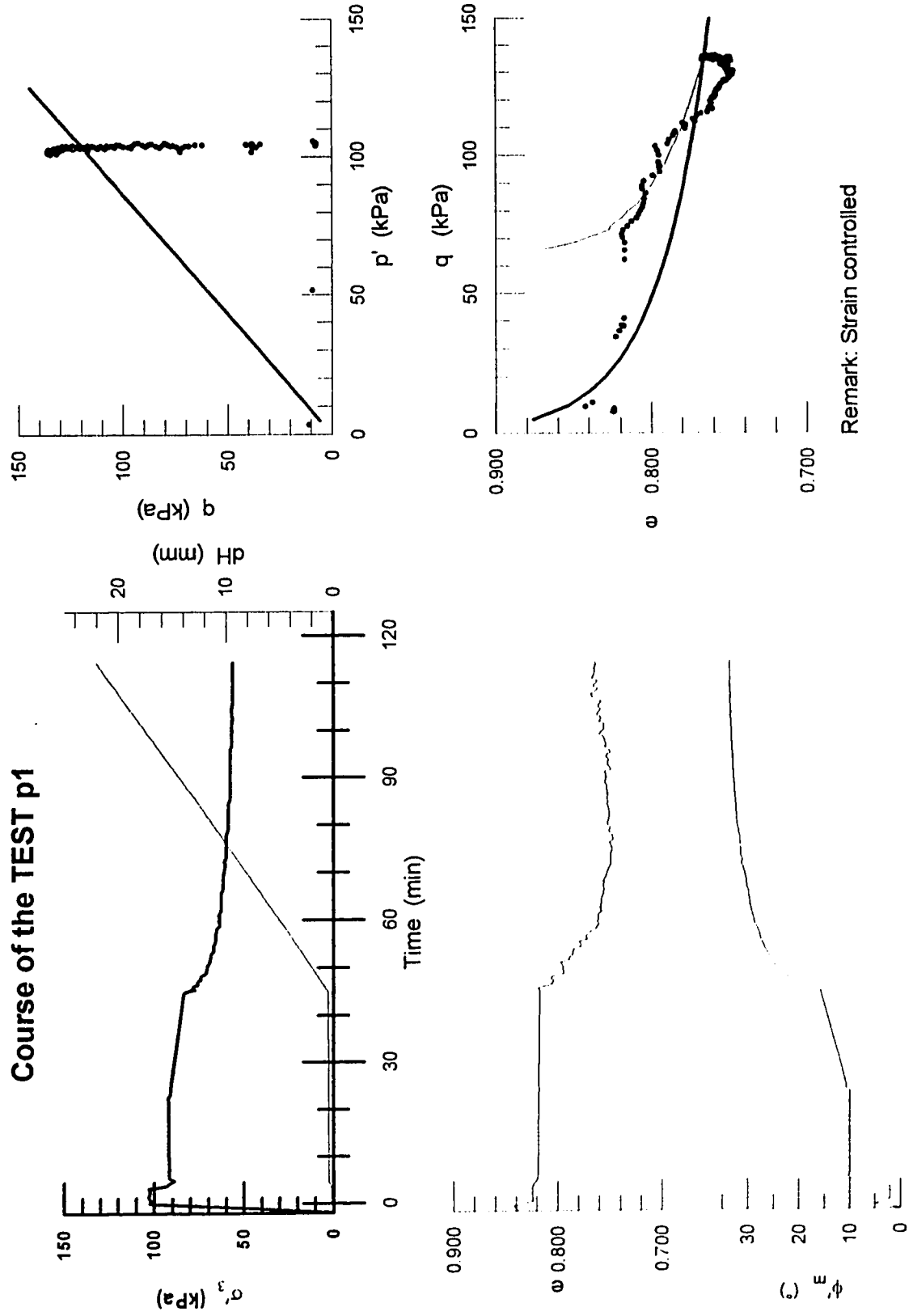
Course of the TEST #compr1



Course of the TEST compr2

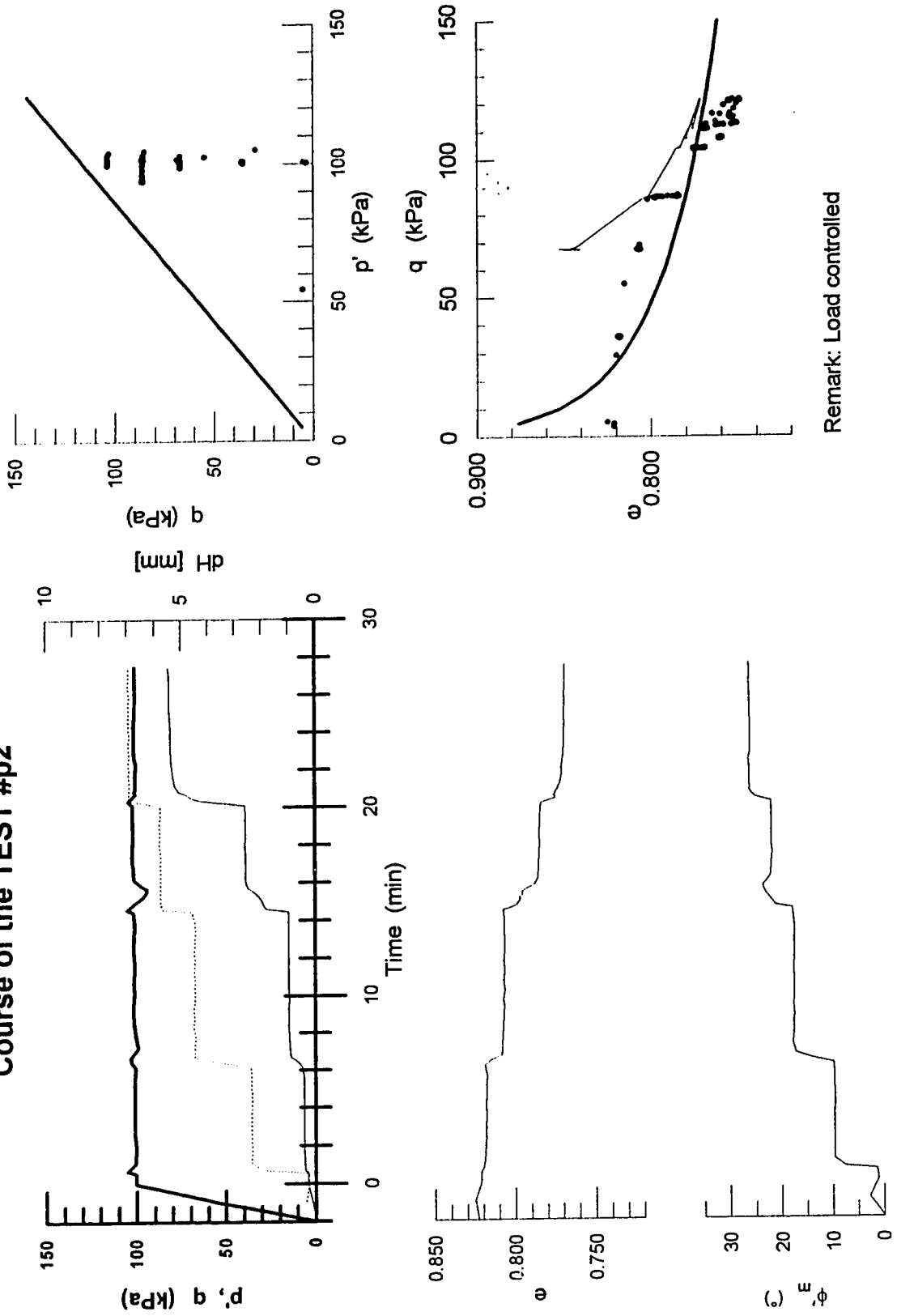


Course of the TEST p1

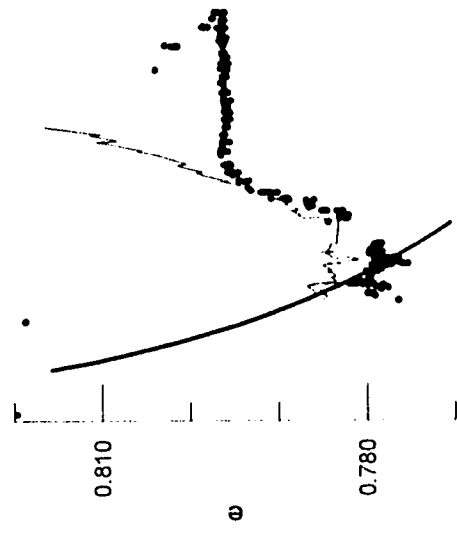
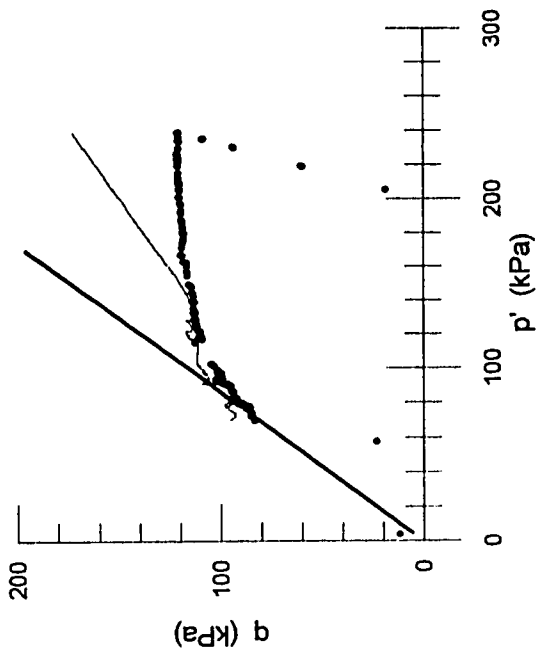


Remark: Strain controlled

Course of the TEST #p2



Remark: Load controlled



Course of the TEST #spec

